THROMBIN, THROMBUS, THROMBI:
MECHANISMS OF THROMBUS FORMATION UNDER FLOW

By

Michelle Anne Berny-Lang

A DISSERTATION

Presented to the Department of Biomedical Engineering
of the Oregon Health & Science University
School of Medicine
in partial fulfillment of
the requirements for the degree of

Doctor of Philosophy
in Biomedical Engineering

December 2010

Department of Biomedical Engineering
School of Medicine
Oregon Health & Science University

CERTIFICATE OF APPROVAL

This is to certify that the Ph.D. dissertation of
Michelle Anne Berny-Lang
has been approved

Owen J. T. McCarty, Ph.D.
Assistant Professor, Thesis Advisor

András Gruber, M.D.
Associate Professor

David H. Farrell, Ph.D.
Professor

Sandra Rugonyi, Ph.D.
Assistant Professor

Monica T. Hinds, Ph.D.
Assistant Professor

To my dad,

You and I used to climb a tree…

To my mom,

For never being more than a phone/Skype call away.

TABLE OF CONTENTS

List of Figures

Chapter 1: Introduction

Chapter 2: Common Materials and Methods

Chapter 3: Thrombin Mutant W215A/E217A Acts as a Platelet GPIb Antagonist

Chapter 7: Conclusions and Future Directions

List of Tables and Equations

Tables

Chapter 3: Thrombin Mutant W215A/E217A Acts as a Platelet GPIb Antagonist

Equations

Chapter 2: Common Materials and Methods

Chapter 5: Rational Design of an Ex Vivo Model of Thrombosis

List of Abbreviations

Ab	antibody
ACD	acid citrate dextrose
ADAMTS13	a disintegrin and metalloproteinase with a thrombospondin type 1 motif, member 13
ADP	adenosine diphosphate
AF	Alexa fluor
ANOVA	analysis of variance
APC	activated protein C
AT-III	antithrombin III
BSA	bovine serum albumin
CHO cells	Chinese hamster ovary cells
CTI	corn trypsin inhibitor
CVD	cardiovascular disease
DIC	differential interference contrast
DMEM	Dulbecco's Modified Eagle Medium
EC	endothelial cell
ECM	extracellular matrix
EPCR	endothelial protein C receptor
FBS	fetal bovine serum
FII	coagulation factor II, prothrombin
FIIa	activated coagulation factor II, thrombin
FITC	fluorescein isothiocyanate
FIX(a)	(activated) coagulation factor IX

Fluo-4 AM	Fluo-4 acetoxymethyl ester
FV(a)	(activated) coagulation factor V
FVII(a)	(activated) coagulation factor VII
FVIIai	inhibited form of activated factor VII
FVIII(a)	(activated) coagulation factor VIII
FX(a)	(activated) coagulation factor X
FXI(a)	(activated) coagulation factor XI
FXII(a)	(activated) coagulation factor XII
FXIII(a)	(activated) coagulation factor XIII
Gla	γ-carboxyglutamic acid
GP	glycoprotein
GPCR	G-protein-coupled receptor
GPIb	glycoprotein Ib or CD42b
GPRP	H-Gly-Pro-Arg-Pro-OH
LRR	leucine-rich repeat
mAb	monoclonal antibody
MCAO	middle cerebral artery occlusion
MES	2-(N-morpholino)ethanesulfonic acid
OG	Oregon Green
PAR	protease-activated receptor
PBS	phosphate buffered saline
PMSF	phenylmethylsulfonyl fluoride
PPACK	D-phenylalanyl-L-prolyl-L-arginine chloromethyl ketone

PPP	platelet poor plasma
PRP	platelet rich plasma
PS	phosphatidylserine
RBC	red blood cell
S195A	active-site thrombin mutant Ser195Ala
SDS-PAGE	sodium dodecyl sulfate polyacrylamide gel electrophoresis
SEM	standard error mean
TF	tissue factor
TFPI	tissue factor pathway inhibitor
TTC	2,3,5-triphenyltetrazolium chloride
TW	thrombin mutant Thr172Tyr/Glu217Ala
TWE	thrombin mutant Thr172Tyr/Trp215Ala/Glu217Ala
TxA_2	thromboxane A2
v/v	volume/volume
VTE	venous thromboembolism
vWF	von Willebrand factor
WAVE-1	Wiskott-Aldrich syndrome protein (WASP)-family verprolin-homologous protein
WE	thrombin mutant Trp215Ala/Glu217Ala
w/v	weight/volume
Z-GGR-AMC	Z-Gly-Gly-Arg aminomethyl coumarin
α_{IIb}	CD41
β_3	CD61

Acknowledgements

A paragraph is not enough to extend my sincere gratitude to my thesis advisor, Dr. Owen McCarty. I am extremely grateful for the countless hours Owen has dedicated to help me improve and grow as a scientist (perhaps we should retire the/my chair in your office!). His tireless work ethic, attention to detail, and infectious enthusiasm is inspirational and has continually motivated me to work harder and strive for more. It has been a rewarding experience to participate in the development of Owen's laboratory and I look forward to seeing its future growth and successes.

I extend my thanks to Dr. András Gruber for always encouraging me to see the big picture. I appreciate his unbridled creativity and am thankful for his participation on my thesis committee. Dr. David Farrell has prompted my interest in the fibrinogen world and I would like to thank him for his experimental ideas and assistance, and critical review of this dissertation. My knowledge of fluid dynamics has been strongly enhanced by Dr. Sandra Rugonyi and I am grateful that she was part of my thesis committee. It has been a pleasure to work next door to Dr. Monica Hind's lab throughout my graduate career. I appreciate her willingness to serve on my defense committee.

I am grateful to Dr. Johan Heemskerk for welcoming me into his laboratory. I wish to thank him for his guidance and support and for pushing me to think independently. Hartelijk bedankt to Marion Feijge, Marijke Kuijpers, Imke Munnix, Saskia Schols, Karen Gilio, Judith Cosemans, Paola van der Meijden, and Reyhan Nergiz-Unal for their help, friendship, and for tolerating my Dutch (or lack thereof).

I would like to thank Dr. Enrico Di Cera and Leslie Pelc (St. Louis University) and Dr. Paul Bock (Vanderbilt University) and Dr. Peter Panizzi (Massachusetts General Hospital) for providing crucial reagents and thoughtful advice on my research. I am also grateful to Dr. Steve Watson (University of Birmingham, UK) for guidance and collaborative research efforts.

I have had the privilege of working with an outstanding group of individuals in both the McCarty lab and the Gruber lab. Tara Adams has been not only a helpful, insightful, and supportive co-worker, but also a caring friend. Members of the McCarty and Gruber team have helped and supported my research while making graduate school more enjoyable. I feel fortunate to have worked with Joseph Aslan, Garth Tormoen, Asako Itakura, Jiaqing Pang, Tal Eshel-Green, Robert Conley, Erik Tucker, and Sawan Hurst. Each summer was brightened by the addition of our summer interns, thanks to David Kyle Robinson, Madeline Midgett, Jacqueline Gertz, Ishan Patel, Patrick Simonson, Brian Fuchs, and Cassandra Loren.

None of this would be possible without the continuous love, support, and encouragement of my friends and family. I am especially appreciative of my parents, Mike and Dana, who have believed in me without fail. I wish to thank them for everything, including the 50+ times they listened with interest to my ISTH 2007 presentation. And finally, I extend my deepest thanks to my husband, partner, and best friend, Chris. This thesis is just as much yours as it is mine.

Abstract

Thrombin, Thrombus, Thrombi: Mechanisms of Thrombus Formation Under Flow

Michelle A. Berny-Lang

Department of Biomedical Engineering
School of Medicine
Oregon Health & Science University

December 2010
Thesis Advisor: Owen J. T. McCarty, Ph.D.

In the event of vascular injury, careful orchestration of blood platelet recruitment and coagulation protein activation functions to stop blood loss. Elucidation of the molecular mechanisms that mediate hemostasis is essential to understanding the dysfunction of this process under pathological conditions. This dissertation centers on characterizing the role of the coagulation enzyme thrombin in hemostasis, utilizing biophysical techniques to reveal unique interactions of thrombin with platelets and thrombi.

The platelet receptor GPIb has been shown to mediate platelet-thrombin interactions in solution. Functional results presented here extend these findings to demonstrate that GPIb supports platelet interactions with both wild-type thrombin and the thrombin mutant, WE, under shear flow.

In addition to its capacity for thrombin binding, the platelet surface is key in thrombin formation, supporting activation of prothrombin (the precursor to thrombin) by factor Xa.

Upon formation, however, the fate and distribution of thrombin remains unclear. Results described in this thesis confirm binding of factor Xa and prothrombin to platelets, and emphasize the role of fibrin(ogen) in thrombin distribution on thrombi.

Elevated rates of thrombosis are observed in patients with cancer, which may correlate to the expression and release of procoagulant molecules by tumor cells. In order to evaluate the mechanisms of thrombus formation, a novel *ex vivo* model of occlusive thrombus formation was developed. Utilizing this model, tumor cells were shown to promote the formation of occlusive thrombi in a manner dependent upon tissue factor and the activity of thrombin.

Collectively, this dissertation provides new insights into the function of thrombin in hemostasis and thrombosis.

Chapter 1: Introduction

1.1 Cardiovascular Disease and Hemostasis

Cardiovascular disease (CVD), defined as high blood pressure, coronary heart disease, heart failure, or stroke, has consistently ranked as the number one cause of death in the United States since 1900, with the exception of the influenza epidemic in 1918 (Lloyd-Jones, *et al.*). While advances in prevention and treatment of CVD have improved outcomes and reduced mortality rates, the incidence of CVD-related mortality remains staggeringly high (Lloyd-Jones, *et al.*). Statistics from the most recent year of analysis indicate that more than 38% of deaths in the United States in 2007 were due to CVD (Xu, *et al.* 2010). Within CVD, dysfunction of the hemostatic system, as in myocardial infarction or stroke, is implicated in a significant number of deaths (Furie, *et al.* 2008; Lloyd-Jones, *et al.*). Further understanding of the mechanisms that drive normal hemostasis or derail hemostasis in a pathologic situation will improve prevention and treatment strategies for CVD.

Hemostasis is a process that relies on the intricate interplay between vascular cells and blood proteins to minimize blood loss at sites of vascular damage. Upon injury to the vasculature, exposed extracellular matrix (ECM) proteins trigger a series of events that lead to the formation of a hemostatic plug. The exposed ECM proteins bind von Willebrand factor (vWF) from the blood, which recruits blood platelets (the “first

responder" cells) to the injury site. Concurrent exposure of tissue factor (TF) on vascular cells initiates blood coagulation, resulting in the generation of the key coagulation enzyme, thrombin, and subsequent deposition of fibrin, functioning to stabilize the developing clot (as reviewed by Furie, *et al.* 2008). Offsetting the balance of the hemostatic system can result in a spectrum of events, ranging from uncontrolled bleeding through hemorrhage or uncontrolled clot formation in thrombosis. This chapter will detail the primary cells and proteins involved in hemostasis and discuss how their functions are altered in disease states.

1.2 Vascular Cells

1.2.1 Overview of vascular cells

Platelets, red blood cells (RBCs), and leukocytes (white blood cells) comprise the cellular components of blood, with their traditional roles being hemostasis, oxygen transport, and immunity, respectively. Beyond their traditional functions, RBCs and leukocytes also contribute to hemostasis. For example, in flowing blood, RBCs are heavily concentrated at the axis of the vessel, forcing platelets to the vessel wall through margination, allowing the platelets to continually assess vascular integrity (Aarts, *et al.* 1988; Woldhuis, *et al.* 1992). Leukocytes are recruited to thrombi, interact with platelets, and can express molecules, such as TF, that influence coagulation (Ahn, *et al.* 2005; Bouchard, *et al.* 2003; Kirchhofer, *et al.* 1997). In addition to blood cells, endothelial cells (ECs), which line the vasculature, contribute substantially to hemostasis. Among a multitude of hemostatic functions, under normal conditions, ECs secrete inhibitors of platelet activation, helping to maintain platelets in a basal state (Radomski, *et al.* 1987).

However, upon injury; ECs increase expression and secretion of procoagulant and adhesive molecules, including TF and vWF, which promote coagulation and platelet recruitment (Camerer, *et al.* 1996; Ribes, *et al.* 1989; Sporn, *et al.* 1986; Wu, *et al.* 1996). Each of the vascular cells plays a cooperative role in hemostasis, facilitating and contributing to the essential function of the platelet.

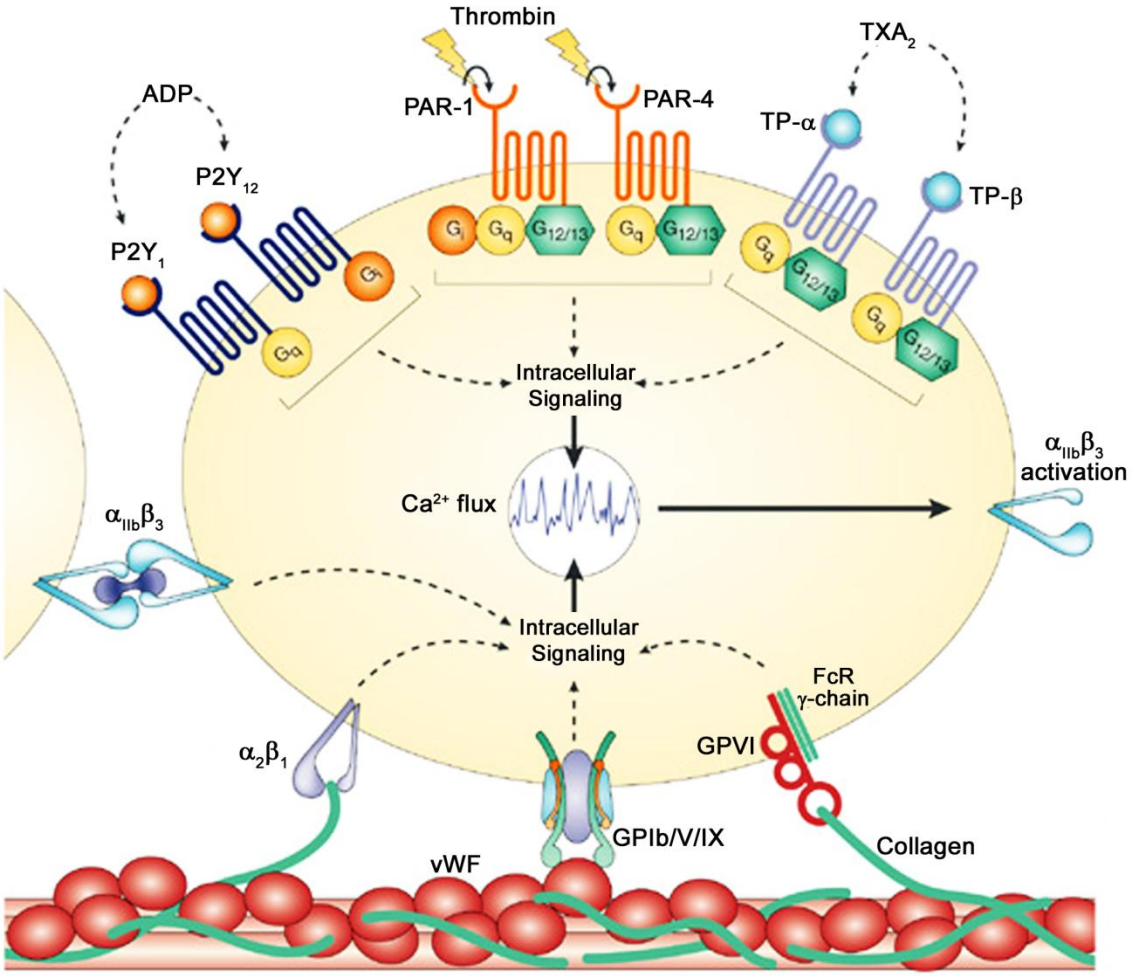

Figure 1.1. Major adhesion and agonist receptors on the platelet surface. Platelet interactions with exposed collagen are mediated by vWF-GPIb/IX/V interactions and by binding of $\alpha_2\beta_1$ and GPVI to collagen. Platelet-platelet binding is supported by the integrin $\alpha_{IIb}\beta_3$. Interactions of adhesion receptors and agonist receptors ($P2Y_1$, $P2Y_{12}$, PAR-1, PAR-4, TP-α, and TP-β) with their ligands induce signaling cascades that elicit intracellular calcium fluxes. Figure adapted and reprinted with permission from Nature Publishing Group, Nature Reviews Drug Discovery (Jackson, *et al.* 2003).

1.2.2 Platelets

Platelets are the smallest of the blood cells, ~3μm in diameter and anucleate; they are present at 150-400 billion cells per liter. Platelets are formed from mature megakaryocytes in the bone marrow and live for 5-10 days in circulation (Italiano, *et al.* 1999; Najean, *et al.* 1969).

Platelet responses are mediated by unique platelet membrane receptors. Through glycoprotein Ib (GPIb), also termed CD42b, platelets interact with vWF at sites of vascular injury (Figure 1.1). GPIb is expressed on the platelet membrane as part of the GPIb/IX/V complex, comprised of four transmembrane polypeptides, GPIbα, GPIbβ, GPIX and GPV, with ~25,000 copies of GPIb-IX and ~12,000 copies of GPV present on platelets (Andrews, *et al.* 1997). Importantly, vWF binding has been mapped to GPIbα (Vicente, *et al.* 1990). The kinetics of the GPIb-vWF bond support platelet tethering and rolling under flow conditions (Doggett, *et al.* 2002). Firm adhesion at sites of damaged endothelium requires additional adhesive molecules, including activated integrins. Integrins are present on a variety of cells types and mediate cell-cell and cell-protein interactions. Composed of a heterodimeric complex of α and β subunits, the subunit composition of the receptor designates its specificity (Wegener, *et al.* 2008). Integrins are generally expressed on the cell surface in a low affinity, inactive state. Conformational changes that lead to a high affinity, active state are induced by intracellular signals or ligand binding (Liddington, *et al.* 2002). Following platelet rolling on vWF, adhesion to the subendothelium is mediated by integrins specific for collagen ($\alpha_2\beta_1$), laminin ($\alpha_6\beta_1$), and other matrix proteins (Inoue, *et al.* 2006; Santoro, *et al.* 1988). Collagen-dependent

platelet adhesion, aggregation, and activation are dependent on an additional receptor, GPVI , from the immunoglobulin superfamily of receptors (Moroi, *et al.* 1989). As platelets actively bind the ECM, additional platelets are recruited to generate platelet aggregates at the injury site. As illustrated in Figure 1.1, platelet-platelet interactions are supported by integrin $\alpha_{IIb}\beta_3$ (CD41/CD61), the most abundant platelet receptor, present at a copy number of ~80,000 (Wagner, *et al.* 1996). This receptor bridges platelets mainly through the plasma proteins fibrinogen and vWF, and is thus crucial for platelet aggregate formation (Marguerie, *et al.* 1979; Ruggeri, *et al.* 1982).

In addition to the adhesive platelet receptors, platelets express several receptors designed to interact with platelet agonists and elicit cellular responses. Most agonist receptors are G-protein-coupled receptors (GPCRs), a family of proteins with 7 transmembrane domains that activate intracellular signaling pathways. Critical platelet GPCRs include the protease-activated receptors (PARs), which are activated by the coagulation enzyme thrombin, and receptors for the secondary mediators of platelet activation, adenosine diphosphate (ADP) and thromboxane A_2 (TxA_2) (as reviewed by Offermanns 2006). Thrombin is one of the most potent physiological platelet activators and functions through PAR-1 and PAR-4 expressed on human platelets (Figure 1.1) to induce platelet activation and aggregation (Kahn, *et al.* 1999). ADP (released from platelets and RBCs) is a weak platelet antagonist alone, but acting through the receptors $P2Y_1$ and $P2Y_{12}$ (Figure 1.1), it amplifies the platelet response due to other agonists and increases the stability of platelet aggregates (Jin, *et al.* 2001; Leon, *et al.* 1997; Woulfe, *et al.* 2001). In parallel to ADP, TxA_2, also released from platelets, potentiates platelet activation and

stabilizes aggregates through the TP receptors (Hirata, *et al.* 1991; Paul, *et al.* 1999; Svensson, *et al.* 1976).

Interactions of both the adhesive and agonist receptors with their ligands trigger intracellular signaling cascades that result in platelet activation. In their basal state, platelets circulate in a discoid shape, but upon activation, undergo a dramatic structural change into a spherical structure with spiky projections of the cytoskeleton, termed filopodia (Zucker, *et al.* 1985). During activation, platelets exocytose granules, namely the dense granules and α-granules, which contain molecules that influence platelet adhesion and activation, coagulation, and inflammation (Reed 2004). Platelets have 3-8 dense granules of 200-300 nm in diameter that house low molecular weight molecules such as ADP, ATP, serotonin, and calcium (Gunay-Aygun, *et al.* 2004; McNicol, *et al.* 1999). The more prevalent α-granules (50-80 per platelet) are 200-500 nm in size and contain a multitude of high molecular weight proteins, including vWF, fibrinogen, the coagulation cofactors V and VIII, as well as a wide array of chemokines and cytokines (Blair, *et al.* 2009). The membrane of both dense and α-granules contains platelet membrane receptors, which, upon exocytosis of the granules, are expressed on the platelet membrane surface. Key receptors in the α-granule membrane are P-selectin (CD62P), responsible for platelet interactions with leukocytes, and the integrin $\alpha_{IIb}\beta_3$ (as reviewed by Furie, *et al.* 2001).

Intracellular signaling pathways evoked by platelet receptor-ligand interactions, result in an increase in cytosolic calcium (Figure 1.1). Calcium is released intracellularly from

stores in the sarcoplasmic reticulum or allowed to enter the cell via calcium release-activated channels in the plasma membrane (Bergmeier, *et al.* 2009; Hallam, *et al.* 1985; Jardin, *et al.* 2007). Sustained increases in intracellular calcium affect the distribution of membrane phospholipids, promoting exposure of the negatively charged lipid phosphatidylserine (PS) on the outer membrane surface (Bevers, *et al.* 1982; Bevers, *et al.* 1983; Dachary-Prigent, *et al.* 1995; Keuren, *et al.* 2005). In the presence of calcium, the exposed PS provides a surface for binding and activation of the γ-carboxyglutamic acid (Gla)-containing coagulation factors II, VII, IX, X (Shearer 1990; Sunnerhagen, *et al.* 1995); see Figure 1.2. In addition to platelet-coagulation factor interactions via PS, platelets support interactions with coagulation proteins through specific membrane receptors. As an example, GPIbα, the major platelet receptor for vWF, also interacts with protein C, factor XI, and the essential coagulation protein thrombin (Baglia, *et al.* 2004; White, *et al.* 2008; Yamamoto, *et al.* 1986). Therefore, combined with their adhesive and aggregatory functions, platelets also play a critical role in localizing coagulation factors at the site of vessel injury.

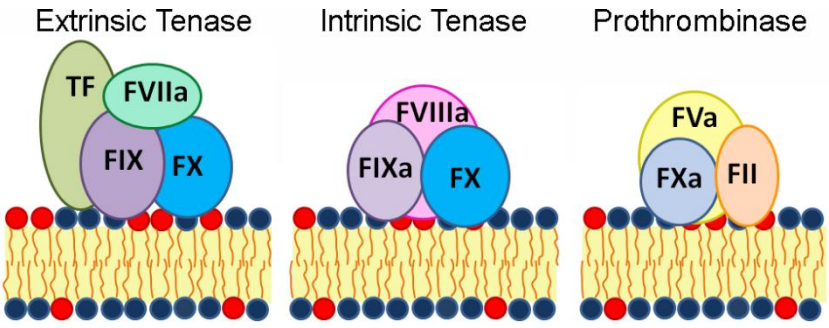

Figure 1.2. Coagulation factor activation complexes on the platelet surface. Coagulation factors bind to the platelet membrane surface in a calcium-mediated interaction between PS (red) and coagulation factor Gla domains. Left, the TF-FVIIa complex promotes activation of FIX and FX in the extrinsic tenase complex. Middle, FIXa and the cofactor FVIIIa associate on the platelet surface to activate FX in the intrinsic tenase complex. Right, prothrombin (FII) is activated to thrombin by FXa and cofactor FVa in the prothrombinase complex. Figure design based on review by Mann (Mann, *et al.* 2003).

1.3 Coagulation

1.3.1 Overview of coagulation

Concurrent with platelet adhesion and aggregate formation is the activation of the coagulation system. In coagulation, zymogen coagulation proteins in the blood are sequentially activated into their enzyme, or active, forms (Figure 1.3). Following vascular injury, TF is exposed on ECs and subsequently binds to activated factor VII (FVIIa), initiating a cascade of events leading to thrombin generation (as reviewed by Mann, *et al.* 2003). The FVIIa-TF complex is associated with negatively charged phospholipids, PS, on the membrane surface of activated blood cells, and, as part of the extrinsic tenase complex (Figure 1.2), assembles with and activates FIX and FX (Lawson, *et al.* 1991). Following activation, FIXa and the cofactor FVIIIa assemble on the membrane surface to form the intrinsic tenase complex (Figure 1.2), responsible for additional generation of FXa (Ahmad, *et al.* 2003; Ahmad, *et al.* 2003). After arrangement of a third complex on the membrane surface, the prothrombinase complex (Figure 1.2), FXa, in conjunction with cofactor FVa, catalyzes prothrombin (FII) activation to thrombin (Kamath, *et al.* 2008; Tracy, *et al.* 1985). Thrombin is released by FXa cleavage of the zymogen precursor prothrombin at Arg320 and Arg271 (Krishnaswamy, *et al.* 1987). Alternatively, thrombin can be formed by cleavage of prethrombin-1, a thrombin precursor released when thrombin cleaves prothrombin (Anderson, *et al.* 2003). Regardless of the route by which thrombin is initially formed, thrombin stimulates its own subsequent generation through the activation of the cofactors V and VIII, and factor XI (Figure 1.3), which results in rampant thrombin generation in the presence of activated platelets (Maas, *et al.* 2010; Rick, *et al.* 1978; Suzuki, *et al.* 1982).

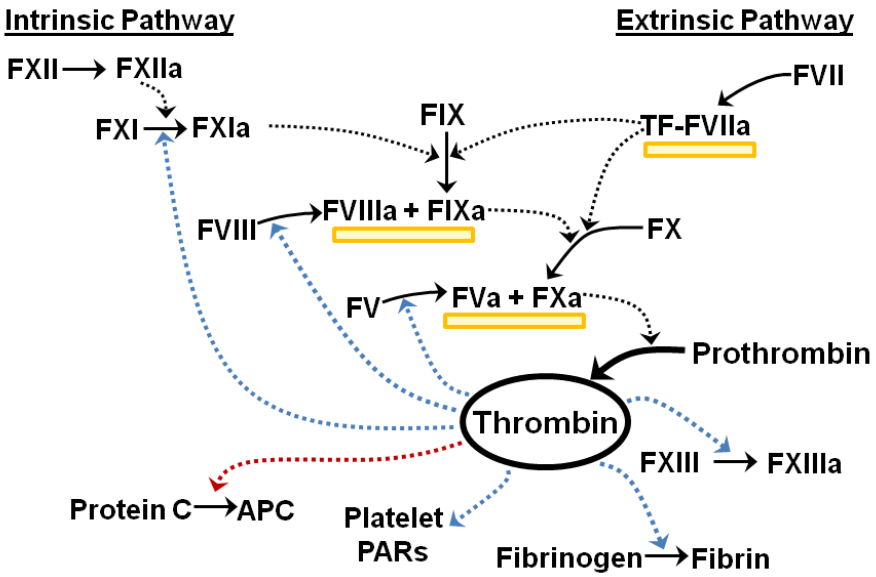

Figure 1.3. The critical role of thrombin in hemostasis. Coagulation is triggered by upstream activation of the extrinsic or intrinsic pathways, resulting in thrombin generation through FXa cleavage of prothrombin on the cell membrane surface (yellow boxes). Thrombin has a multitude of functions in hemostasis, including activation of platelet PARs, cleavage of fibrinogen into fibrin, and activation of FXI, FXIII, cofactors V and VIII, and protein C. The enzymatic functions of thrombin and other coagulation enzymes are indicated by dashed lines. Procoagulant actions of thrombin are indicated by blue lines, and anticoagulant actions by red lines.

Thrombin generation does not go uncontrolled and is regulated by three important mechanisms: tissue factor pathway inhibitor (TFPI), antithrombin III (AT-III), and activated protein C (APC). TFPI functions to disrupt the extrinsic tenase complex, preventing the formation of FIXa and FXa, therefore, hindering thrombin production (Crawley, *et al.* 2008). Alternatively, AT-III inhibits several of the activated coagulation factors involved in thrombin production, including FXa and thrombin itself (Mann, *et al.* 2003). As a third mechanism, thrombin controls its own regulation through generation of activated protein C (APC). Activation of protein C by thrombin is orchestrated on the EC surface by the membrane protein thrombomodulin and the endothelial protein C receptor (EPCR) (Esmon, *et al.* 1981; Xu, *et al.* 2005). APC functions to inactivate the cofactors

Va and VIIIa, resulting in a down regulation of thrombin generation (Fulcher, *et al.* 1984; Kisiel, *et al.* 1977; Walker, *et al.* 1979).

Prior to inactivation, however, thrombin plays a central role in hemostasis through cleavage of fibrinogen and activation of FXIII. Thrombin cleaves the blood protein fibrinogen into fibrin monomers (Blomback, *et al.* 1978). Monomers spontaneously polymerize and are crosslinked by thrombin-activated FXIII (Ferry 1952; Siebenlist, *et al.* 2001). Crosslinked fibrin is deposited on platelet aggregates, functioning to stabilize the developing platelet plug (Falati, *et al.* 2002; Lord 2007). The intersection of the coagulation pathway with the platelet deposition pathway results in the formation of a stable thrombus (blood clot) at the site of vascular injury, preventing loss of blood into the extravascular space.

1.3.2 Thrombin structure and corresponding function

When thrombin is generated by proteolytic cleavage of prothrombin, the resulting protein is a 37-kDa serine protease involved in a plethora of biological functions beyond its role in hemostasis, ranging from tumor growth and metastasis to inflammation to embryonic development (as reviewed by Di Cera 2003). Among its hemostatic functions are the cleavage of fibrinogen to fibrin, activation of FV, VIII, XI, XIII, and protein C, and the activation of platelets. Major structural features of thrombin include the active-site cleft, anion-binding exosites I and II, the 60- and γ (autolysis)-loops, and the sodium (Na^+) binding site (Crawley, *et al.* 2007; Di Cera 2007), as shown in Figure 1.4. The active site of thrombin, containing the catalytic triad of His57, Asp102, and Ser195, is similar to

other serine proteases (Adams, *et al.* 2006; Di Cera, *et al.* 2001). A single point mutation of S195 to an A (mutant S195A) eliminates catalytic activity (Krem, *et al.* 2003). Unique to thrombin are exosites I and II (Figure 1.4), which are responsible for mediating substrate/effector interactions with thrombin, contributing to the specificity of the enzyme. For example, the thrombin inhibitor, heparin, binds thrombin via exosite II, while fibrinogen binds via exosite I (De Cristofaro, *et al.* 2003). Also involved in thrombin's specificity are the 60- and γ-loops, and, importantly, the Na^+ binding site (Davie, *et al.* 2006). When thrombin is Na^+ bound, it adopts a fast conformation, with enhanced substrate binding and catalysis. Conversely, without Na^+, thrombin is in a slow form (Huntington 2009). The form of thrombin has important consequences for the pro- and anti-coagulant functions of the enzyme. In comparison to the slow form, fast thrombin has higher specificity (greater than 20-fold) for fibrinogen, fibrin, and PARs (procoagulant). The slow form retains comparable specificity for protein C in the presence of thrombomodulin (anticoagulant) (Di Cera 2003; Di Cera 2007; Di Cera, *et al.* 2001). Mutants with disruptions in the Na^+ binding site have been developed by Dr. Enrico Di Cera's laboratory with the aim of generating an anticoagulant thrombin. One such mutant, W215A/E217A (WE) was found to have dramatically reduced capacity to cleave fibrinogen (20,000-fold reduction) and PARs (1000-fold reduction), and yet retains the ability to activate protein C in the presence of thrombomodulin (Cantwell, *et al.* 2000). In a baboon model of thrombosis, administration of WE enhanced APC levels and effectively reduced platelet and fibrin deposition, without increased bleeding (Gruber, *et al.* 2002; Gruber, *et al.* 2007). While great advancements have been made in the determination of the structural features that regulate thrombin's activity, the

mechanisms responsible for mediating interactions between wild-type and mutant thrombin with blood cells and clots remain critical areas of research.

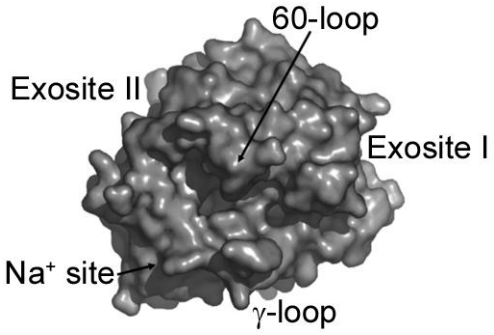

Figure 1.4. The structure of thrombin. Important structural features on the surface of the coagulation enzyme thrombin are shown. The active site containing the catalytic triad is located in the center, below the 60-loop (indicated by arrow). In this orientation, with respect to the active site, the anion-binding exosites I and II are located east and northwest, respectively. The Na^+ binding site (indicated by arrow) is oriented to the southwest of the active site, with the γ-loop south of the active site. Figure adapted and reprinted with permission from John Wiley and Sons, Journal of Thrombosis and Haemostasis (Di Cera 2007).

1.3.3 Thrombin interactions with platelets and fibrin(ogen)

The structure of thrombin mediates its interactions with cells and coagulation proteins; specificity for receptors on platelets and for fibrin(ogen) is largely mediated by the anion-binding exosites.

Platelet interactions: Thrombin interacts with platelets through the PARs. Of the four PARs identified (PAR1 through PAR4), human platelets are known to express PAR1 and PAR4 (Kahn, *et al.* 1999). Both platelet PARs interact with thrombin exosite I, resulting in cleavage of the receptors and subsequent platelet activation (Lane, *et al.* 2005). Thrombin interactions with PARs are mediated by an additional platelet receptor, GPIbα (Coughlin 2005). Whether thrombin exosite I, exosite II, or both are involved in GPIbα binding is controversial, but it is known that when thrombin is bound to GPIbα, PAR

hydrolysis is enhanced (Adams, *et al.* 2006; De Candia, *et al.* 2001). In addition to platelet activation via PARs, GPIb-bound thrombin can cleave the GPV portion of the GPIb/IX/V complex or act directly through GPIb to induce intracellular platelet signaling (Ramakrishnan, *et al.* 2001; Soslau, *et al.* 2001). Although interactions between GPIb and thrombin have been described on the molecular level, the physiological implications of these interactions remain to be determined.

Fibrin(ogen) interactions: One of the major procoagulant roles of thrombin is the cleavage of fibrinogen to insoluble fibrin. Accordingly, fibrin(ogen) contains multiple binding sites for thrombin. Fibrinogen is a dimeric molecule composed of two sets of three disulfide-linked polypeptides chains: Aα, Bβ and γ (Weisel 2005). The resulting protein is comprised of two outer D domains, linked by a central E domain (Mosesson 2005). In the reaction of fibrinogen cleavage, thrombin binds to Aα via exosite I and releases fibrinopeptide A, exposing a fibrin polymerization site and initiating fibrin assembly. Further, thrombin can interact with Bβ, through exosite I, to cleave fibrinopeptide B (Lane, *et al.* 2005). Release of fibrinopeptide B reveals an additional fibrin polymerization site (Adams, *et al.* 2006.; Crawley, *et al.* 2007).

Beyond the sites involved in fibrinogen cleavage, additional non-substrate binding sites for thrombin have been identified on fibrin(ogen). Following formation of fibrin monomers, thrombin has been shown to bind with low affinity to the N-terminal E domain (Meh, *et al.* 1996). A high affinity binding site for thrombin has been identified in the γ' chain of the D domain of fibrinogen (Meh, *et al.* 1996). The γ' variant of

fibrinogen results from alternative mRNA splicing of the fibrinogen γ chain. When human fibrinogen is formed, the majority of molecules contain two γA chains, the most frequently occurring variant of the γ chain. An alternatively spliced γ variant, the γ' chain, is present in approximately 10% of fibrinogen molecules (Lovely, *et al.* 2002; Lovely, *et al.* 2008). During processing of the γA transcript, the 9th intron is spliced out and the 9th and 10th exons join. Alternatively, during γ' processing a site within the 9th intron is polyadenylated, cleaving off exon 10 (Lovely, *et al.* 2002). This γ' variant gives rise to a high affinity thrombin binding site which interacts with thrombin exosite II (Mosesson 2005). The role that thrombin binding sites on fibrin(ogen) play in fibrin formation have been elucidated, however, the potential role these bindings site may play in thrombin recruitment and retainment on developing thrombi requires further investigation.

1.4 Dysfunction of Hemostasis and Relation to Disease

Hemostatic dysfunction is commonly observed in cardiovascular disease, and also presents in many other disease states. At any step along the hemostatic pathway, an alteration in cellular or protein composition can disturb hemostasis and drive it towards bleeding or thrombosis. Bleeding commonly manifests from mutations in or deficiencies of coagulation factors, dysfunction of or low number of platelets, or from autoantibodies or pharmacological agents that disrupt coagulation factor or platelet functions. Deficiencies in FVIII or FIX result in the severe bleeding disorders hemophilia A and B, respectively (Ratnoff, *et al.* 1973). Low expression or mutations of the platelet receptors GPIb (Bernard-Soulier syndrome) or $\alpha_{IIb}\beta_3$ (Glanzmann thrombasthenia) are associated

with bleeding tendencies (George, *et al.* 1981; Sebastiano, *et al.* 2010). Pharmacological agents, including aspirin (inhibitor of TxA_2 formation), warfarin (inhibitor of carboxylation of the Gla-domain coagulation factors), and heparin (inhibitor of thrombin), can inhibit thrombosis, but may also cause bleeding (Awtry, *et al.* 2000; Garcia, *et al.* 2010; Gray, *et al.* 2008; Lovelock, *et al.* 2010). On the other side of the balance, unregulated clot formation can lead to the development of occlusive thrombi and subsequent infarction (tissue death due to lack of oxygen), such as myocardial infarction (heart attack) or cerebral infarction (stroke). Virchow's triad defines the elements associated with thrombosis to be alterations in blood flow, alterations in the blood vessel wall, or abnormal blood coagulability (Mann 2006). Blood flow changes can occur at locations of stasis or eddies, or in stenosed vessels. Alterations of the vessel wall include the increased expression of tissue factor upon endothelial damage (Camerer, *et al.* 1996; Wu, *et al.* 1996). Increased blood coagulability, in parallel to bleeding, can be caused by altered expression or mutations of coagulation factors, as evidenced by the hypercoagulable mutations of factor V Leiden and prothrombin G20210A (Segal, *et al.* 2009; Segers, *et al.* 2009).

Disease states ranging from diabetes, to HIV, to cancer, have been shown to alter hemostatic profiles (Biondi-Zoccai, *et al.* 2003; Mosesson, *et al.* 1972; Noble, *et al.* 2010; Shen, *et al.* 2004). Dating as far back as the 1820's, associations between cancer and thrombosis have been observed (Bouillard, *et al.* 1823; Trousseau 1865). The presence of thrombosis in cancer correlates with a significant reduction in survival time and thrombotic complications represent a primary cause of death in cancer patients

(Blom, *et al.* 2005; Heit, *et al.* 2000; Tesselaar, *et al.* 2007). How the hemostatic processes are affected in disease states, including cancer, remains a crucial area for active research.

1.5 Thesis Overview

Vascular injury triggers carefully orchestrated platelet deposition and coagulation pathways that function to stop blood loss. Elucidation of the molecular mechanisms that control normal hemostasis is essential to understanding how hemostasis can be disrupted in disease. This thesis centers on the coagulation enzyme thrombin, revealing unique interactions of the protein with platelets and thrombi and expounding upon the fundamental role that thrombin plays in thrombus formation.

The ability of the platelet receptor GPIb to mediate thrombin binding in solution has received considerable attention in the hemostasis field. How these interactions occur under the shear flow conditions of the vasculature and the implications of these interactions in hemostasis are currently under investigation. Studies in Chapter 3 highlight the role of GPIb in mediating platelet interactions with both wild-type thrombin and WE under shear flow.

In addition to its capacity for thrombin binding, the platelet surface is key in thrombin formation. Catalyzed by assembly of the prothrombinase complex on PS-exposing platelets, prothrombin is cleaved into active thrombin by FXa (Kamath, *et al.* 2008; Tracy, *et al.* 1985). Although the ability of the platelets to support thrombin generation is

well characterized, the fate and distribution of thrombin following formation remains unclear. Further, the majority of studies on the prothrombinase complex have been performed in purified systems, requiring additional analysis on how these reactions occur in the dynamic environment of flowing blood. Studies in Chapter 4 utilize a novel method of thrombus formation under flow to investigate the role of platelets and fibrin(ogen) in supporting the binding of coagulation factors FXa, prothrombin, and thrombin on clots.

In order to evaluate the role of thrombin and other hemostatic components in thrombus formation, many animal models have been employed. These models utilize a variety of animals (mouse, rat, baboon, etc.) to induce thrombi in diverse vasculature beds from large arteries to small capillaries (Bodary, *et al.* 2009). Together with animal models, a validated *ex vivo* model of thrombus formation is needed. Chapter 5 describes the development of an *ex vivo* model of occlusive thrombus formation.

While the key triggers for thrombus formation in healthy individuals are the exposure of ECM proteins and TF, which lead to thrombin generation, the thrombotic complications associated with disease states are mediated by often ill-defined pathways. In metastatic cancer, cells migrate from the primary tumor into the vasculature to invade new tissues (Chiang, *et al.* 2008). Tumor cells have been shown to express procoagulant molecules, including TF (Zhou, *et al.* 1998), therefore, in Chapter 6, the ability of tumor cells to promote coagulation and occlusive thrombus formation is investigated.

The studies outlined in Chapters 3-6 provide new insights into the process of thrombus formation and the role of thrombin in hemostasis and thrombosis. In Chapter 7, the key findings from my thesis research are summarized and areas of interest for future work are highlighted.

Chapter 2: Common Materials and Methods

2.1 Ethical Considerations

Studies in this thesis were conducted using blood from both human and murine sources. All human donors were healthy and gave full informed consent in accordance with the Declaration of Helsinki. Experiments using human donors were performed under approval of the Oregon Health & Science University Institutional Review Board or the Medical Ethics Committee of Maastricht University (Chapter 4). All animal experiments were conducted under approval of the Oregon Health & Science University or the Maastricht University (Chapter 4) Institutional Animal Care and Use Committees. Animals were maintained using housing and husbandry in accordance with local and national legal regulations.

2.2 Collection of Human Blood and Preparation of Blood Cells or Plasma

2.2.1 Blood collection

Human venous blood was drawn by venipuncture from healthy male or female volunteers, age 18 or older, who had been aspirin-free for at least two weeks prior. Blood was collected into an anticoagulated syringe. The anticoagulant used was varied based upon the experimental procedure.

2.2.2 Platelet preparation

Blood was drawn into a one-tenth volume of sodium citrate (3.8% w/v). Acid citrate dextrose (ACD; 85 mmol/L sodium citrate, 111 mmol/L glucose, 78 mmol/L citric acid) was added to freshly drawn blood at a one-tenth volume. Blood was transferred to polypropylene tubes and platelet-rich plasma (PRP) was prepared by centrifugation at 200*g* for 20 minutes. Platelets were isolated from PRP by centrifugation at 1000*g* for 10 minutes in the presence of prostacyclin (0.1 µg/mL, Cayman Chemical; Ann Arbor, MI). Platelet pellets were gently resuspended in Tyrodes buffer (129 mmol/L NaCl, 0.34 mmol/L Na_2HPO_4, 2.9 mmol/L KCl, 12 mmol/L $NaHCO_3$, 20 mmol/L HEPES, 5 mmol/L glucose, 1 mmol/L $MgCl_2$; pH 7.3) containing prostacyclin (0.1 µg/mL) and a one-tenth volume of ACD. Platelets were washed again by centrifugation at 1000*g* for 10 minutes and resuspended in Tyrodes buffer. Platelet concentration was determined with a hemacytometer and adjusted to the desired concentration with Tyrodes buffer.

2.2.3 Red blood cell preparation

Red blood cells (RBCs) were isolated following the initial centrifugation of whole blood for platelet preparation procedures (200*g* for 20 minutes). Following removal of PRP, RBCs were pelleted by centrifugation at 2000*g* for 10 minutes, and then washed (3×) with RBC buffer (10 mmol/L HEPES, 14 mmol/L NaCl, 5 mmol/L glucose; pH 7.4).

2.2.4 Platelet-poor plasma preparation

Blood was drawn into a one-tenth volume of sodium citrate (3.2% w/v) and transferred to polypropylene tubes. Plasma was separated from blood components by centrifugation of

citrated whole blood at 2150*g* for 10 minutes. Plasma was considered platelet-poor after two consecutive centrifugation steps at 2150*g*. Platelet-poor plasma (PPP) from three donors was pooled and stored frozen at -80°C until use.

2.3 Flow Assays

The interactions involved in hemostasis occur in the dynamic, actively changing environment of flowing blood. Vessels experience a variety of forces, with wall shear stresses ranging from 10-70 dynes/cm^2 in arteries and 1-6 dynes/cm^2 in veins, corresponding to shear rates of 260-1800 s^{-1} and 30-160 s^{-1}, respectively (Kroll, *et al.* 1996; Lipowsky, *et al.* 1978; Lipowsky, *et al.* 1980; Papaioannou, *et al.* 2005). Accounting for the effects of flow and shear stress allows for more thorough characterization of the interactions involved in hemostasis. To recreate the shear stresses experienced in vessels, flow systems with rectangular perfusion chambers have been designed (Doroszewski, *et al.* 1977; Forrester, *et al.* 1984; Lawrence, *et al.* 1987). Under the simplifying assumptions that flow is laminar and steady state, velocity is unidirectional and fully developed, the width of the chamber is much greater than the height, and the fluid is Newtonian (a reasonable assumption for blood at shear rates over 100s^{-1} (Katritsis, *et al.* 2007)), wall shear stress through a rectangular chamber can be calculated by the following equation:

$$\text{(2.1):} \quad \tau_w = \frac{6\mu Q}{wh^2}$$

where τ_w is the shear stress at the wall, μ is the fluid viscosity, Q is the volumetric flow rate, and w and h are the dimensions of the chamber (width and height). The wall shear rate (γ_w) is proportional to the shear stress:

$$\gamma_w = \frac{\tau_w}{\mu} \quad (2.2)$$

Based upon the dimensions of the rectangular chamber and the viscosity of blood (approximated as 0.04 Poise (Kroll, *et al.* 1996)), the volumetric flowrate can be adjusted to create physiological levels of shear in the chamber.

2.3.1 Cell-protein interactions under flow

For flow perfusion assays designed to assess the interactions of cells (platelets) with proteins under flow, rectangular chambers (0.2 mm × 2.0 × mm × 50 mm glass capillaries; VitroCom, Mountain Lakes, NJ) were coated with proteins of interest for 1 hour at room temperature. Following washing with phosphate buffered saline (PBS), capillaries were treated with denatured bovine serum albumin (BSA, 5 mg/mL in PBS) for 1 hour at room temperature to prevent non-specific interactions. After a second wash with PBS, the capillary was inserted into a silicone tubing system and mounted on the stage of an inverted microscope. The silicone tubing connected a fluid reservoir (for buffer or blood) to the capillary to a syringe on a syringe pump (Figure 2.1). The syringe pump pulled fluid through the tubing lines and into the capillary. The tubing lines were primed with Tyrodes buffer, then blood was pulled by the syringe pump at the appropriate volumetric flow rate to yield the desired wall shear stress. Following blood perfusion, the system was perfused with additional Tyrodes buffer to wash out unbound

blood cells and proteins. Images were obtained during or after perfusion to assess interactions and adhesion under flow.

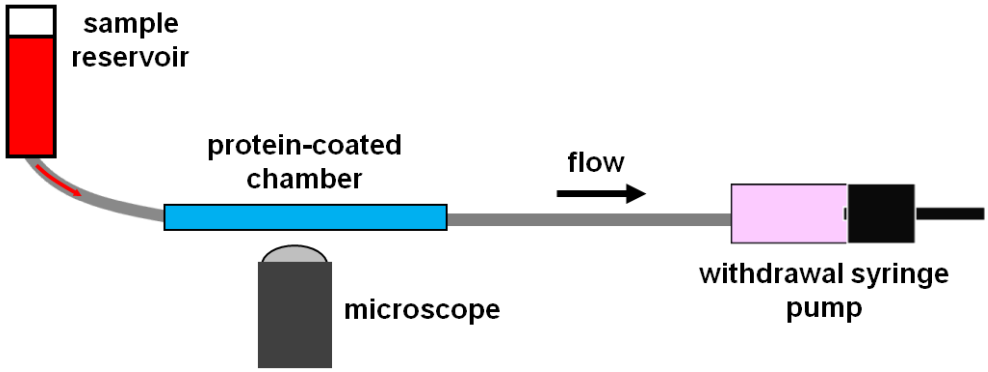

Figure 2.1. Schematic of the flow system. Anticoagulated whole blood or reconstituted blood (washed platelets and RBCs) are added to a sample reservoir. The blood sample is pulled through a protein-coated chamber at desired shear conditions with a syringe pump. The flow chamber is mounted above a microscope for imaging of platelet interactions and aggregate formation during and after perfusion.

2.3.2 Whole blood perfusion with coagulation

In order to evaluate the impact of coagulation on cell-protein interactions under shear flow, we developed an experimental model of thrombus formation in the presence of coagulation under flow. Rectangular chambers were coated in the same manner as above, input into a silicone tubing system, and mounted on the microscope stage. Two syringe pumps were utilized to perfuse fluids into the capillary (Figure 2.2). Effluent from the capillary exit was collected into a waste container. Sodium citrate anticoagulated whole blood (0.38 % w/v sodium citrate final) was co-perfused with recalcification buffer (Tyrodes buffer containing 75 mmol/L $CaCl_2$, 37.5 mmol/L $MgCl_2$, and 50 pmol/L tissue factor) at a 10:1 ratio. The fluids mixed immediately before entry into the chamber, allowing coagulation to occur.

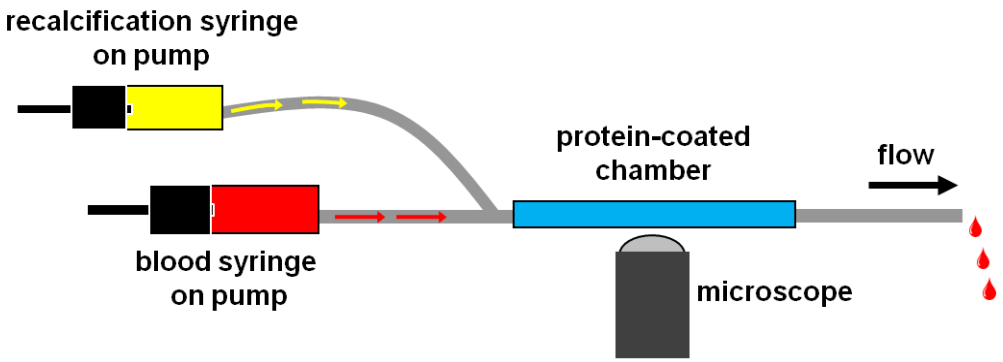

Figure 2.2. Schematic of the coagulation flow system. Two syringe pumps co-perfused sodium citrate-anticoagulated whole blood with recalcification buffer ($CaCl_2$/$MgCl_2$/TF) to trigger coagulation in the protein-coated perfusion chamber. To monitor platelet adhesion, fibrin formation, and thrombus formation, the perfusion chamber was mounted above a microscope.

2.4 Common Reagents

Unless otherwise specified, reagents used for blood collection, preparation of blood components, or for flow chamber assays were from Sigma-Aldrich (St. Louis, MO). Recombinant tissue factor (TF, Innovin) was purchased from Dade Behring (Marburg, Germany or Deerfield, IL) and fibrillar collagen was from Chrono-Log (Havertown, PA). The serine protease inhibitor D-phenylalanyl-L-prolyl-L-arginine chloromethyl ketone (PPACK) was purchased from Calbiochem (San Diego, CA).

2.4.1 Fluorescently labeled coagulation factors

To generate active-site, fluorescently labeled coagulation factors, human prothrombin, thrombin and FXa were purified from plasma and characterized by Dr. Paul Bock's laboratory (Bock 1992; Panizzi, *et al.* 2006) or purchased from commercial sources (Haematologic Technologies Inc, Essex Junction, VT). Purified factors were active-site labeled with N^{a}- [(acetylthio)acetyl]-D-Phe-Pro-Arg chloromethyl ketone, followed by mild treatment with NH_2OH and reaction of the thiol generated with 5- (and 6)-

iodoacetamido-2′,7′-difluorofluorescein (OG488-iodoacetamide) (Bock 1992; Panizzi, *et al.* 2006). It was confirmed that all active-site labeled factors lacked protease activity, but retained normal binding properties (Bock 1992; Panizzi, *et al.* 2006).

Chapter 3: Thrombin Mutant W215A/E217A Acts as a Platelet GPIb Antagonist

Michelle A. Berny, Tara C. White, Erik I. Tucker, Leslie A. Bush-Pelc, Enrico Di Cera, András Gruber, Owen J.T. McCarty

3.1 Abstract

Thrombin containing the mutations Trp215Ala and Glu217Ala (WE) selectively activates protein C and has potent antithrombotic effects in primates. The aim of this study was to delineate the molecular mechanism of direct WE-platelet interactions under static and shear conditions. Purified platelets under static conditions bound and spread on immobilized wild-type but not WE thrombin. In PPACK-anticoagulated blood under shear flow conditions, platelets tethered and rolled on both wild-type and WE thrombin, and these interactions were abrogated by the presence of a glycoprotein Ib (GPIb)-blocking antibody. Platelet deposition on collagen was blocked in the presence of WE, but not wild-type thrombin or prothrombin. WE also abrogated platelet tethering and rolling on immobilized von Willebrand factor in whole blood under shear flow. These observations demonstrate that the thrombin mutant WE, while not activating platelets, retains the ability to interact with platelets through GPIb, and inhibits GPIb-dependent binding to von Willebrand factor-collagen under shear.

This work was originally published by Wolters Kluwer Health
Arteriosclerosis, Thrombosis, and Vascular Biology 2008; Volume 28, Pages: 329-334
Reprinted with permission

3.2 Introduction

Studies conducted in this thesis were designed to investigate the role of thrombin in thrombus formation under flow. As platelets are a critical thrombus component, we first aimed to characterize interactions between platelets and thrombin in the presence of shear. In solution, thrombin can interact with platelets through the PARs and the GPIb/IX/V complex, but the ability of the anticoagulant thrombin mutant, WE, to interact with platelets remains to be determined. Here, we demonstrate that GPIb mediates thrombin-platelet and WE-platelet interactions under flow, and provide evidence that WE can antagonize the binding of GPIb to vWF.

3.3 Background

The serine protease thrombin plays a central role in thrombosis and hemostasis. During clot formation *in vivo*, thrombin generation by factor Xa from prothrombin is localized to the surface of activated platelets. Additionally, thrombin stimulates its own generation through the activation of factor XI and the cofactors V and VIII, leading to rampant thrombin generation in the presence of activated platelets. The primary procoagulant functions of thrombin are the cleavage of soluble fibrinogen to insoluble fibrin and the activation of platelets via cleavage of protease-activated receptors (PARs), resulting in platelet cytoskeletal reorganization events critical to thrombus stability. Thrombin binds to the platelet receptor GPIbα (CD42b), the major platelet receptor for von Willebrand

factor (vWF) that is required for normal hemostasis (Andrews, *et al.* 2004). Thrombin has also been shown to proteolytically inactivate ADAMTS13, a reprolysin-like metalloprotease that inactivates large multimeric forms of vWF, which is crucial for shear-dependent platelet aggregation during hemostasis and thrombosis (Jackson 2007).

In the presence of thrombomodulin, however, thrombin acts as an indirect anticoagulant through the enzymatic activation of protein C. Activated protein C (APC) in turn inactivates factors Va and VIIIa, resulting in the downregulation of thrombin generation (Dahlback, *et al.* 2005). Thrombin thus orchestrates a series of site-specific procoagulant and anticoagulant events that result in hemostatic plug formation at the site of a breech in the vasculature, while preventing intravascular expansion of the hemostatic process, thus preserving vessel patency.

A comprehensive library of Ala mutants was recently used to map the thrombin epitopes recognizing fibrinogen, protein C, and thrombomodulin, to identify residues that contribute differentially to the procoagulant and anticoagulant functions of thrombin (Di Cera, *et al.* 2007; Xu, *et al.* 2005). As Trp215 and Glu217 participate in fibrinogen recognition via distinct interactions, the double mutant thrombin W215A/E217A (WE) was rationally engineered through the combination of mutations around the active site that individually reduce fibrinogen binding but not protein C activation (Cantwell, *et al.* 2000). The mutant has drastically reduced (3 to 5 orders of magnitude) catalytic activity toward fibrinogen and PAR-1; however, in the presence of thrombomodulin, the activity of WE toward protein C is restored to 10% of the wild-type thrombin (Pineda, *et al.*

2004). Recent studies have shown that infusion of low doses of WE elicited safe and potent antithrombotic effects in a baboon model of platelet-dependent thrombosis (Gruber, *et al.* 2002; Gruber, *et al.* 2007). The unexpected finding from this study was that the lowest dose of WE, which produced no significant systemic anticoagulation and only a 5-fold baseline increase in circulating APC levels, was markedly more antithrombotic than infusion of exogenous APC producing detectable anticoagulation and a 9-fold baseline APC level increase. Moreover, a disproportionately high level of radiolabeled WE was detected in the thrombus. Collectively, these data suggest that the platelet-rich thrombus is capable of effectively capturing and immobilizing WE, thereby providing a possible mechanism for increased local activity via APC generation or other antithrombotic mechanisms on the thrombus surface. Thus, the goal of current study was to elucidate the molecular mechanisms mediating WE-platelet interactions under shear flow conditions that can occur on the intraluminal surface of thrombi. Our studies have demonstrated that the thrombin mutant WE, while not activating platelets, retains the ability to interact with platelets through GPIb. Furthermore, WE inhibits GPIb-dependent platelet deposition on thrombin, aggregation on collagen, and rolling on immobilized vWF under shear, suggesting that WE may act as a platelet GPIb-vWF antagonist in addition to selectively activating protein C.

3.4 Materials and Methods

3.4.1 Reagents

The recombinant human thrombin mutants Trp215Ala/Glu217Ala (WE), Thr172Tyr/Glu217Ala (TW), Thr172Tyr/Trp215Ala/Glu217Ala (TWE), and Ser195Ala

(S195A) were expressed, purified, and tested by Dr. Enrico Di Cera's laboratory (Ayala, *et al.* 2001; Cantwell, *et al.* 2000; Di Cera, *et al.* 2001; Krem, *et al.* 2003). Thrombin mutants were concentrated to 10 mg/mL in 50 mmol/L choline chloride, 20 mmol/L 2-(N-morpholino)ethanesulfonic acid (MES), pH 6.0. It is noteworthy that presence of diluent (1:500; corresponding to 20 µg/mL thrombin mutant) alone did not affect platelet function in any of the assays tested. vWF was a kind gift from Dr. Michael Berndt (Monash University, Clayton, Australia). The anti-GPIb monoclonal antibody (mAb) 6D1 was a generous gift from Dr. Barry Coller (Rockefeller University, New York, NY), and the anti-GPIb mAb SZ2 was purchased from Beckman Coulter (Fullerton, CA). Prothrombin and fibrinogen were purchased from Enzyme Research Laboratories (South Bend, IN). Chinese hamster ovary (CHO) cells stably expressing the platelet glycoprotein (GP) Ib-IX complex (CHOαβIX cells) or only GP Ibβ and IX (CHOβIX cells) (Dong, *et al.* 2001) were kind gifts from Dr. José López (Puget Sound Blood Center, Seattle, WA). Wild-type thrombin and all other reagents were from Sigma-Aldrich (St. Louis, MO).

3.4.2 Platelet preparation from Rac1 or WAVE-1 deficient mice

Mice deficient in Rac1 or Wiskott-Aldrich syndrome protein (WASP)-family verprolin-homologous protein (WAVE-1) were kindly donated by Drs. Laura Machesky (The Beatson Institute for Cancer Research, UK) and Steve Watson (University of Birmingham, UK) and Victor Tybulewicz (National Institute for Medical Research, UK) (Calaminus, *et al.* 2007; Dahl, *et al.* 2003; McCarty, *et al.* 2005; Walmsley, *et al.* 2003; Zambrowicz, *et al.* 1998). Animals were euthanized and blood was drawn by cardiac puncture into a one-tenth volume of ACD. PRP was prepared by centrifugation at 200*g*

for 6 minutes. Mouse platelets were isolated from PRP by centrifugation at 1000*g* for 6 minutes in the presence of prostacyclin (0.1 µg/mL). Platelet pellets were gently resuspended in Tyrodes buffer (described in Section 2.2.2) containing prostacyclin and a one-tenth volume of ACD, then washed by centrifugation at 1000*g* for 6 minutes. Washed mouse platelets were resuspended to the desired concentration in Tyrodes buffer.

3.4.3 Platelet static and flow adhesion assays

Glass coverslips were incubated with a solution of wild-type or mutant thrombin (50 µg/mL), prothrombin (50 µg/mL), fibrillar collagen (100 µg/mL), fibrinogen (50 µg/mL), or vWF (50 µg/mL) overnight at 4°C. Surfaces were then blocked with denatured BSA (5 mg/mL) for 1 hour followed by washing with PBS before use in adhesion assays.

For static spreading experiments, washed platelets (2×10^7/mL) were incubated on protein-coated coverslips at 37°C for 45 minutes, followed by washing with modified Tyrodes buffer to remove unbound cells (McCarty, *et al.* 2005; McCarty, *et al.* 2004). Platelet spreading was imaged using Köhler illuminated Nomarski differential interference contrast (DIC) optics with a Zeiss 63× oil immersion 1.40 NA plan-apochromat lens on a Zeiss Axiovert 200M microscope (Carl Zeiss; Jena, Germany) and recorded using Stallion 4.0 (Intelligent Imaging Innovations Inc; Denver, CO). The degree of adhesion and surface area coverage was computed using Image J software (McCarty, *et al.* 2005; McCarty, *et al.* 2004).

For flow adhesion assays, protein-coated coverslips were assembled onto a flow chamber (Glyotech; Gaithersburg, Maryland) and mounted on the stage of an inverted microscope (Zeiss Axiovert 200M). In selected experiments, reconstituted blood (equal volumes washed platelets at 6×10^8/mL and red blood cells) or PPACK (40 μmol/L) anticoagulated whole blood was perfused through the chamber for 3 minutes at wall shear rates of 300 to 1000 s^{-1}, and imaged using DIC microscopy in both real-time and after washing with Tyrodes buffer. The number of tethering and rolling platelets was determined off-line by reviewing the real-time videos (McCarty, *et al.* 2005; McCarty, *et al.* 2004).

3.4.4 Analysis of data

For paired data, statistical significance between means was determined by the paired Student's t-test. Statistical significance of differences between means for 3 or more conditions was determined by ANOVA. If means were shown to be significantly different, multiple comparisons were performed by the Tukey test. Probability values of $P<0.01$ were selected to be statistically significant.

3.5 Results

3.5.1 Molecular mechanisms of platelet cytoskeletal reorganization on thrombin-coated surfaces

To characterize the molecular basis of platelet-thrombin interactions, we gently pipetted purified platelets over surface immobilized thrombin and monitored platelet morphology using Nomarski DIC microscopy. To assess the direct ability of thrombin to support platelet binding, these experiments were performed in the presence of apyrase and

indomethacin, inhibitors of the secondary mediators ADP and thromboxane A2 (TxA_2), respectively. Consistent with our previous reports (Thornber, *et al.* 2006), immobilized thrombin supported human platelet adhesion and lamellipodia formation (Figure 3.1). In light of the fact that thrombin has been shown to induce robust activation of the small GTPase Rac1 in platelets (McCarty, *et al.* 2005), we aimed to investigate the role of Rac1 in mediating platelet spreading on immobilized thrombin. As shown in Figure 3.1, immobilized thrombin supported wild-type murine platelet adhesion and activation, as evidenced by generation of filopodia and full lamellipodia. Strikingly, lamellipodia formation was abolished in Rac1-deficient platelets on thrombin, although Rac1–/– platelets retained the ability to form filopodia. In contrast, full lamellipodia formation was observed in the absence of the actin scaffolding protein WAVE-1 (Figure 3.1). The presence of the actin polymerization-inhibitor cytochalasin D abrogated filopodia and lamellipodia formation for wild-type, Rac1–/–, and WAVE-1–/– platelets on thrombin.

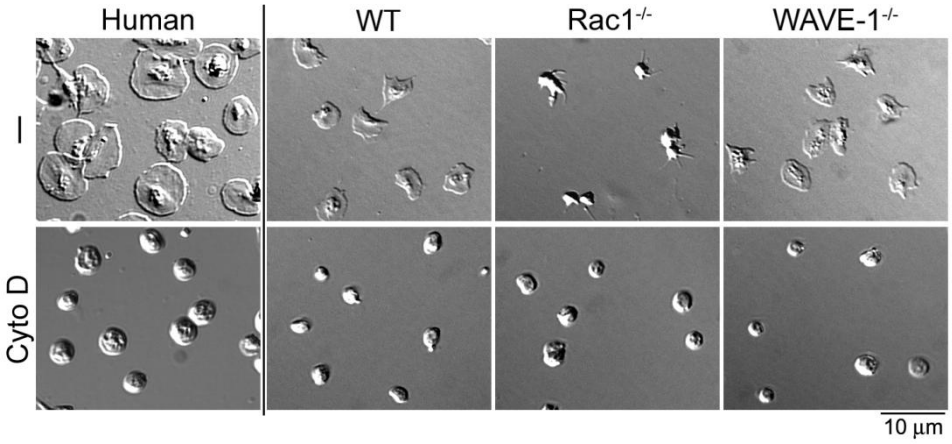

Figure 3.1. The role of Rac1 and WAVE-1 on spreading of platelets on immobilized thrombin. Washed human platelets (2×10^7/mL) or murine platelets (2×10^7/mL) from wild-type, Rac1–/–, or WAVE-1–/– mice were placed on thrombin coated coverslips for 45 minutes at 37°C and imaged using DIC microscopy. Experiments were performed in the absence or presence of the actin-polymerization inhibitor cytochalasin D (Cyto D; 10 µmol/L). Images are representative of at least 3 experiments. These data were produced by Owen McCarty.

We next investigated the role of proteolysis in platelet adhesion to immobilized thrombin. Our results demonstrate that platelet adhesion and activation were abrogated in the presence of PPACK (40 μmol/L), which blocks the active site of thrombin (Figure 3.2). Similarly, platelets failed to adhere to surface-immobilized thrombin Na^+-binding site mutants WE, TW, or TWE (Figure 3.2). Platelets also failed to bind to the active site mutant S195A, which has been shown to retain the Na^+-binding properties of wild-type thrombin (Krem, *et al.* 2003) or to surface-immobilized prothrombin or BSA (Figure 3.2). It is noteworthy that the presence of WE in solution did not affect the degree of platelet adhesion to immobilized thrombin, collagen or fibrinogen under static conditions (Table 3.1). Moreover, both the rate and extent of thrombin-induced platelet aggregation was unaffected by the presence of WE.

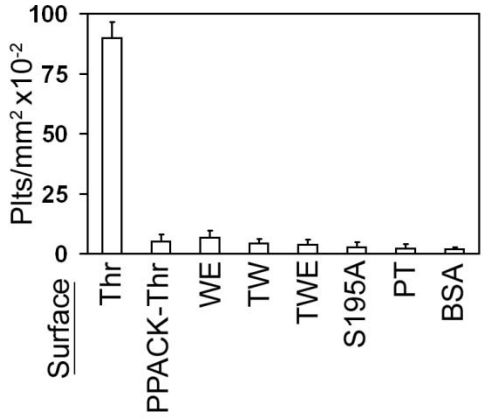

Figure 3.2. Platelet binding to wild-type or mutant thrombin. Washed human platelets (2×10^7/mL) were placed on coverslips coated with either thrombin (Thr), PPACK-treated thrombin, WE, TW, TWE, S195A, prothrombin (PT), or BSA for 45 minutes at 37°C, and imaged using DIC microscopy. The number of adherent platelets were recorded for 3 fields of view (0.013 mm^2) and expressed as mean ± SEM from at least 3 experiments.

Taken together, our data show that Rac1, but not WAVE-1, is required for regulating platelet lamellipodia formation on thrombin, and that this mechanism is not activated by immobilized WE.

Table 3.1. Effects of WE on platelet binding to immobilized ligands.

Surface	Solution Treatment	Platelet adhesion (cells/mm^2 × 10^{-2})	P-value
BSA	—	5.6 ± 1.7	—
thrombin	—	60.0 ± 8.3	P = 0.17
thrombin	WE	51.3 ± 7.1	
collagen	—	61.1 ± 5.4	P = 0.44
collagen	WE	54.1 ± 4.1	
FG	—	90.1 ± 5.5	P = 0.40
FG	WE	84.5 ± 1.1	

Purified human platelets (2×10^7/ml) were placed on BSA, thrombin, collagen, or fibrinogen-coated coverslips for 45 minutes at 37°C. In designated experiments, washed platelets were resuspended in buffer containing vehicle or exogenously added WE (20 μg/ml) in the presence of the ADP-scavenger apyrase (2 U/mL) and TxA_2 inhibitor indomethacin (10 μmol/L) prior to exposure to the protein surface. Adherent platelets are reported as mean ± SEM of 3-6 experiments. Reported P-values compare adhesion in the absence or presence of WE.

3.5.2 Platelet interactions with immobilized thrombin under flow

We investigated thrombin-platelet interactions under shear stress that better characterized the microenvironment of thrombus formation in the intraluminal boundary layer of blood flow. We assessed platelet adhesion and aggregation after perfusion of reconstituted blood over immobilized thrombin at a shear rate of 300 s^{-1}. Tightly-packed platelet aggregates (33.5 ± 1.3 aggregates/mm^2 × 10^{-2}) consisting of 10 to 50 platelets were seen on thrombin after perfusion of reconstituted blood for 3 minutes (Figure 3.3A). These platelet aggregates were stable and we did not observe a significant level of embolization. In accord with previous reports (Weeterings, *et al.* 2006), platelet aggregation on thrombin was significantly reduced in the presence of the blocking anti-GPIb mAb SZ2 (20 μg/mL), resulting in 46.4 ± 1.3 aggregates/mm^2 × 10^{-2} consisting of 1 to 5 platelets

(Figure 3.3B). Interestingly, platelet aggregation on immobilized thrombin in the presence of exogenously added WE (20 µg/mL) was reduced to a similar degree as was observed in the presence of SZ2, resulting in 45.9 ± 1.4 aggregates/mm^2 × 10^{-2} consisting of 1 to 5 platelets (Figure 3.3C). This was further evidenced by a reduction in the percentage of platelet aggregate surface coverage on thrombin in the presence of WE (58.5 ± 4.2% versus 16.8 ± 3.6% surface coverage on thrombin in the presence of vehicle or WE, respectively). Minimal platelet adhesion was observed on thrombin in the presence of PPACK (Figure 3.3D), whereas platelets failed to firmly adhere on WE, S195A, prothrombin, or BSA under flow (Figure 3.3E-H).

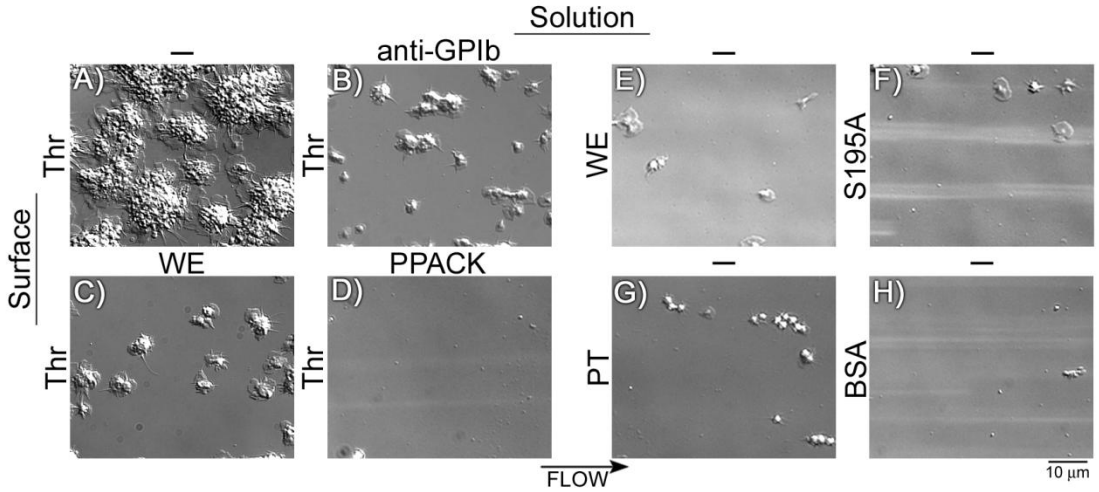

Figure 3.3. Platelet adhesion to wild-type or mutant thrombin under flow. Reconstituted human blood was perfused at a shear rate of 300s^{-1} for 3 minutes over thrombin-coated slides in the presence of vehicle (A), the blocking GPIb mAb SZ2 (B), exogenously added WE (C), or PPACK (D). In separate experiments, reconstituted blood was perfused over immobilized WE (E), S195A (F), prothrombin (G), or BSA (H). Images are representative of at least 3 experiments. David Kyle Robinson from the McCarty laboratory assisted in generating these data.

As activation of platelets is not mandatory for GPIb-mediated binding to ligands such as vWF (Nesbitt, *et al.* 2002), we aimed to investigate whether inactive thrombin, which failed to support firm adhesion (Figure 3.3D), retained the ability to support GPIb-mediated events. We perfused PPACK-anticoagulated whole blood over immobilized

thrombin and monitored platelet interactions under shear flow conditions in real-time using DIC microscopy. Platelet tethering and rolling was observed on immobilized wild-type thrombin in whole blood (Figure 3.4A,B). Furthermore, platelet tethering and rolling was observed on WE thrombin, although to a lesser extent than compared with wild-type thrombin (Figure 3.4C). Platelets failed to arrest and adhere on wild-type or WE thrombin in the presence of PPACK, suggesting that a proteolytic event was required for platelet firm adhesion. The presence of either the function-blocking anti-GPIb mAb SZ2 or exogenously added WE (20 μg/mL) in solution abrogated platelet interactions on both wild-type and WE thrombin (Figure 3.4). In contrast, the presence of vehicle, wild-type thrombin, or prothrombin (20 μg/mL) in solution did not affect the extent of platelet tethering and rolling. Platelets failed to interact with immobilized prothrombin or BSA.

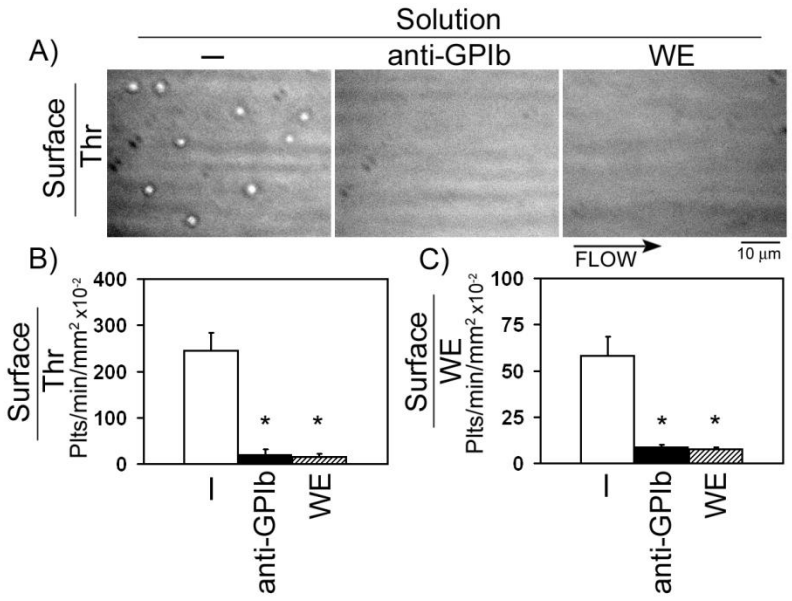

Figure 3.4. The platelet receptor GPIb interacts with thrombin and WE under flow. Human whole blood anticoagulated with PPACK was perfused over immobilized wild-type thrombin or WE at a shear rate of 300 s^{-1} for 3 minutes. A, Representative micrographs of platelet tethering on wild-type thrombin in the presence of vehicle, the blocking GPIb mAb SZ2, or WE (20 μg/mL) are shown. The cumulative number of tethering platelets on wild-type thrombin (B) or WE (C) was recorded for a single field of view (0.013 mm^2) for 30 seconds and expressed as mean ± SEM from at least 3 experiments. *P<0.01 with respect to vehicle. Madeline Midgett from the McCarty laboratory performed experiments to generate data in panel C.

To assess the ability of WE to bind to GPIbα, radiolabeled WE thrombin (^{125}I-WE) was incubated with CHOαβIX cells expressing GPIbα (and GPIbβ and GPIX to facilitate GPIbα expression). Our data show that GPIbα-expressing CHO cells bound 2.1-fold more ^{125}I-WE as compared with CHOβIX cells, which lack GPIbα (Figure 3.5). Moreover, ^{125}I-WE binding to CHOαβIX cells was reduced by nearly 50% in the presence of the anti-GPIb mAb SZ2. CHOαβIX cells supported 6.4-fold more binding of ^{125}I-WE relative to ^{125}I-BSA. Additionally, CHOαβIX cells were observed to tether and roll when perfused over immobilized WE at a shear rate of 150 s^{-1}, and this rolling was inhibited by the presence of the anti-GPIb mAb SZ2. Overall, our data demonstrate that WE, although unable to support PAR-dependent platelet activation, retains the ability to bind GPIb, supports GPIb-dependent platelet rolling, and inhibits GPIb-dependent platelet tethering on thrombin under flow conditions that are typical of the intravascular environment.

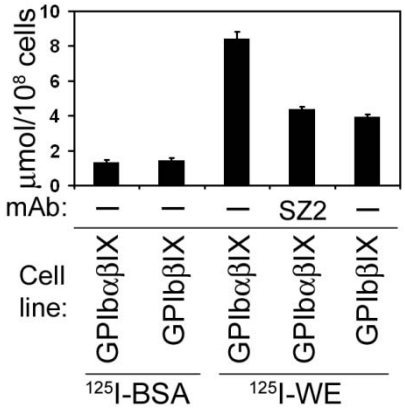

Figure 3.5. Characterization of WE binding to GPIbα. WE thrombin and BSA were radiolabeled with ^{125}I (^{125}I-WE, 0.37 µCi [10 kBq]/µg; ^{125}I-BSA, 1.15 µCi [10 kBq]/µg, >85% protein bound after dialysis). 300 µl of 1×10^6 CHOαβIX cells/ml (which express GPIbα) or CHOβIX cells (which lack GPIbα) in HBSS were incubated for 30 min with 15 µg/ml ^{125}I-WE or ^{125}I-BSA in the absence or presence of the anti-GPIb mAb SZ2 (20 µg/ml). Radiolabeled WE and BSA retention was determined and expressed as µmol of radiolabeled protein bound per 1×10^8 cells. Experiments were performed by Owen McCarty with assistance from Sawan Hurst from András Gruber's laboratory.

3.5.3 The thrombin mutant WE inhibits platelet adhesion to collagen and rolling on vWF under flow conditions

It is well established that GPIb plays an essential role in mediating platelet aggregate formation on immobilized collagen under shear flow (Kulkarni, *et al.* 2000; Yuan, *et al.* 1999). In accord with these reports, our data demonstrate that perfusion of PPACK-anticoagulated whole blood over collagen resulted in substantial platelet aggregate formation on collagen fibers at a shear rate of 1000 s^{-1} (Figure 3.6Ai), whereas platelet adhesion and aggregation was severely reduced in the presence of the GPIb mAb 6D1 (Figure 3.6Aii). Strikingly, the presence of WE in solution also inhibited platelet deposition on collagen (Figure 3.6Aiii) in a dose-dependent manner with an IC_{50} of 7.98 µg/mL (Figure 3.6B). In contrast, the presence of vehicle, wild-type thrombin (20 µg/mL), S195A (20 µg/mL), or prothrombin (20 µg/mL) did not reduce platelet aggregate formation on collagen (Figure 3.6Aiv-vi).

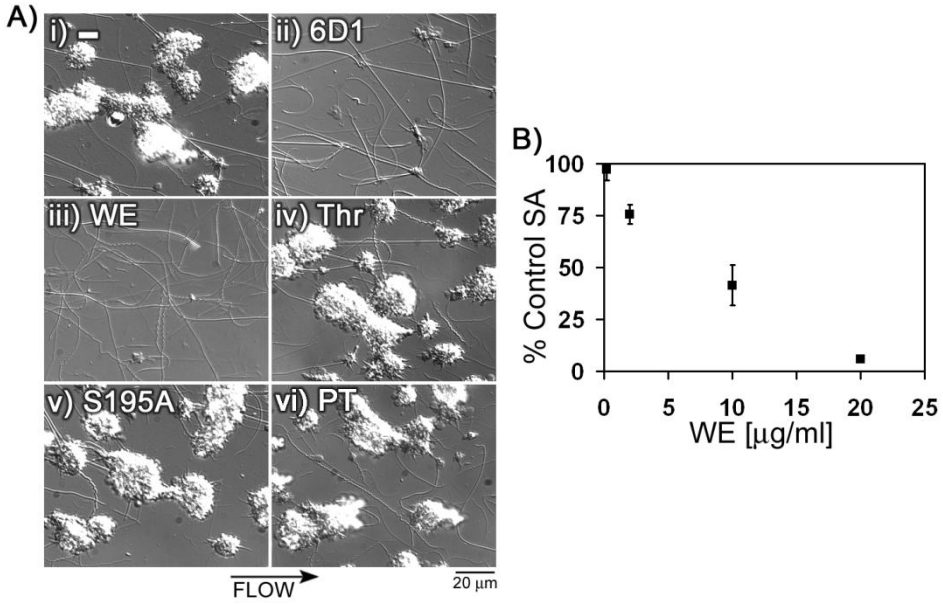

Figure 3.6. The thrombin mutant WE inhibits platelet adhesion on immobilized collagen under flow. Human whole blood anticoagulated with PPACK was perfused over collagen-coated slides at a shear rate of 1000 s^{-1} for 3 minutes. A, In selected experiments, whole blood was incubated with vehicle (i), the blocking GPIb mAb 6D1 (ii), WE (iii), wild-type thrombin (Thr, iv), S195A (v), or prothrombin (PT, vi) at a final concentration of 20 µg/mL. Images are representative of at least 3 experiments. B, Experiments were performed in the presence of varying concentrations of WE (0.2, 2, 10, 20 µg/mL). The surface coverage of adherent platelets was recorded for 3 fields of view (0.013 mm^2) and analyzed using ImageJ software. WE in solution inhibited platelet deposition on immobilized collagen in a dose-dependent manner with an IC_{50} of 7.98 µg/mL. Values are expressed as mean ± SEM from at least 3 experiments.

To determine the molecular mechanisms by which WE inhibits platelet aggregation on collagen under flow, we perfused PPACK-anticoagulated whole blood over immobilized vWF at a shear rate of 1000 s^{-1} and monitored platelet tethering and rolling in real-time with DIC microscopy. Our results show that platelets tethered and rolled on vWF under flow (Figure 3.7A), while the presence of the anti-GPIb mAb 6D1 dramatically reduced the degree of rolling platelets (Figure 3.7B). Importantly, the presence of WE in solution dramatically reduced the degree of platelet rolling on vWF (Figure 3.7AB). In contrast, the presence of vehicle, wild-type thrombin, S195A, or prothrombin had no effect on platelet-vWF interactions (Figure 3.7B). Taken together, our data suggest that WE acts as a potent platelet GPIb antagonist by blocking vWF-platelet binding under shear flow

conditions that typically occur at the blood-thrombus interface, whereas it does not appear to block platelet adhesion and activation in the absence of shear, which typically occurs in wound blood.

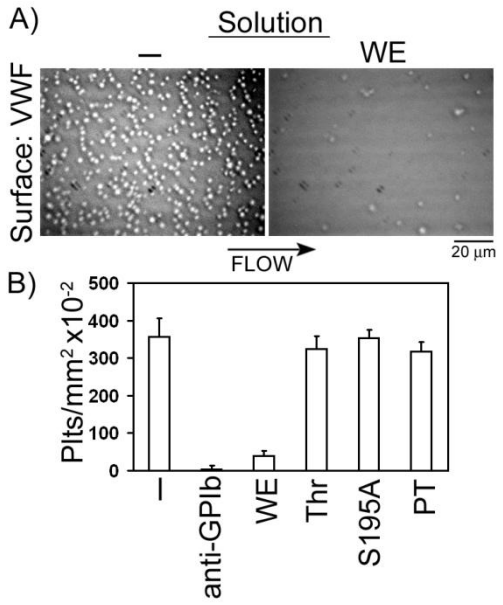

Figure 3.7. Evaluation of platelet rolling on immobilized vWF under flow. Human whole blood anticoagulated with PPACK was perfused over vWF-coated slides at a shear rate of 1000 s^{-1}. A, Representative micrographs of platelet tethering on vWF in the presence of vehicle or WE (20 μg/mL). B, In selected experiments, whole blood was incubated with either vehicle, the blocking GPIb mAb 6D1, WE, wild-type thrombin (Thr), S195A, or prothrombin (PT). The number of tethering platelets was recorded at a single time point for each field of view (0.013 mm^2) after 30 seconds of flow and expressed as mean ± SEM.

3.6 Discussion

The studies here provide insight into the molecular mechanisms that mediate WE-platelet interactions. Specifically, the data extend previous observations that GPIb serves as a ligand for thrombin (Weeterings, *et al.* 2006). Significantly, these studies reveal that WE, in addition to serving as a protein C activator, has the capability of functioning as a specific platelet GPIb-vWF antagonist.

The platelet receptor GPIb-IX-V consists of GPIbα disulfide-linked to GPIbβ, noncovalently complexed with GPIX and GPV in the ratio 2:2:2:1 (Jackson 2007). The 282 N-terminal residues of GPIbα contain binding sites for vWF, thrombin, and the coagulation factors XI and XIIa. The GPIbα leucine-rich region (LRR) 59 to 128 has been implicated in contributing to vWF binding (Shen, *et al.* 2006), whereas thrombin binding is centered around an anionic region containing 3 sulfated tyrosine residues (Tyr276, Tyr278, and Tyr279) (Dong, *et al.* 1994; Ward, *et al.* 1996).The thrombin binding site for GPIbα has been localized to thrombin exosite II. Functional assays revealed that residue Arg233 of exosite II is critical for GPIbα binding (De Cristofaro, *et al.* 2001; Yun, *et al.* 2003), whereas crystallography studies demonstrated that Arg233 makes contacts with several backbone oxygen atoms of the acidic region of GPIbα (Celikel, *et al.* 2003; Dumas, *et al.* 2003). Moreover, both crystal structures suggested that GPIbα might bind simultaneously to one thrombin molecule through exosite II and to vWF. Interestingly, both crystal structures revealed that thrombin exosite I binds GPIbα, thereby permitting two thrombin molecules to bind to a single GPIbα molecule, although the two studies differed markedly regarding their interpretation of this binding (Celikel, *et al.* 2003; Dumas, *et al.* 2003). It has been proposed that a conformational change in GPIbα is induced after thrombin exosite II binding, and that this conformational change permits a second thrombin molecule to bind, via exosite I, to a distinct location on GPIbα. Whether thrombin forms a dimer between two GPIbα molecules on the same platelet or bridges two GPIbα molecules on adjacent platelets has been debated (Sadler 2003), and is yet unknown.

Our studies suggest that WE specifically blocks GPIb binding to vWF, as evidenced by the ability of WE to inhibit GPIb-dependent platelet deposition on collagen and platelet rolling on vWF under shear flow. Pineda and colleagues have recently solved the x-ray crystal structure of WE, which revealed that the mutation of Trp215 and Glu217 resulted in a collapse of the 215 to 217 strand that crushes the primary specificity pocket (Pineda, *et al.* 2004). The collapse results from the abrogation of the stacking interaction between Phe227 and Trp215 and the polar interactions of Glu217 and Thr172 and Lys224. Other notable changes are a rotation of the carboxylate group of Asp189, breakage of the H-bond between the catalytic residues Ser195 and His57, breakage of the ion pair between Asp222 and Arg187, and significant disorder in the 186- and 220-loops that define the Na^+-binding site (Pineda, *et al.* 2004). Along these lines, it is possible that the ability of WE to block GPIb-mediated binding to vWF is attributable to steric hindrance resulting from the conformational modulation of thrombin-GPIbα binding due to the Trp215Ala and Glu217Ala mutations. In addition, it is important to note that, in contrast to the catalytically inactive forms of thrombin (PPACK-thrombin, S195A), WE retains the ability to cleave PAR receptors, albeit at a rate that is reduced 1000-fold compared with wild-type (Cantwell, *et al.* 2000). In light of the fact that it has been shown that thrombin binding to GPIbα facilitates PAR receptor cleavage and synergistic signaling (Soslau, *et al.* 2001), perhaps this dramatic increase in the residence time for the GPIb-WE-PAR receptor complex precludes the ability of vWF to bind to GPIb. This would explain why forms of thrombin which are unable to bind PAR receptors, such as S195A, fail to inhibit GPIb-vWF-mediated interactions. We do not at present know whether binding of WE to GPIb modifies the catalytic efficiency of WE toward protein C. Our findings, however,

raise the possibility that the platelet surface may act as a catalyst for local protein C activation by WE in the presence of intraluminal levels of shear that characterize the surface of non-occlusive thrombi in large vessels. Such a mechanism of local APC generation would explain the superb antithrombotic efficacy of low dose of WE observed *in vivo* (Gruber, *et al.* 2007).

In summary, the present study dissects the molecular mechanisms of mutant thrombin WE interactions with platelets. Specifically, in contrast to the Rac1-dependent platelet lamellipodia formed on wild-type thrombin, we show that WE is unable to support platelet adhesion or cytoskeletal reorganization. We demonstrate that WE is a ligand for the platelet receptor GPIb, and that the binding of WE, but not wild-type or active-site blocked thrombin, inhibits GPIb binding to vWF. The combination of GPIb-dependent local accumulation of WE under shear and generation of APC in conjunction with inhibition of GPIb-vWF binding would provide a mechanism for the surprising hemostatic safety and antithrombotic activity of the double mutant WE thrombin.

Chapter 4: Spatial Distribution of Factor Xa, Thrombin, and Fibrin(ogen) on Thrombi at Venous Shear

Michelle A. Berny, Imke C. A. Munnix, Jocelyn M. Auger, Saskia E. M. Schols, Judith M. E. M. Cosemans, Peter Panizzi, Paul E. Bock, Steve P. Watson, Owen J. T. McCarty, Johan W. M. Heemskerk

4.1 Abstract

The generation of thrombin is a critical process in the formation of venous thrombi. In isolated plasma under static conditions, phosphatidylserine (PS)-exposing platelets support coagulation factor activation and thrombin generation; however, their role in supporting coagulation factor binding under shear conditions remains unclear. We sought to determine where activated factor X (FXa), (pro)thrombin, and fibrin(ogen) are localized in thrombi formed under venous shear. Fluorescence microscopy was used to study the accumulation of platelets, FXa, (pro)thrombin, and fibrin(ogen) in thrombi formed *in vitro* and *in vivo*. Co-perfusion of human blood with tissue factor resulted in formation of visible fibrin at low, but not at high shear rate. At low shear, platelets demonstrated increased calcium signaling and PS exposure, and supported binding of FXa and prothrombin. However, once cleaved, (pro)thrombin was observed on fibrin fibers, covering the whole thrombus. *In vivo*, wild-type mice were injected with fluorescently labeled coagulation factors and venous thrombus formation was monitored

in mesenteric veins treated with $FeCl_3$. Thrombi formed *in vivo* consisted of platelet aggregates, focal spots of platelets binding FXa, and large areas binding (pro)thrombin and fibrin(ogen). FXa bound in a punctate manner to thrombi under shear, while thrombin and fibrin(ogen) distributed ubiquitously over platelet-fibrin thrombi. During thrombus formation under venous shear, thrombin may relocate from focal sites of formation (on FXa-binding platelets) to dispersed sites of action (on fibrin fibers).

This work was originally published by the Public Library of Science
PLoS ONE 2010; Volume 5, Number 4, Pages: e10415
Reprinted with permission

4.2 Introduction

The studies performed in Chapter 3 describe a critical role for the platelet surface receptor GPIb in thrombin-platelet interactions under flow. In coagulation, the platelet surface provides a platform for thrombin generation. By supporting association of FXa with the cofactor FVa, the platelet surface catalyzes prothrombin cleavage. Activated thrombin influences thrombus development, but how it is retained at the site of thrombus formation is unclear. To provide further insight into the contributions of thrombin to thrombus formation, experiments in Chapter 4 were designed to determine where FXa, prothrombin, thrombin are distributed on thrombi in the presence of shear. Data presented here suggest an important role for fibrin(ogen) in the recruitment of thrombin to thrombi.

4.3 Background

The application of microscopic imaging technologies to *in vivo* models of thrombus formation has provided new fundamental insight into the roles of platelets and

coagulation factors in the thrombus formation process (Furie, *et al.* 2005; Munnix, *et al.* 2007; Nesbitt, *et al.* 2009). These studies have challenged the traditional understanding that platelets control arterial thrombus formation, while the coagulation system is implicated in venous thrombosis, where shear rates are low. For instance, exposure of tissue factor (TF) and activation of TF-induced thrombin generation is now also considered to play a key role in thrombi formed in the arterial circulation (Dubois, *et al.* 2007; Kuijpers, *et al.* 2008). Conversely, platelets contribute to the thrombotic process in veins by responding to thrombin and then providing interaction and activation sites for coagulation factors (Butenas, *et al.* 2001). *In vitro* studies indicate that platelets mediate thrombin generation and coagulation by exposing phosphatidylserine (PS) on their membrane surface following prolonged increases in cytosolic calcium (Dachary-Prigent, *et al.* 1995; Leon, *et al.* 2004; Vanschoonbeek, *et al.* 2004). PS provides a binding surface for the assembly of the coagulation tenase and prothrombinase complexes, which convert factor X into activated factor X (FXa) and prothrombin into thrombin, respectively (Tracy, *et al.* 1985; Zwaal, *et al.* 1997). Through static experiments, the concept was developed that the amount and pattern of thrombin generation and, hence, of fibrin clot formation, is stringently controlled by platelets (Beguin, *et al.* 1997; Heemskerk, *et al.* 2002). In contrast, other studies have shown that the formation of fibrin is dependent upon the shear rate, with lower shear rates supporting more fibrin generation (Inauen, *et al.* 1990; Weiss, *et al.* 1986). Therefore, the role of procoagulant platelets in the regulation of thrombus formation under flow conditions is unclear. In the present paper, we utilized *in vitro* and *in vivo* approaches to evaluate the ability of PS-exposing platelets to support coagulation factor binding in thrombi formed under flow conditions.

4.4 Materials and Methods

4.4.1 Reagents

Alexa Fluor (AF) 647 and Oregon Green (OG488) labeled annexin A5, AF546 and OG488 labeled human fibrinogen, Fluo-4 acetoxymethyl ester (Fluo-4 AM) and labeled goat anti-rat antibody were from Invitrogen (Leiden, The Netherlands). Rat anti-mouse CD41 monoclonal antibody (mAb) and fluorescein isothiocyanate (FITC) labeled anti-CD61 mAb were from BD Biosciences (San Diego, CA). FITC-labeled anti-human fibrinogen antibody was from WAK Chemie (Steinbach, Germany) and the fibrin-specific mAb (anti-fibrin II β chain, clone T2G1) from Accurate Chemical & Scientific Corporation (Westbury, NY). Recombinant hirudin (Refludan) was purchased from Schering-Plough (Kenilworth, NJ). The fluorogenic thrombin substrate Z-Gly-Gly-Arg aminomethyl coumarin (Z-GGR-AMC) came from Bachem (Bubendorf, Switzerland), plasmin from Enzyme Research Laboratories (South Bend, IN), fibrinogen antiserum from MP Biomedicals (Irvine, CA) and purified human D-dimer from Cell Sciences (Canton, MA). Unlabeled wild-type annexin A5, with high-affinity binding to PS, and the quadruple-mutant, M1234 annexin A5, where all calcium-dependent binding sites were mutated to abolish binding to PS, were purchased from Nexins Research (Hoeven, The Netherlands). All other reagents were purchased from Sigma-Aldrich (St. Louis, MO).

4.4.2 Human whole blood platelet activation and thrombus formation under shear

Glass coverslips or capillaries were coated with fibrinogen (1 mg/mL) or fibrillar collagen (100 µg/mL) for 1 hour at room temperature. Coverslips were assembled into a parallel-plate flow chamber and mounted on the stage of an inverted fluorescence

microscope (Diaphot 200; Nikon; Tokyo, Japan) (Siljander, *et al.* 2004). As described in Section 2.3.3, citrate-anticoagulated human blood was perfused into the flow chamber via a pulse-free syringe pump. Coagulation was triggered with a second syringe pump, allowing co-perfusion at one-tenth of the main flow rate with $CaCl_2$/TF medium (75 mmol/L $CaCl_2$, 37.5 mmol/L $MgCl_2$ and 50 pmol/L TF). Blood perfusion rates were selected to result in initial wall shear rates of 200 s^{-1}, 500 s^{-1}, or 1000 s^{-1}; blood was perfused for a total of 15 minutes at all shear rates. Phase contrast and fluorescence images were recorded with a 40× oil immersion objective using 2 intensified CCD cameras controlled by Visitech software (Sunderland, UK) (Munnix, *et al.* 2007; Siljander, *et al.* 2004).

Changes in cytosolic calcium, $[Ca^{2+}]_i$, of adherent platelets were measured during whole blood perfusion. Washed platelets from acid citrate dextrose-anticoagulated blood were loaded with the calcium indicator Fluo-4 and added to citrate-anticoagulated blood from the same donor to yield 20% fluorescent platelets. During blood perfusion, fluorescence images were recorded at 4 frames per second. Using Visitech software, image series were analyzed for regions-of-interest representing one adherent platelet, to give changes in fluorescence (F) per cell. Pseudo-ratioing of F traces resulted in F/F_o curves, representing increases in single-cell fluorescence above baseline and corresponding to increases in intracellular calcium, $[Ca^{2+}]_i$ (Auger, *et al.* 2005).

Thrombi formed in flow chambers were labeled for 5 minutes with indicated OG488-conjugated coagulation factors (0.3-1 µmol/L) or antibodies (20 µg/mL) in combination

with AF647-annexin A5 (14 nmol/L). After washing with Tyrode-HEPES buffer (136 mmol/L NaCl, 2.7 mmol/L KCl, 10 mmol/L HEPES, 2 mmol/L $MgCl_2$, 2 mmol/L $CaCl_2$, 5.6 mmol/L glucose, 0.1% BSA, 1 U/mL heparin; pH 7.45) to remove unbound fluorescent probes, thrombi were imaged with a 60× oil objective and confocal laser scanning microscope using a BioRad-Zeiss 2100 multiphoton system (Munnix, *et al.* 2007). Control experiments were performed with heat-treated fluorescent probes, which did not incorporate into the thrombi. Single-color fluorescence scanning images were analyzed for fluorescence coverage, intensity, and distribution patterns with Image Pro software (Media Cybernetics, Silverspring, MD). The pixel overlap of two overlay images with different fluorescence colors (Pearson's correlation coefficient, R_r) was also calculated. This parameter is a value from −1 to +1, which describes the overlap between two colored patterns and is independent of pixel intensity values.

4.4.3 Real-time measurement of thrombin generation during whole blood flow

Citrate-anticoagulated blood containing the fluorogenic thrombin substrate, Z-GGR-AMC (420 µmol/L), was co-perfused with $CaCl_2$/TF over fibrinogen as described above. After perfusion for 10 minutes at 200 s^{-1}, real-time accumulation of fluorescence due to substrate cleavage was recorded under stasis. Fluorescent images were obtained every 2 seconds with Visitech software. Regions of interest corresponding to the site of a thrombus were analyzed for fluorescence changes. Traces were then converted into first-derivative curves using Thrombinoscope software (Maastricht, The Netherlands) developed for thrombin generation measurement in plasma (Hemker, *et al.* 2000).

4.4.4 Measurement of fibrin formation from whole blood flow

To measure fibrin formed under various flow conditions, blood was co-perfused with TF/$CaCl_2$ for 15 minutes into fibrinogen- or collagen-coated capillaries as described above. Following blood perfusion, capillaries were washed with Tyrode-HEPES buffer, then treated with lysis buffer (20 mmol/L Tris, 300 mmol/L NaCl, 2 mmol/L EGTA, 2% NP-40, 2 mmol/L PMSF) for 5 minutes, followed by treatment with plasmin (1 µmol/L) for 1 hour to degrade fibrin. Eluates from capillaries were collected, separated by SDS-PAGE (6% acrylamide) and western-immunoblotted with fibrinogen antiserum for the 200 kDa fibrin degradation product D-dimer. D-dimer levels on blots were compared with a standard curve of purified D-dimer (1-100 ng).

4.4.5 In vivo thrombus formation

Thrombus formation was provoked in mesenteric veins of 4-5 week old wild-type C57Bl/6 mice (Kuijpers, *et al.* 2008). Mice were anesthetized by subcutaneous injection of ketamine (0.1 mg/g body weight) and xylazine (0.02 mg/g body weight); anesthesia was maintained throughout the experiment. Fluorescently labeled coagulation factors were injected via the tail vein (31-37 µmol/L in 70 µL of 50 mmol/L Hepes and 125 mmol/L NaCl; pH 7.4). In selected experiments, mice were injected with OG488- or AF647-labeled goat anti-rat antibody (40 µg) and rat anti-mouse CD41 mAb (2.5 µg in 70 µL saline). Mesenteric vessels, venules with a diameter of ~100 µm and arterioles with a diameter of ~60 µm (Kuijpers, *et al.* 2008), were exteriorized and treated topically with 30 µL of 500 mmol/L $FeCl_3$. The treatment led to the damage and loss of the endothelial cell layer in mesenteric veins (Kuijpers, *et al.* 2008). Vessels were observed

with a 40× water immersion objective on an upright Olympus BX-61WI microscope system (Middlesex, UK). Low fluorescence intensities were visualized with a CCD camera and a high-performance GEN III image intensifier (Kalia, *et al.* 2008). Immediately after $FeCl_3$ application, simultaneous brightfield and fluorescence images were captured at 30 frames per second by high-speed shutter and wavelength changing systems (Celi, *et al.* 2003). Image acquisition was controlled by Slidebook 4.10.12 software (Intelligent Imaging Innovations, Denver, CO).

Recorded images were processed with Slidebook software. Fluorescence intensities were corrected for autofluorescence by eliminating all pixels with a lower intensity than the average background intensity (determined per frame for a user-defined region of interest). Using the threshold criteria, all pixel intensities greater than the background were integrated. No further image processing was done. Exported raw images were analyzed by Metamorph software 7.5.0 (Molecular Devices, Downingtown, PA) to determine the increase in fluorescence of selected thrombi. Masks corresponding to the site of the thrombus were created and sum intensities of pixels above background were calculated. After background subtraction, pixel sizes >3 of all fluorescence features above background were listed. Features were grouped according to pixel size (4-9, 10-30, 31-99, 100-309, etc.), and total numbers of positive pixels per group were determined.

4.4.6 Analysis of data

Statistical significance was determined by Tukey's multiple comparison test and ANOVA.

4.5 Results

4.5.1 Thrombus formation and platelet activation under shear

To develop a reproducible method of thrombus formation under shear, human whole blood was co-perfused with $CaCl_2$/TF into fibrinogen-coated flow chambers. Imaging after 15 minutes of perfusion revealed that the fibrinogen surface was covered with platelet-rich thrombi and fibrin fibers at low shear (200 s^{-1}), while at 500 s^{-1} only thrombi were formed, and at 1000 s^{-1} a monolayer of platelets was present (Figure 4.1A). In the presence of the thrombin inhibitor, hirudin, only a monolayer of platelets was observed on fibrinogen at 200 s^{-1} (Figure 4.1A). To evaluate the extent of fibrin formation on fibrinogen surfaces, thrombi were lysed and the fibrin degradation product, D-dimer was evaluated by western blotting. In accordance with previous studies (Inauen, *et al.* 1990; Weiss, *et al.* 1986), D-dimer levels were maximal at low shear (200 s^{-1}), indicating that fibrin formation was greatest at the lowest shear rate (Figure 4.1C). A parallel set of results was observed on collagen surfaces (Figure 4.1B,D).

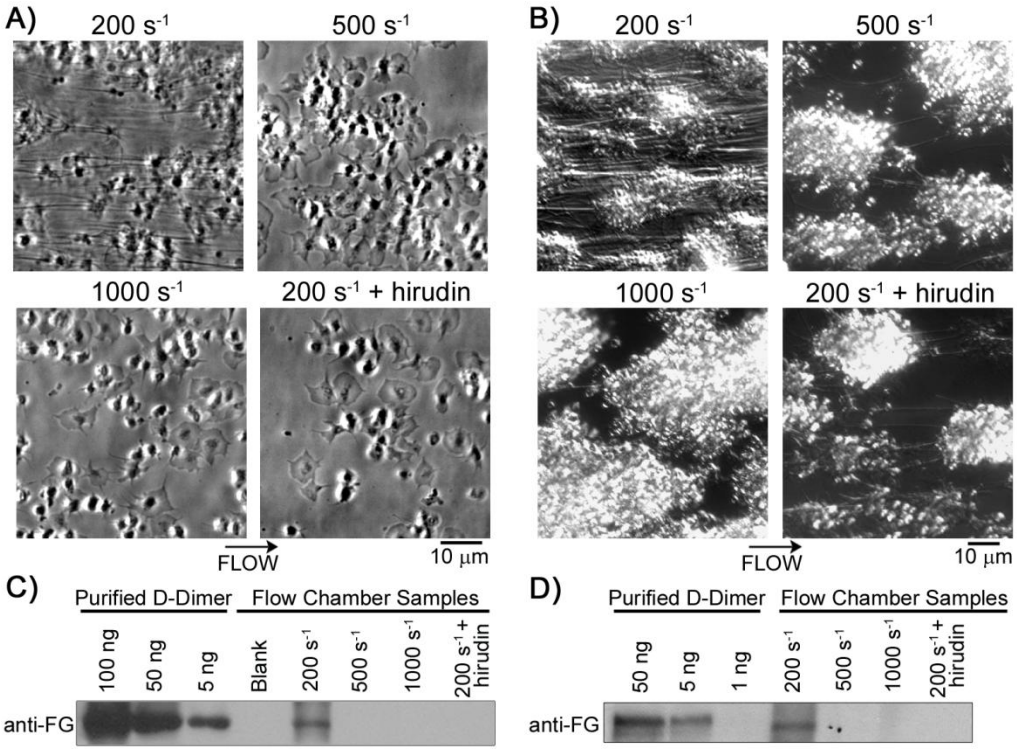

Figure 4.1. Thrombus formation and fibrin deposition on fibrinogen or collagen under shear. Human whole blood was co-perfused with $CaCl_2$/TF over fibrinogen or collagen for 15 minutes shear rates of 200 s^{-1}, 500 s^{-1}, or 1000 s^{-1}. Experiments were performed in the presence of vehicle or hirudin (2.9 μmol/L). Representative micrographs of platelet adhesion and fibrin formation on fibrinogen (A) or collagen (B) are shown. Following perfusion, flow chambers were washed and sequentially treated with lysis buffer and plasmin. Samples from fibrinogen-coated (C) or collagen-coated (D) chambers were analyzed for fibrin formation by western blot analysis, as measured by the fibrin degradation product, D-dimer. Lysis of fibrinogen-coated capillaries prior to blood perfusion served as a control (Blank). Western blots were performed by Jiaqing Pang from the McCarty laboratory.

We next aimed to determine if thrombi formed at 200 s^{-1} could support thrombin generation. Blood containing a fluorogenic thrombin substrate, Z-GGR-AMC, was co-perfused with $CaCl_2$/TF into the fibrinogen-coated chamber. Following 10 minutes of perfusion at 200 s^{-1}, thrombi were fluorescently imaged. Measurement of the cleavage of the substrate (as indicated by an increase in fluorescence) pointed to a transient accumulation of thrombin, which was ablated in the presence of hirudin (Figure 4.2A,B).

To determine the platelet response during blood perfusion, platelet activation was monitored by loading cells with Fluo-4, an intracellular calcium probe. Fluo-4 loaded cells were added to whole blood and perfused with $CaCl_2$/TF over fibrinogen. Calcium responses were monitored with fluorescence microscopy. Adherent platelets demonstrated an increase in cytosolic calcium under shear, with the highest amplitude calcium response observed at 200 s^{-1} (Figure 4.2C-E). The increased response at low shear was partially dependent upon the generation/availability of thrombin, as hirudin treatment significantly reduced calcium responses at 200 s^{-1}. As high cytosolic calcium can lead to PS exposure, adherent platelets were stained with OG488-annexin A5, which binds PS with high affinity. The number of PS-exposing platelets was greatest at low shear, and was reduced in the presence of hirudin (Figure 4.2F). Together, these results demonstrate that platelet-fibrin thrombi formed at low shear contain PS-exposing platelets and promote TF-induced thrombin generation.

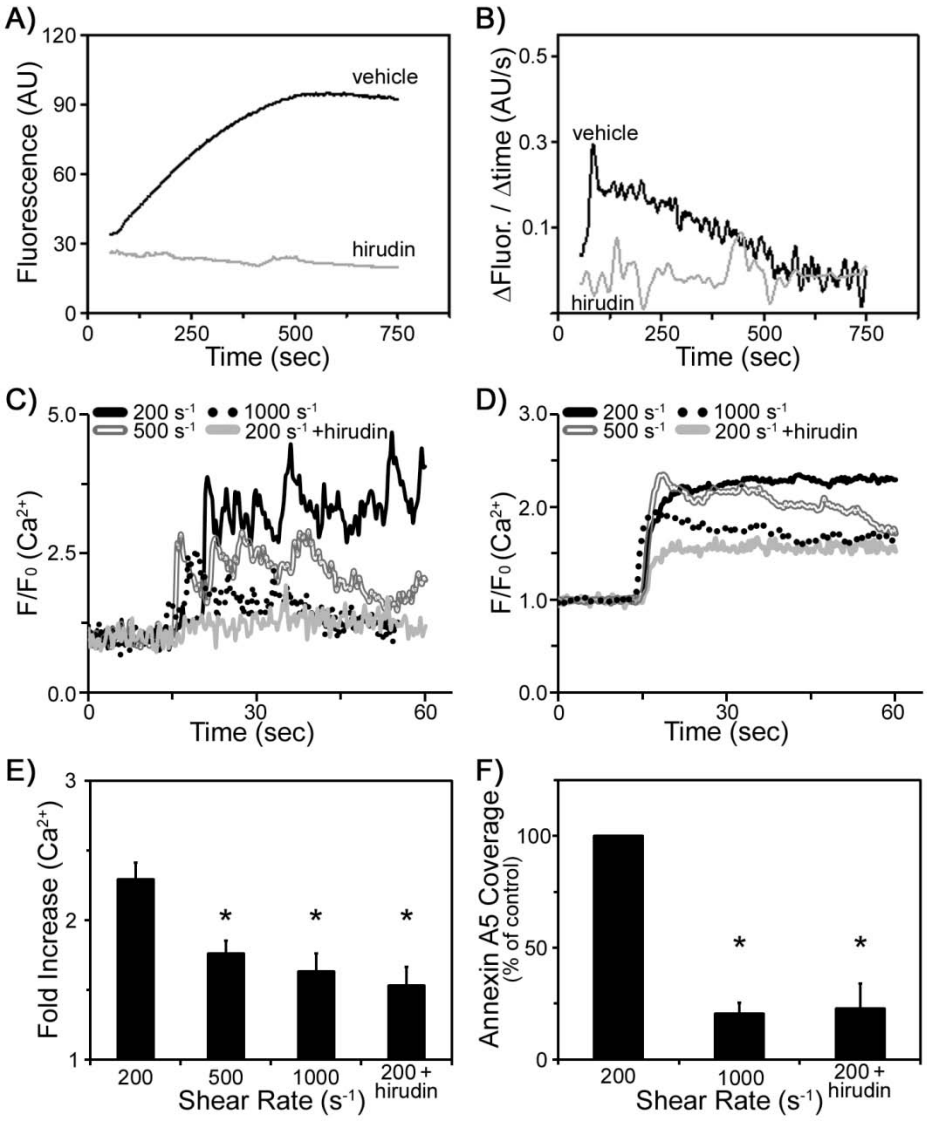

Figure 4.2. Thrombin generation and platelet activation under shear. Human whole blood was co-perfused with $CaCl_2$/TF over fibrinogen in the presence of vehicle or hirudin (2.9 µmol/L). A-B, The fluorogenic thrombin substrate, Z-GGR-AMC (420 µmol/L) was added to whole blood prior to perfusion. The accumulation of fluorescence from cleaved Z-GGR-AMC after 10 minutes of flow at 200 s^{-1} is shown. A, Increase in fluorescence intensity from thrombus area; B, first-derivative curves of transient thrombin generation. C-E, Platelets loaded with the calcium indicator Fluo-4 were added to whole blood before perfusion. Platelet calcium responses under flow are shown. C, Traces of F/F_o values of platelets after adhesion representing $[Ca^{2+}]_i$; D, average F/Fo traces; E, fold increase of calcium responses during 1 minute of adhesion. F, Following blood perfusion, adherent cells were labeled with OG488-annexin A5. The graph indicates accumulation of PS-exposing platelets (fraction of platelets staining with OG488-annexin A5 as a percentage of 200 s^{-1} control). Mean ± SEM (n = 3-5). *P<0.05.

4.5.2 Characterization of coagulation factor distribution on thrombi under shear

We next aimed to determine the localization of coagulation factors and the site of thrombin generation during thrombus formation. Thrombi were formed by perfusion of whole blood and $CaCl_2$/TF at 200 s^{-1} over fibrinogen, and were labeled with fluorescently labeled coagulation factors or antibodies in combination with AF647-labeled annexin A5 (Figure 4.3A). Staining with fluorescently labeled anti-CD61 (integrin β_3) mAb showed the presence of platelet aggregates (20-45 μm in size), surrounded by annexin A5-binding platelets (Munnix, *et al.* 2007). We next evaluated the binding of FXa, which has been shown to assemble on the platelet surface as part of the prothrombinase complex. The labeling of OG488-FXa substantially overlapped with PS-exposing (annexin A5-binding) platelets. Quantitatively, this was demonstrated by a high Pearson's overlap coefficient R_r between labels of 0.56 (Figure 4.3C). OG488-FXa binding was restricted to small structures, resulting in a fluorescence surface area coverage of 9.6 ± 1.2% (Figure 4.3B).

In marked contrast, OG488-prothrombin, a substrate of the prothrombinase complex, distributed over thrombi and fibrin fibers. As prothrombin can be enzymatically cleaved into thrombin in the presence of active proteases, labeling was performed in the presence of the serine protease inhibitor PPACK. Our results show that the distribution of OG488-prothrombin in the presence of PPACK overlapped with the binding distribution of AF647-annexin A5 (Figure 4.3A), resulting in an increase in the overlap coefficient R_r of prothrombin and annexin A5 labeling (Figure 4.3C). Moreover, the OG488-prothrombin fluorescence surface area coverage was drastically reduced in the presence of PPACK (Figure 4.3B). To confirm that prothrombin cleavage was responsible for the altered label

distribution, we investigated the binding of OG488-active site-labeled thrombin. Our results demonstrate that OG488-active site-labeled thrombin bound ubiquitously to fibrin-platelet structures, as evidenced by a fluorescence area coverage of 35.0 ± 4.0% and a low overlap (R_r = 0.10) with annexin A5 (Figure 4.3).

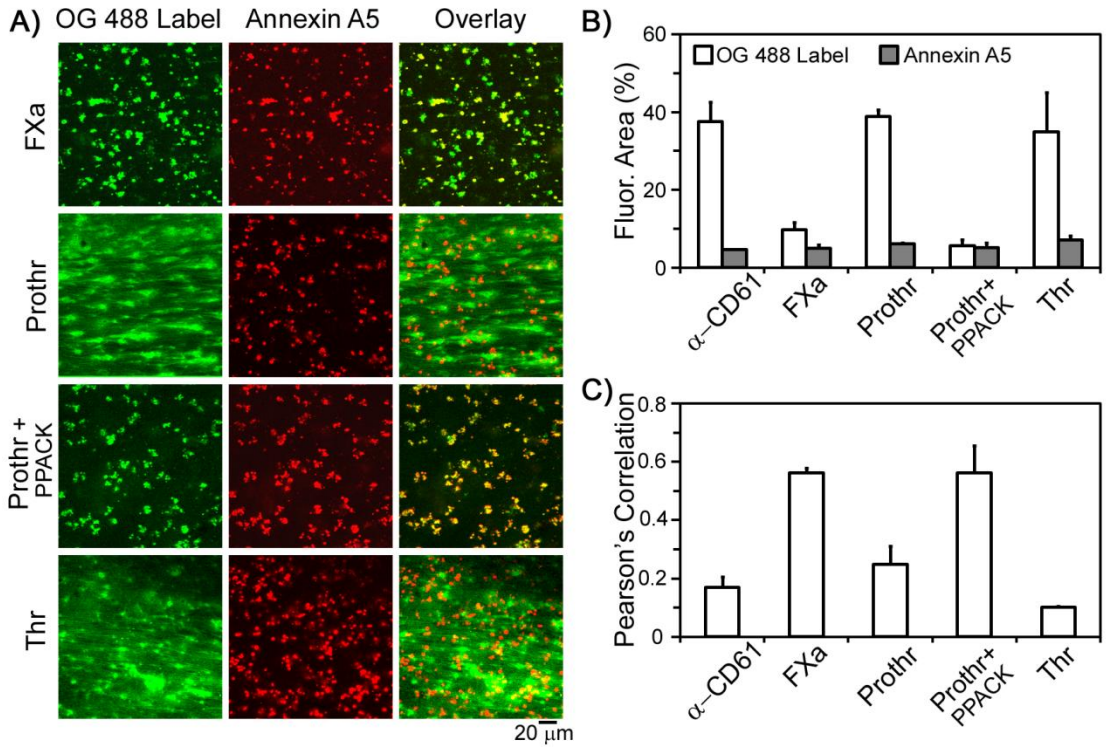

Figure 4.3. Localization of factor Xa (FXa) and (pro)thrombin on thrombi formed under shear. Human whole blood was co-perfused with $CaCl_2$/TF at 200 s^{-1} over fibrinogen. Thrombi were dual-labeled with AF647-annexin A5 (14 nmol/L, *red*) and active-site OG488-labeled coagulation factors (1 µmol/L, *green*) or an antibody to the integrin β_3 (α-CD61, 20 µg/ml, *green*). Where indicated, serine proteases were inhibited during labeling with PPACK (40 µmol/L). A, Confocal images in *green* are shown for OG488-labeled FXa, prothrombin (Prothr), or thrombin (Thr) fluorescence; images in *red* indicate annexin A5 binding. B, Fluorescence surface area coverage for each *green* label and annexin A5. C, Pearson's correlation coefficient, showing overlap between PS-exposing platelets and *green* labels. Mean ± SEM (n = 3-5). Johan Heemskerk and Imke Munnix of the Heemskerk laboratory assisted with confocal imaging and image analysis.

Utilizing OG488-labeled human fibrinogen or fluorescently coupled antibodies to fibrin(ogen), the distribution of fibrin(ogen) was determined on thrombi formed under shear. Fluorescent fibrinogen bound ubiquitously to the platelet thrombi and fibrin fibers

(Figure 4.4A,B), as evidenced by a high surface area coverage (45.3 ± 7.7%) and low overlap with annexin A5 (0.17). Similarly, fluorescently-labeled antibodies against fibrinogen or fibrin bound in a ubiquitous manner on platelet-fibrin thrombi, resulting in a low overlap with annexin A5 (0.20 and 0.12 for anti-fibrinogen and anti-fibrin antibodies, respectively; Figure 4.4C). In contrast, substantial overlap was observed when thrombi were dual stained with OG488-prothrombin and AF547-fibrinogen (R_r = 0.79).

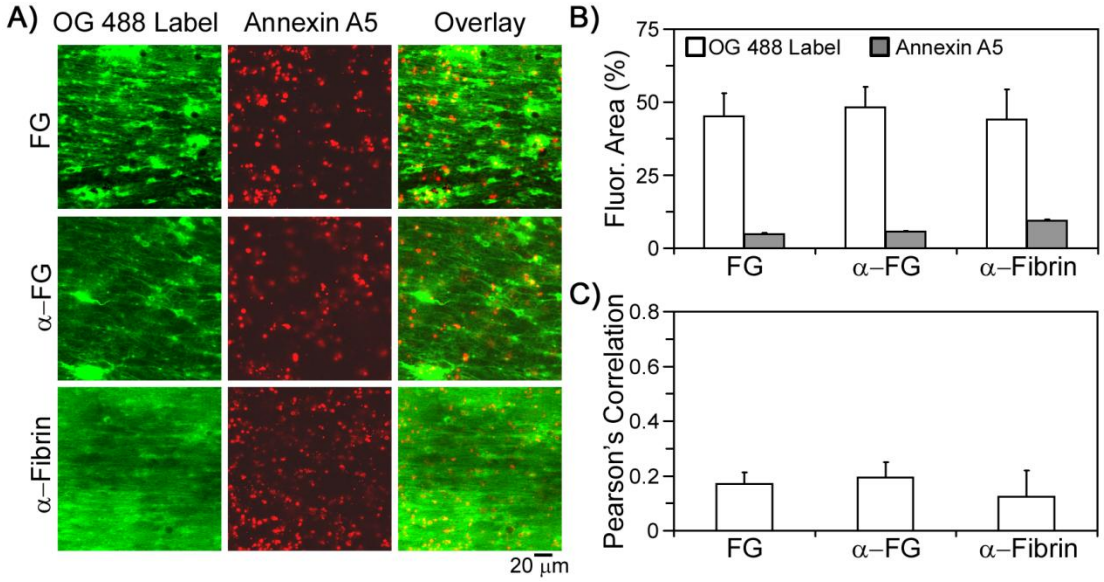

Figure 4.4. Spatial localization of fibrin(ogen) and procoagulant platelets during thrombus formation. Thrombi were formed by a 15 minute co-perfusion of whole blood and $CaCl_2$/TF at 200 s^{-1} over fibrinogen. Dual-labeling was with AF647-annexin A5 (14 nmol/L, *red*) and the indicated fibrin(ogen) labels (*green*). A, Confocal fluorescence images in *green* are shown for OG488-fibrinogen (FG, 0.3 μmol/L), anti-fibrinogen antibody (α-FG, 20 μg/mL), or anti-fibrin antibody (α-Fibrin, 20 μg/mL). Images in *red* indicate staining of PS-exposing platelets. B, Fluorescence surface area coverage for each OG488 label and annexin A5. C, Pearson's correlation coefficient (R_r), between annexin A5 and each *green* label. Mean ± SEM (n = 3-5 experiments). Johan Heemskerk and Imke Munnix of the Heemskerk laboratory assisted with confocal imaging and image analysis.

To determine the role of PS-exposing platelets in fibrin generation in the low shear model of thrombus formation, flow experiments were performed using blood pretreated with wild-type or mutant annexin A5 (0.28 μmol/L). When blood containing wild-type annexin A5 was co-perfused with $CaCl_2$/TF over fibrinogen and post-labeled with

OG488-fibrinogen, there was a marked decrease in OG488-fibrinogen labeling and absence of fibrin formation (Figure 4.5). In contrast, pretreatment of blood with M1234 annexin A5 mutant (lacking the four calcium binding sites required for interaction with PS) had no effect on fibrin formation or the distribution of OG488-fibrinogen on the thrombus surface (Figure 4.5). Collectively, these results reveal the distinct distribution of FXa, prothrombin, and thrombin on thrombi formed under shear, and confirm the important role of exposed PS for fibrin formation under flow.

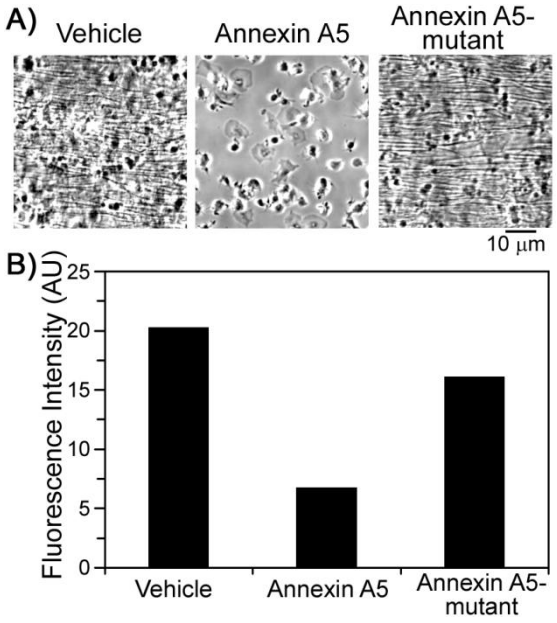

Figure 4.5. Role of PS-exposing platelets in fibrin formation during thrombus formation. Thrombi were formed on fibrinogen by co-perfusion of whole blood and $CaCl_2$/TF at a shear rate of 200 s^{-1}. Blood samples were incubated with vehicle, annexin A5, or mutant M1234 annexin A5 (each 0.28 μmol/L) before perfusion. Thrombi were labeled with OG488-fibrinogen (0.3 μmol/L). A, Representative phase-contrast micrographs of platelets and fibrin after 15 minutes of perfusion. B, Relative accumulation of labeled fibrin(ogen). Data are presented as integrated fluorescence intensity per microscopic field. Results of 1 representative experiment are shown.

4.5.3 Heterogeneous incorporation of coagulation factors in venous thrombi in vivo

To evaluate the incorporation of coagulation factors into thrombi formed *in vivo*, thrombus formation was studied by brightfield and fluorescence microscopy following

$FeCl_3$-induced damage of mouse mesenteric veins with mean wall shear rates of ~345 s^{-1} (Kuijpers, *et al.* 2008). Video images were recorded following injection of OG488-labeled fibrinogen, prothrombin, FXa or anti-CD41 (integrin α_{IIb}) mAb. Images showed accumulation of labeled platelets and coagulation factors following vascular damage (Figure 4.6). Although the rate of label accumulation was similar for all probes, marked differences were observed in the patterns of label incorporation (Figure 4.6). Whereas labeled fibrinogen and prothrombin distributed as large fluorescent structures of the size of the whole thrombus, labeling of FXa and platelets (anti-CD41 mAb) was confined to numerous 15-45 μm sized structures. As confirmed by morphometric analysis of the label distribution patterns, our results show that about 80% of labeled fibrinogen and prothrombin, but only 25% of labeled platelets and FXa, accumulated into features of >3100 pixels (Figure 4.6C).

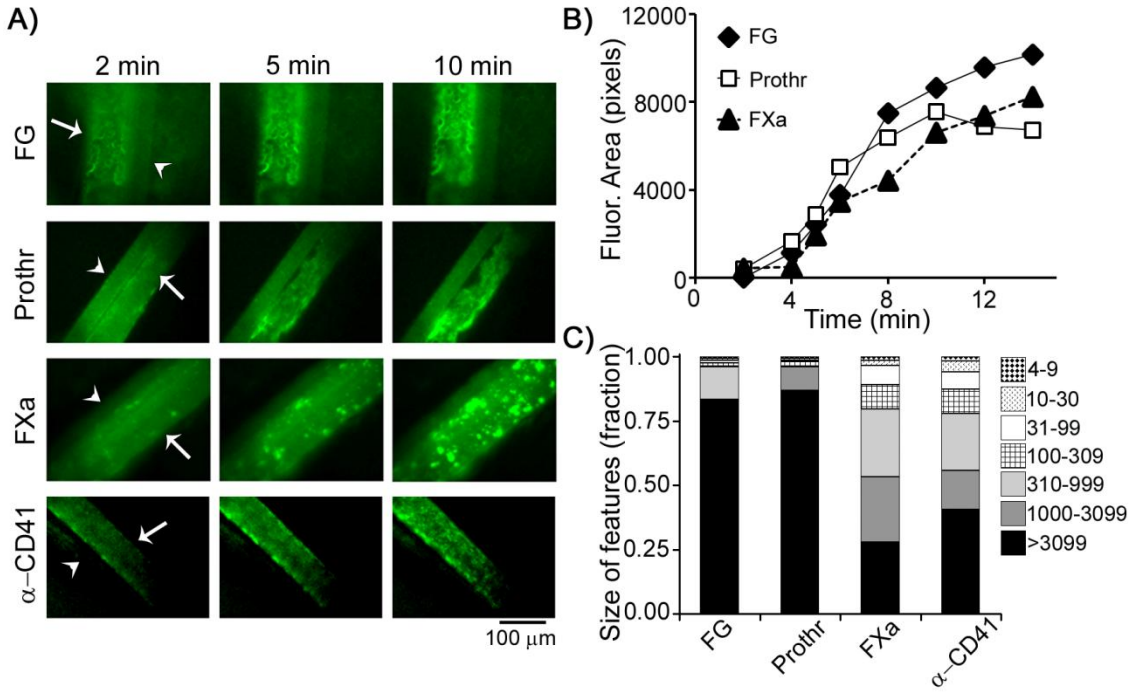

Figure 4.6. Incorporation of labeled coagulation factors during venous thrombus formation *in vivo*. Mice were injected with OG488-labeled fibrinogen (FG), prothrombin (Prothr), factor Xa (FXa), or anti-CD41 mAb (anti-platelet integrin α_{IIb}). Thrombus formation in exteriorized mesenteric vessels was induced by 30 µL of 500 mmol/L $FeCl_3$ (n = 3-5). A, Fluorescence images of venous thrombi (arrows) and adjacent arteries (arrowheads). B, Increase in fluorescence surface area coverage over time. C, Distribution of fluorescence in smaller or larger features. These experiments were performed by Imke Munnix of the Heemskerk laboratory and Jocelyn Auger from Steve Watson's laboratory. Johan Heemskerk assisted in image analysis.

4.6 Discussion

Our study was designed to investigate the distribution of coagulation factors on thrombi under shear. Our data demonstrate that FXa and prothrombin (in the presence of PPACK) bound in a punctate manner on the thrombus surface under shear, overlapping substantially with annexin A5-binding, PS-exposing platelets. This finding is in accord with previous studies in purified systems that have shown that the tenase and prothrombinase complexes assemble on peripheral blood cell surfaces (Ahmad, *et al.* 2003; Ahmad, *et al.* 2003; Kamath, *et al.* 2008; Tracy, *et al.* 1985). Our observation that fibrin formation was abrogated in the presence of supraphysiological concentrations of

annexin A5 (Kaneko, *et al.* 1996; Masuda, *et al.* 2004), demonstrates the functional role of coagulation factor interactions with exposed PS during thrombus formation.

While FXa and prothrombin labeling was punctate, thrombin and fibrin(ogen) were ubiquitously distributed over fibrin-platelet structures, with a large surface area coverage and low overlap with annexin A5. Thrombin is a critical player in blood coagulation and is known to bind to the platelet surface and to fibrin(ogen) (Adams, *et al.* 2006; Beguin, *et al.* 1997; Kahn, *et al.* 1999; Marguerie, *et al.* 1979; Mosesson 2005); however, where thrombin is localized during clot formation is largely unknown. Thrombin interacts with fibrin(ogen) though multiple low and high affinity binding sites (Fredenburgh, *et al.* 2008; Meh, *et al.* 1996). Importantly, a high affinity thrombin binding site exists on an alternatively spliced variant of fibrinogen (γ′-fibrinogen), which is present in ~10% of circulating fibrinogen molecules and becomes incorporated into fibrin (Lovely, *et al.* 2002; Mosesson, *et al.* 1972; Pospisil, *et al.* 2003). Thrombin bound to this high affinity site on fibrin(ogen) has been shown to be enzymatically active and protected from inhibition by the heparin-antithrombin complex (Fredenburgh, *et al.* 2008; Weitz, *et al.* 1998). Therefore, our findings of thrombin distribution on platelet-fibrin clots suggest that fibrin may play an important role in localizing thrombin to clots. Our results point to an initial binding of prothrombin to the FXa-containing prothrombinase complex at PS-exposing platelets (thrombin formation), followed by redistribution of active thrombin to the platelet-fibrin thrombus.

Previous *in vivo* experiments with wild-type C57Bl/6 mice have shown that $FeCl_3$-induced thrombus formation in the mesenteric venules relies on the exposure of collagen, activation of the TF/activated factor VII pathway, thrombin, and platelet activation (Kuijpers, *et al.* 2008; Munnix, *et al.* 2007). While exposed extracellular matrix proteins play an essential role in mediating the first steps of platelet recruitment in damaged vessels, fibrinogen plays a predominant role in platelet aggregate formation. Rapid deposition of fibrin(ogen) is observed in $FeCl_3$-induced damage of mesenteric venules (Furie, *et al.* 2007), allowing deposited fibrin(ogen) to become a substrate for subsequent platelet recruitment, adhesion, and aggregation. Under low shear venous conditions, an essential role has been established for fibrinogen in supporting platelet aggregation and adhesion to the growing platelet plug through interactions with $\alpha_{IIb}\beta_3$ (Coller 1980; Nachman, *et al.* 1982; Ni, *et al.* 2000; Ni, *et al.* 2003). Our *in vitro* work points to a role for fibrin(ogen) in supporting thrombin localization during thrombus formation. We therefore designed a series of experiments to characterize the distribution of coagulation factors on thrombi formed by $FeCl_3$-provoked damage of mesenteric venules *in vivo*. In parallel with our *in vitro* studies, a punctate distribution of FXa was observed, in accord with the notion that FXa binding is localized to the platelet surface during thrombus formation. Importantly, our *in vivo* data demonstrate that fibrin(ogen) and (pro)thrombin incorporated into large structures and were distributed throughout the thrombi. Taken together, our studies point to an important role for fibrin(ogen) in retaining the key coagulation enzyme thrombin on clots formed under shear.

Chapter 5: Rational Design of an *Ex Vivo* Model of Thrombosis

Michelle A. Berny, Ishan A. Patel, Tara C. White-Adams, Patrick Simonson, András Gruber, Sandra Rugonyi, Owen J. T. McCarty

5.1 Abstract

The underlying pathogenesis of cardiovascular disease is the formation of occlusive thrombi. While many well-defined animal models recapitulate the process of intravascular thrombosis, there is a need for validated *ex vivo* models of occlusive thrombus formation. Using the force of gravity to provide a constant pressure gradient, we designed and validated an *ex vivo* model of thrombosis. Times to occlusion on a collagen matrix in our model were within the range of occlusion times observed in murine thrombosis models. Prolongation of time to occlusion in the presence of platelet $\alpha_{IIb}\beta_3$ antagonists or inhibitors to thrombin or activated factor X is in agreement with established mechanisms of thrombus formation. The use of this model may be expanded to characterize the mechanisms of thrombosis and to determine the efficacy of pharmacological agents designed to prevent occlusive thrombus formation.

This work was originally published by Springer
Cellular and Molecular Bioengineering 2010; Volume 3, Number 2, Pages: 187-189
Reprinted with permission

5.2 Introduction

In Chapters 3 and 4, assays were conducted in the presence of shear flow to assess the platelet receptors involved in interactions with thrombin and to determine the localization of thrombin on thrombi. Thrombin contributes not only to hemostatic thrombus formation, but also to the pathological development of occlusive thrombi. In order to better characterize the role of thrombin and other hemostatic components in pathologic thrombus formation, an *ex vivo* model of occlusive thrombus formation was developed and validated in Chapter 5.

5.3 Background

Upon damage to vessel walls, exposed extracellular matrix (ECM) proteins and tissue factor (TF) trigger a series of events that lead to the formation of a hemostatic plug in order to prevent blood from escaping a damaged blood vessel. A number of *in vitro* models have been established to simulate primary hemostasis under physiologically relevant shear and pressure conditions (Gorog 1986; Gorog, *et al.* 1984; Kratzer, *et al.* 1985; Muga, *et al.* 1995). While the activation of platelets and the coagulation cascade are essential for normal hemostasis, intravascular formation of occlusive thrombi represents the underlying pathogenesis of cardiovascular diseases (Denis, *et al.* 2007; Harker, *et al.* 1991; Renne, *et al.* 2005; Tucker, *et al.* 2009). Although there currently exist a number of well-defined animal models of thrombosis, whereby the time to vessel occlusion is measured, there is a need for validated *ex vivo* models to determine the propensity of blood to form an occlusive thrombus. *In vitro* flow adhesion models have been widely utilized to study receptor-ligand mediated interactions under physiologically

relevant levels of shear (McCarty, *et al.* 2004), illuminating the initial steps of platelet recruitment and activation on ECM proteins under flow. However, these parallel-plate or capillary flow models are driven by a constant volumetric flow rate, in contrast to the pressure gradient that maintains blood circulation *in vivo*. The current study describes the design of an *ex vivo* model of intravascular occlusive thrombus formation in blood driven by a constant pressure gradient.

5.4 Model Development

Our thrombosis model uses gravity to drive blood flow through a capillary tube under a constant pressure gradient (Figure 5.1A). The height of the blood required to drive this system was calculated using the Navier-Stokes equation within the capillary tube, which for the *z*-direction in Cartesian coordinates, is:

$$(5.1):\ \rho_b\left(\frac{\partial u_z}{\partial t}+u_x\frac{\partial u_z}{\partial x}+u_y\frac{\partial u_z}{\partial y}+u_z\frac{\partial u_z}{\partial z}\right)=-\frac{\partial P}{\partial z}+\mu_b\left(\frac{\partial^2 u_z}{\partial x^2}+\frac{\partial^2 u_z}{\partial y^2}+\frac{\partial^2 u_z}{\partial z^2}\right)$$

where ρ_b is blood density, t time, u velocity, P pressure (including effects due to gravitational forces), and μ_b blood viscosity. Under the assumptions that the flow is laminar and steady state (does not change with time); velocity is unidirectional, and only flows in z direction; the flow is fully developed and does not change as a function of z; the width (x-direction) of the capillary is much larger than the depth (y-direction) and thus velocity is only a function of y; blood behaves as a Newtonian, incompressible, and isothermal fluid in this model, the Navier-Stokes equation simplifies to Equation 5.2:

$$(5.2):\quad \frac{\partial P}{\partial z}=\ \mu\frac{\partial^2 u_z}{\partial y^2}$$

Upon integration of Equation 5.2, we employed the following boundary conditions for pressure: at the entrance of the capillary ($z = 0$), the pressure term was defined as the atmospheric pressure (P_a) plus the pressure resulting from the height of the blood ($z = h_b$) in the reservoir ($\rho_b g h_b$). At the exit of the capillary ($z = -h_c$), the pressure term was defined as the atmospheric pressure (P_a) minus the pressure resulting from the height of the capillary ($\rho_b g h_c$) plus the pressure term from the depth that the capillary was submerged in phosphate buffered saline (PBS; $\rho_{pbs} g h_{pbs}$). In addition, boundary conditions for velocity were: at the wall, velocity was zero due to the assumption of a no slip boundary condition; at the center of the tube (width in the *y*-direction was defined as $2a$), the velocity was maximum and the gradient of velocity in the *y*-direction (the shear rate) was zero. Thus solving the equation resulted in the formula given in Equation 5.3, whereby the shear rate at the wall (γ_w) can be evaluated for a given width of the capillary tube (a) and height of the reservoir of blood (h_b).

$$(5.3): \quad \gamma_w = a\left[\frac{\rho_b g(h_c + h_b) - \rho_{pbs} g h_{pbs}}{h_c \mu_b}\right]$$

where γ_w is wall shear rate, ρ_b is the density of the blood, ρ_{pbs} is the density of the PBS, h_c is the height of the capillary tube, h_b is the height of the blood in the reservoir, h_{pbs} is the depth that the capillary is submerged in PBS, g is acceleration due to gravity, μ_b is viscosity of blood, a is 1/2 the width of the capillary along the short-axis. Thus, an initial capillary wall shear rate of 350 s^{-1} can be achieved in a 0.2 × 2.0 × 50 mm glass capillary tube (Vitrotube™ Catalog # 5002, VitroCom, Mountain Lakes, NJ) by maintaining the height of blood (h_b) in the reservoir at 2.2 cm.

Glass capillary tubes were coated with fibrillar collagen (100 µg/mL) for 1 hour at room temperature and blocked with denatured BSA (5 mg/mL) for 1 hour. Collagen-coated capillaries were vertically mounted below a reservoir (Figure 5.1A). Whole blood samples (1 mL) were recalcified with $CaCl_2$ and $MgCl_2$ (final concentrations 7.5 and 3.75 mmol/L, respectively) and serially added to the reservoir in order to maintain a constant height of blood. Recalcified blood was allowed to drain from the reservoir, through the capillary, into a PBS bath. Time to occlusion of the capillary was recorded as the time blood first exited from the capillary into the PBS until the time blood ceased to flow from the capillary (occlusion). Experiments were observed over a 40 minute period. If occlusion did not occur after 40 minutes, experiments were terminated and a time point of 40 minutes was recorded.

5.5 Results

Our data show that recalcified blood occluded in the collagen-coated capillary tube after a mean time of 17.4 ± 1.7 minutes (Figure 5.1B). Time to occlusion was significantly increased in BSA-coated capillary tubes (30.6 ± 1.7 minutes, $p < 0.05$). No occlusion was observed in the absence of recalcification. When the platelet receptor $\alpha_{IIb}\beta_3$ was inhibited with the $\alpha_{IIb}\beta_3$ antagonist, eptifibatide (20 µg/mL; Cor Therapeutics Inc, South San Francisco, CA), occlusion times in collagen-coated capillaries were extended to 30.0 ± 3.3 minutes (Figure 5.1B). Occlusive thrombus formation was thrombin dependent, as recalcified blood pretreated with the direct thrombin inhibitor, hirudin (20 µg/mL; CIBA-Geigy Pharmaceuticals, Horsham, UK), failed to occlude in the capillary over 40 minutes of blood flow. In the presence of the activated factor X inhibitor, rivaroxaban (10

μmol/L; Bayer Healthcare, Leverkusen, Germany), occlusion times were also greater than 40 minutes (Figure 5.1B). Further, pretreatment of blood with activated protein C (APC, 5 μg/mL; Haematologic Technologies Inc, Essex Junction, VT), a natural anticoagulant which inhibits activated factors V and VIII (White, *et al.* 2008), prolonged occlusion times to 39.4 ± 0.6 minutes.

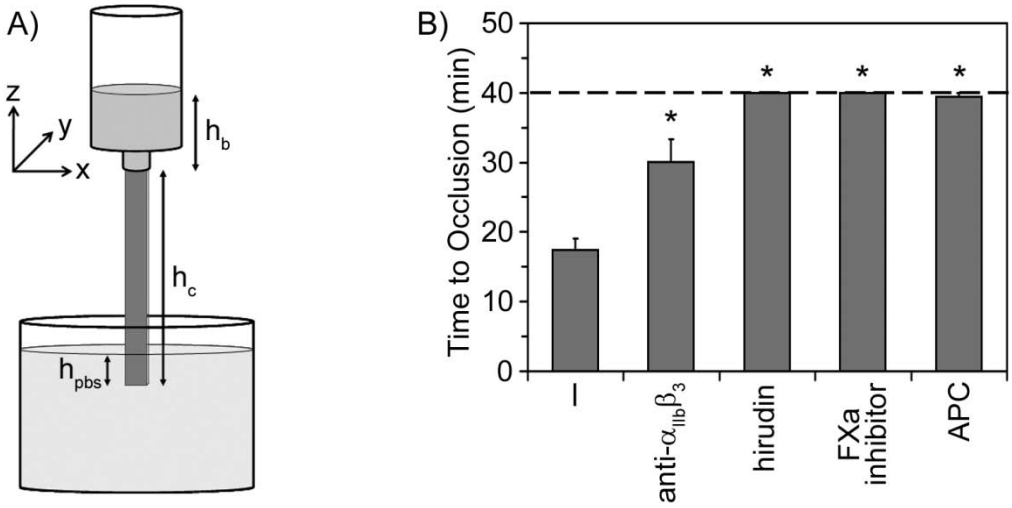

Figure 5.1. Pressure driven occlusive thrombus formation on a collagen matrix. A, Diagram of *ex vivo* model of thrombus formation. B, Sodium citrate anticoagulated whole blood was recalcified with $CaCl_2$ and $MgCl_2$ (7.5 and 3.75 mmol/L final concentrations, respectively), added to the reservoir and allowed to drain through collagen-coated capillary tubes into a PBS bath. Experiments were performed in the presence of PBS (−), the integrin $\alpha_{IIb}\beta_3$ antagonist eptifibatide (anti-$\alpha_{IIb}\beta_3$), the thrombin inhibitor hirudin, the activated factor X (FXa) inhibitor rivaroxaban, or activated protein C (APC). Time to occlusion is reported as mean ± SEM from at least three experiments. Statistical significance of differences between means was determined by ANOVA. *P < 0.05 with respect to PBS-treatment (−). These experiments were performed by Ishan Patel and Patrick Simonson of the McCarty laboratory.

5.6 Discussion

This aim of this study was to develop an *ex vivo* model of occlusive thrombus formation that successfully recapitulates the process of intravascular thrombosis. The times to occlusion (17 minutes) we observed on collagen were within the range of times to occlusion reported for mouse vessels exposed to $FeCl_3$ (Renne, *et al.* 2006; Renne, *et al.*

2005; White, *et al.* 2008). Prolongation of time to occlusion in the presence of known antithrombotic reagents is in agreement with established mechanisms of thrombus formation (Heemskerk, *et al.* 2002; Phillips, *et al.* 2005). The use of this model may be expanded to evaluate the occlusion times on a variety of surfaces to determine the mechanisms that regulate the coagulation cascade under a physiologically relevant constant pressure gradient, to characterize the efficacy of pharmacological agents designed to prevent occlusive thrombus formation, and to determine the role that vascular tortuosity plays in intravascular thrombosis.

Chapter 6: Promotion of Experimental Thrombus Formation by the Procoagulant Activity of Breast Cancer Cells

Michelle A. Berny-Lang, Joseph E. Aslan, Garth W. Tormoen, Ishan A. Patel, Paul E. Bock, András Gruber, Owen J. T. McCarty

6.1 Abstract

The routine observation of tumor emboli in the peripheral blood of patients with carcinomas raises questions about the clinical relevance of these circulating tumor cells. Thrombosis is a common clinical manifestation of cancer and circulating tumor cells may play a pathogenetic role in this process. The presence of coagulation-associated molecules on cancer cells has been described, but the mechanisms by which circulating tumor cells augment or alter coagulation remains unclear. In this study we utilized suspensions of a metastatic adenocarcinoma cell line, MDA-MB-231, and a non-metastatic breast epithelial cell line, MCF-10A, as models of circulating tumor cells to determine the thromobogenic activity of these blood-foreign cells. In human plasma, both metastatic MDA-MB-231 cells and non-metastatic MCF-10A cells significantly enhanced clotting kinetics. The effect of MDA-MB-231 and MCF-10A cells on clotting times was cell number-dependent and inhibited by a neutralizing antibody to tissue factor (TF) as well as inhibitors of activated factor X and thrombin. Using fluorescence microscopy, we found that both MDA-MB-231 and MCF-10A cells supported the

binding of fluorescently-labeled thrombin. Furthermore, in a model of thrombus formation under pressure-driven flow, MDA-MB-231 and MCF-10A cells significantly decreased the time to occlusion. Our findings indicate that the presence of breast epithelial cells in blood can stimulate coagulation in a TF-dependent manner, suggesting that tumor cells that enter the circulation may promote the formation of occlusive thrombi under shear flow conditions.

This work has been accepted for publication in *Physical Biology*

6.2 Introduction

Rates of thrombosis are elevated in cancer patients, suggesting that a cancer-associated process can drive pathological thrombus formation. In metastasis, cancer cells can migrate from the primary tumor into the vasculature, exposing cancer cells to the blood. Building upon the novel mechanisms of thrombus formation revealed in this thesis, we applied the assays and techniques developed in Chapters 3-5 to determine the procoagulant activity of tumor cells. Here, results indicate that the presence of breast epithelial cells accelerates coagulation and promotes the development of occlusive thrombi.

6.3 Background

Cancer metastasis is the process whereby cancer cells separate from the primary tumor mass, enter the vascular or lymphatic circulation, exit into a new tissue, and colonize the invaded microenvironment. Metastasis represents a primary cause of morbidity and mortality associated with many cancers. For instance, although early-stage breast cancer

is curable with excision of the primary lesion along with radiation, hormonal therapy and chemotherapy, these treatments are ineffective once a tumor has metastasized. Clinical studies have shown that the presence of micrometastases in bone marrow is associated with the occurrence of clinically overt distant metastasis and death from cancer-related causes, but not with locoregional relapse, in breast cancer patients (Braun, *et al.* 2000). Although significant progress has been made in deciphering the molecular and genetic features of epithelial cancers, much is still unknown about the behavior and effects of cancer cells in the fluid phase during transit through the circulation.

Causal association between thrombosis and cancer was first recognized by Bouillard in the 1820's, then developed by Trousseau in the 1860's, who, observing his own disease, described that patients who present with migratory superficial thrombophlebitis are likely to have underlying pancreatic cancer (Bouillard, *et al.* 1823; Trousseau 1865). Since that time, extensive clinical evidence has established the fact that the blood coagulation system is intricately involved in the metastatic process. Poignantly, venous thromboembolism (VTE) complications, including pulmonary embolism, are the second leading direct cause of death of cancer patients, with the risk of VTE elevated from 7-fold to up to 28-fold as compared to non-cancer patients (Blom, *et al.* 2005; Heit, *et al.* 2000). The median survival of metastatic breast cancer patients who presented with VTE was strikingly short (2 months; range: 1-2) compared with that of metastatic breast cancer patients without thrombosis (13 months; range: 1-44) (Tesselaar, *et al.* 2007). Conversely, in patients with symptomatic VTE, the incidence of concomitant diagnosis of cancer that was previously unknown is between 4-10%, with the stage of cancer often

advanced (Otten, *et al.* 2001; Sorensen, *et al.* 2000). With the accumulating evidence that coagulation activation in cancer is critical to the outcome of the disease, there has been increasing interest in elucidating the coagulation and fibrinolytic pathways that promote cancer metastasis and the cellular pathways that promote thrombosis (Borsig 2008; Camerer, *et al.* 2004; McCarty, *et al.* 2000).

Studies have demonstrated an association between elevated levels of circulating tissue factor (TF) and thrombosis in cancer patients (Mackman 2009). TF is a key protein in the initiation of blood coagulation, assembling with the proteolytic enzyme activated factor VIIa (FVIIa) on blood cell membranes with exposed negatively charged phosphatidylserine (PS). Exposure of PS promotes the assembly of the tenase complex, where the TF-FVIIa complex catalyzes the activation of FIX and FX to FIXa and FXa, respectively (Ahmad, *et al.* 2003). The serine protease, FXa, goes on to assemble with the coagulation protein cofactor, FVa, to form the prothrombinase complex, which catalyzes the generation of thrombin (FIIa) from prothrombin (Mann, *et al.* 2003). The primary procoagulant functions of thrombin are the cleavage of soluble fibrinogen to insoluble fibrin and the activation of platelets via cleavage of protease-activated receptors (PARs) (Di Cera 2003). Additionally, thrombin also stimulates its own generation through the activation of FXI and the cofactors FV and FVIII, leading to rampant thrombin generation (Mann, *et al.* 2003; Pieters, *et al.* 1989). In the present study, we aimed to characterize the molecular pathways by which epithelial cells that originate from breast tumors promote coagulation factor activation and occlusive clot formation under physiologically relevant shear conditions.

6.4 Materials and Methods

6.4.1 Reagents

Recombinant inactivated FVIIa (FVIIai) was obtained from Enzyme Research Laboratories (South Bend, IN). A FITC-conjugated anti-TF antibody was from LifeSpan BioSciences (Seattle, WA) and a neutralizing anti-TF antibody (clone D3H44) was from Genentech (South San Francisco, CA). The FXa inhibitor, rivaroxaban, was obtained from Bayer Healthcare (Leverkusen, Germany) and the direct thrombin inhibitor, hirudin, was obtained from CIBA-Geigy Pharmaceuticals (Horsham, UK). Annexin A5 was purchased from AnaSpec (San Jose, CA). H-Gly-Pro-Arg-Pro-OH (GPRP) was from Calbiochem (Darmstadt, Germany). Dulbecco's Modified Eagle Medium (DMEM) for MDA-MB-231 and MCF-10A cells, fetal bovine serum (FBS), horse serum, cholera toxin, and recombinant trypsin (TrypLE) were from Invitrogen (Carlsbad, CA). All other reagents were purchased from Sigma-Aldrich (St. Louis, MO).

6.4.2 Cell preparation for experiments

MDA-MB-231 and MCF-10A cells were a kind gift from Dr. Tlsty (University of California, San Francisco, CA). Cells were detached with TrypLE for 30 minutes at 37°C, pelleted at 150*g* for 5 minutes, washed with serum-free DMEM, and resuspended to a concentration of 2×10^6/mL in serum-free DMEM. MDA-MB-231 and MCF-10A cells were cultured and prepared with assistance from Joseph Aslan of the McCarty laboratory.

6.4.3 Clotting times and OG-488 thrombin binding

Clotting times of pooled human plasma were measured with a KC4 Coagulation Analyzer (Trinity Biotech, Bray, Co. Wicklow, Ireland). Plasma samples were treated with antibodies or inhibitors to TF, FXa, thrombin, or PS for 3 minutes at room temperature, followed by incubation with vehicle, MDA-MB-231, or MCF-10A cells for 3 minutes at 37°C. Clotting was initiated by the addition of 16.7 mmol/L $CaCl_2$ and the clotting time (recalcification time) was recorded.

For OG-488 thrombin binding experiments, plasma was incubated with OG-488 thrombin (1 μmol/L) and the fibrin polymerization inhibitor, GPRP (10 mmol/L) before addition of MDA-MB-231 or MCF-10 cells (2×10^5/mL). Coagulation was triggered with 16.7 mmol/L $CaCl_2$ and plasma samples were taken 5 minutes later. Samples were imaged with differential interference contrast (DIC) and fluorescence microscopy on a Zeiss Axiovert 200M microscope.

6.4.4 Flow cytometry

MDA-MB-231 or MCF-10A cells (1×10^6/mL) were washed with PBS prior to incubation with a FITC-conjugated anti-TF antibody (1 μg/mL) for 30 minutes at room temperature. Following labeling, cells were analyzed on a FACSCalibur flow cytometer with CellQuest acquisition and analysis software (Becton Dickinson, Franklin Lakes, NJ). Unlabeled cells served as negative controls.

6.4.5 Capillary occlusion assay

As described in Section 5.5, glass capillary tubes (0.2 × 2 mm; VitroCom, Mountain Lakes, NJ) were incubated for 1 hour at room temperature with 100 µg/mL fibrillar collagen, blocked with denatured bovine serum albumin (BSA, 5 mg/mL) for 1 hour, and then vertically mounted below a reservoir. The exit of the capillary was immersed in phosphate buffered saline (PBS). Sodium citrate anticoagulated whole blood (0.38% w/v sodium citrate) was incubated with vehicle, MDA-MB-231, or MCF-10A cells for 5 minutes. Aliquots (500 µL) of treated blood were recalcified by addition of 7.5 mmol/L $CaCl_2$ and 3.75 mmol/L $MgCl_2$ and added to the reservoir to maintain a height of 1.5 cm, yielding an initial wall shear rate of 285 s^{-1} through the capillary, modeled by Equation 5.3 presented in Chapter 5. The time to occlusion of the capillary was recorded over an observation time of 60 minutes.

6.4.6 Analysis of data

Data are presented as mean ± SEM. For paired data, statistical significance between means was determined by the paired Student's t-test. For all other data, one-way ANOVA with the Tukey post-hoc test was employed to determine statistical significance between means. Significance differences for all statistical tests required $P<0.05$.

6.5 Results

6.5.1 Epithelial MDA-MB-231 and MCF-10A cells promote coagulation

To investigate the relationship between metastatic cancer cells and coagulation, we first developed a model of coagulation in the presence of breast epithelial cells lines. In this

work, we utilized two cultured epithelial cell lines derived from human breast tissue and differing in their metastatic potential. MDA-MB-231 is an immortalized human metastatic breast cancer cell line originally derived from a pleural effusion of a patient with metastatic adenocarcinoma of the breast (Cailleau, *et al.* 1974). MCF-10A is an adherent, immortal, non-transformed human mammary epithelial cell line that arose spontaneously from cells that were originally derived from a patient with fibrocystic changes (Soule, *et al.* 1990). We used a plasma recalcification assay to measure the effects of these epithelial cells on coagulation. The clotting of pooled human plasma was initiated by the addition of 16.7 mmol/L $CaCl_2$ and the clotting time (recalcification time) was measured. Our data demonstrate that, in comparison to vehicle controls, the presence of either MDA-MB-231 or MCF-10A cells significantly decreased clotting times in a cell number-dependent manner (Figure 6.1). At the same cell concentration, the metastatic cell line, MDA-MB-231, accelerated coagulation of plasma more effectively than the non-metastatic MCF-10A cell line. Taken together, our data demonstrate that the presence of both metastatic and non-metastatic cells of epithelial origin, in suspension, strongly promotes coagulation of recalcified plasma.

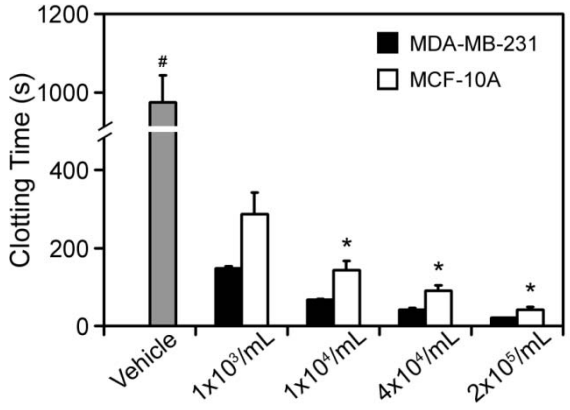

Figure 6.1. Breast epithelial cells support coagulation. Human sodium citrate-anticoagulated plasma was incubated with vehicle or suspensions of cultured MDA-MB-231 or MCF-10A cells (1×10^3 - 2×10^5/mL) for 3 minutes at 37°C. Coagulation of plasma was initiated by recalcification using 16.7 mmol/L $CaCl_2$ (final concentration) and clotting times were recorded on a coagulometer. Data are reported as mean ± SEM, from 6-8 experiments. In comparison to vehicle, clotting times were significantly shortened at all MDA-MB-231 or MCF-10A cell numbers, #P<0.05. *P<0.05 versus corresponding MDA-MB-231 cell concentration.

6.5.2 Mechanisms of MDA-MB-231 and MCF-10A cell procoagulant activity

A number of recent reports have suggested a role for TF in metastasis and the development of cancer-associated thrombosis. TF has been reported to be expressed on the surface of a number of native and cultured cells, including breast cancers, and in general, its surface expression level has been shown to increase with advanced disease (Kakkar, *et al.* 1995). To first determine if MDA-MB-231 and MCF-10A cells express TF, cells were labeled with a FITC-conjugated anti-TF antibody and analyzed by flow cytometry. Results indicate that TF is expressed on the surface of both MDA-MB-231 and MDF-10A cells (Figure 6.2A).

To investigate how TF expression on MDA-MB-231 and MCF-10A cells contributes to their procoagulant activity, we examined the role of the TF pathway in the plasma recalcification assay. When the TF pathway was inhibited by an excess molar

concentration of competitive TF pathway inhibitor, inactivated FVIIa (FVIIai), or an anti-TF antibody, clotting times dramatically increased (Figure 6.2B). Exogenous addition of TF to plasma samples containing MDA-MB-231 or MCF-10A cells caused a further decrease in clotting times. These results indicate that the TF pathway plays an important role in the procoagulant activity of both MDA-MB-231 and MCF-10 cells.

In order to determine the role of the members of the tenase and prothrombinase complexes in procoagulant activity of breast epithelial cells, additional plasma recalcification experiments were performed in the presence of inhibitors of the coagulation enzymes FXa and thrombin. Our data demonstrate that clotting times were prolonged more than 10-fold in the presence of either the FXa inhibitor, rivaroxaban, or thrombin inhibitor, hirudin (Figure 6.2C), indicating that the accelerated coagulation of recalcified plasma, in the presence of suspended epithelial cells, was mediated by thrombin. Inhibition of negatively charged PS on cell-surfaces by addition of a high concentration of annexin A5 (~10,000 times the physiological plasma concentration (Kaneko*, et al.* 1996)) dramatically prolonged clotting times (>20 minutes), suggesting a role for exposure of negatively charged lipids during epithelial cell-induced coagulation. In contrast, pretreating the plasma with the FXIIa inhibitor, corn trypsin inhibitor (CTI, 4 µmol/L), or the anti-FXI monoclonal antibodies, 1A6 or 14E11 (20 µg/ml), had no effect on clotting times in the presence of either MDA-MB-231 or MCF-10A cells, providing evidence against the primary involvement of contact activation and the intrinsic coagulation cascade in the procoagulant activity of these cell lines. Taken together, these results demonstrate that the procoagulant activity of MDA-MB-231 and MCF-10 cells is

primarily dependent upon activation of the extrinsic TF pathway of blood coagulation on the surface of cells.

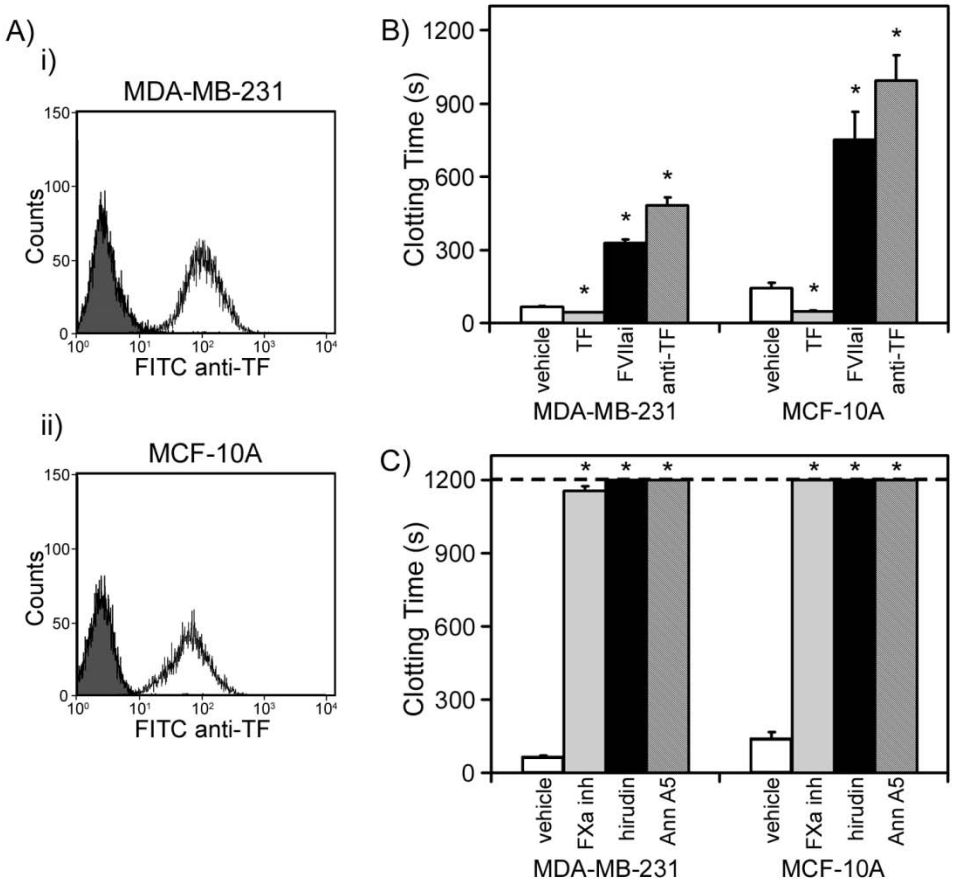

Figure 6.2. Characterization of the procoagulant activity of breast epithelial cells. A, Cultured MDA-MB-231 (i) or MCF-10A cells (ii) at 1×10^6/mL were labeled with a FITC-conjugated anti-TF antibody (1 µg/mL) and analyzed by flow cytometry. Shaded curves represent background fluorescence of unlabeled cells; white curves represent shift in fluorescence in the presence the anti-TF antibody. Representative curves from two or more independent experiments are shown. B&C, Human sodium citrate-anticoagulated plasma was pretreated with (B) vehicle; TF (TF,10 pmol/L); the TF pathway inhibitor, FVIIai (20 µg/mL); or a neutralizing antibody to TF (anti-TF, 20 µg/mL) or (C) vehicle; the FXa inhibitor, rivaroxaban (FXa inh, 10 µmol/L); the thrombin inhibitor, hirudin (20 µg/mL); or the phosphatidylserine binding protein, annexin A5 (Ann A5, 10 µg/mL). Cultured MDA-MB-231 or MCF-10A cells were added to treated plasma at 1×10^4/mL. After 3 minutes of incubation at 37°C, coagulation was initiated by addition of 16.7 mmol/L $CaCl_2$ and clotting times were recorded. Data are reported as mean ± SEM, from 4-8 experiments. If clotting did not occur during 20 minutes of observation, experiments were terminated and a clotting time of 20 minutes was recorded. *P<0.05 versus vehicle treatment.

6.5.3 MDA-MB-231 and MCF-10A cells support the binding of OG-488 thrombin

We next aimed to determine the ability of breast epithelial cells to directly support coagulation factor binding and localization. We have previously shown, in Chapter 4, that both blood platelets and fibrin-rich thrombi support the binding of active site fluorescently-labeled thrombin (OG-488 thrombin) under physiologically relevant shear flow conditions. Plasma was incubated with OG-488 thrombin (1 μmol/L) and the fibrin polymerization inhibitor, GPRP (10 mmol/L) before addition of MDA-MB-231 or MCF-10 cells. Coagulation was triggered with 16.7 mmol/L $CaCl_2$, and plasma samples were taken after 5 minutes. Our data show specific binding of OG-488 thrombin to both MDA-MB-231 and MCF-10A (Figure 6.3), providing direct evidence of the assembly of coagulation factors on the epithelial cell surface under conditions of coagulation.

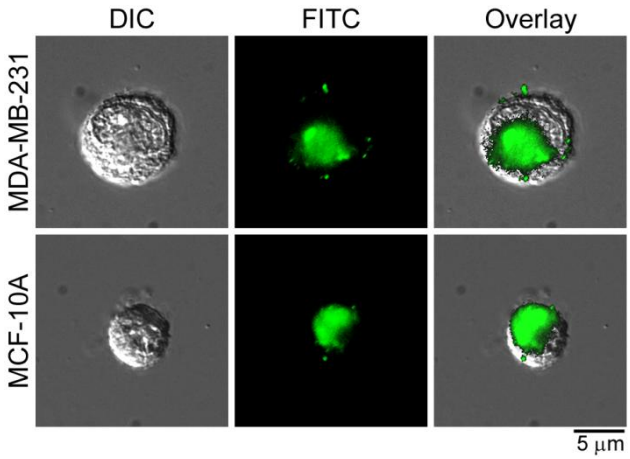

Figure 6.3. Cultured breast epithelial cells bind thrombin under procoagulant conditions. Human sodium citrate-anticoagulated plasma was incubated with suspended MDA-MB-231 or MCF-10A cells (2×10^5/mL) for 3 minutes at 37°C in the presence of OG-488 active-site labeled thrombin (1 μmol/L). Plasma was pretreated with GPRP (10 mmol/L), an inhibitor of fibrin polymerization, to prevent complete gelation. Coagulation was initiated by addition of 16.7 mmol/L $CaCl_2$ and plasma was sampled 5 minutes later. Samples were imaged by DIC and fluorescence microscopy, a representative image of a MDA-MB-231 and MCF-10A cell binding thrombin is shown. OG-488 thrombin fluorescence is indicated in *green*.

6.5.4 MDA-MB-231 and MCF-10A cells decrease the time to occlusion in a ex vivo model of thrombus formation

We next investigated the ability of the cell lines to promote coagulation and occlusive thrombus formation in the presence of shear flow. In our *ex vivo* model of occlusive thrombus formation, recalcified blood was driven by a constant pressure gradient at a physiologically relevant initial wall shear rate of 285 s^{-1} through capillaries coated with fibrillar collagen (diagram of model in Figure 5.1A). Flow through the capillary was monitored until occlusion. Our data demonstrate that the time to capillary occlusion was significantly decreased in the presence of either MDA-MB-231 or MCF-10A cells (Figure 6.4). This reduction in time to occlusion caused by the addition of the cultured tumor cells was erased by the addition of either an anti-TF antibody or the thrombin inhibitor, hirudin (Figure 6.4). These results support the notion that the procoagulant activity of epithelial cells that enter the circulation under pathologic conditions may contribute to thrombus formation in the presence of physiologically relevant shear forces.

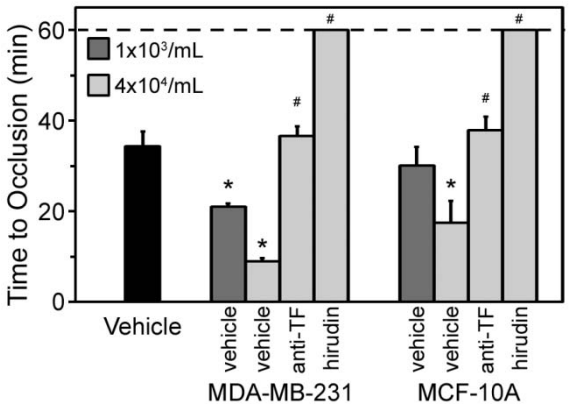

Figure 6.4. Cultured breast epithelial cells promote TF-dependent occlusive thrombus formation in flowing blood, *ex vivo*. Human sodium citrate-anticoagulated whole blood was mixed with vehicle, MDA-MB-231 or MCF-10A cells (4×10^4 or 1×10^3/mL) for 5 minutes at room temperature. In selected experiments, blood was treated with a neutralizing antibody to TF (anti-TF, 20 µg/mL) or the thrombin inhibitor, hirudin (20 µg/mL), in the presence of MDA-MB-231 or MCF-10A cells. Treated blood was recalcified with $CaCl_2$ and $MgCl_2$ (final concentration 7.5 and 3.75 mmol/L, respectively), added to a reservoir to a set height, and allowed to drain through collagen-coated capillaries into a PBS bath, with an initial shear rate of $285s^{-1}$. The time to occlusion (time until blood ceased to flow from the capillary) was recorded. Data are mean ± SEM from 3 or more experiments. *$P<0.05$ versus vehicle treatment in the absence of cells. #$P<0.05$ versus vehicle treatment of corresponding cell type at 4×10^4/mL. Data for these experiments was generated with assistance from Ishan Patel from the McCarty laboratory.

6.6. Discussion

Metastatic cancer has long been linked to coagulopathies such as thromboembolism, a leading cause of death in cancer patients. Here we explore the ability of metastatic and non-metastatic cells of epithelial origin to promote experimental thrombus formation. Using models of coagulation under shear conditions, we show that both non-metastatic MCF-10A cells and aggressively metastatic MDA-MB-231 breast tumor cells can promote coagulation. Metastatic potential, based on cell concentration, correlated with procoagulant activity, as MDA-MB-231 cells were more efficient at forming clots in vitro compared to MCF-10A cells.

Previous work has established that TF is present in greater levels in the serum of cancer patients and that tumor cells express high levels of TF (Kakkar, *et al.* 1995; Mackman 2009; Zhou, *et al.* 1998). Our work concludes that the prothrombotic potential of circulating tumor cells may be, in part, a consequence of TF expression. Indeed, both cell lines expressed TF and a neutralizing antibody against TF abrogated the ability of both MDA-MB-231 and MCF-10A breast epithelial cell lines to accelerate blood clotting. We found that epithelial cell-associated TF is an active cofactor for FVIIa and supports the activation of FX, as addition of the FXa inhibitor, rivaroxaban, also blocks the ability of tumor cells to initiate coagulation. Interestingly, addition of annexin A5, which binds specifically to exposed PS, also delayed clotting. This suggests that epithelial cells can expose phosphatidylserine on their surface, possibly upon activation, and this phosphatidylserine exposure has a role in the ability of the cells to promote thrombus formation. While it is known that tumor cells display more phosphatidylserine on their surface in part due to an altered balance of pro- and anti-apoptotic programs (Aslan, *et al.* 2009; Utsugi, *et al.* 1991; Zwaal, *et al.* 2005), it remains unclear whether this resultant exposure of phosphatidylserine allows cancer cells to assemble procoagulant complexes on their surface, thus allowing the pirating of the coagulation cascade while in the circulation. Additionally, we show that the surface of MDA-MB-231 and MCF-10A cells support the direct binding of thrombin (Figure 6.3). It has been shown that the MDA-MB-231 cells express PARs for thrombin, but the ability of MCF-10A cells to express PARs is unclear (Even-Ram, *et al.* 1998; Henrikson, *et al.* 1999). It is intriguing to speculate that cancer cells express a specific receptor for thrombin, or that perhaps cancer cells can associate with fibrin to establish a platform for thrombin binding and activity.

Whether or not the assembly of thrombin on the surface of cancer cells in the fluid phase plays a role in the process of metastasis remains to be determined.

Our study takes advantage of two well-established breast derived cell lines, MCF-10A and MDA-MB-231. MCF-10A cells were developed from ductal-like epithelial cells derived from a patient with cystic fibrosis (Soule, *et al.* 1990). MDA-MB-231 cells were isolated from the plural effusion from a highly metastatic breast cancer patient (Cailleau, *et al.* 1974). While these cells are at opposite ends of the metastatic spectrum and provide a powerful tool for studying metastasis, we recognize that there are fundamental differences in these cells that could contribute to the observed differences in coagulation response. For instance, the surface expression profile of molecules such as integrins, selectin ligands varies between these two cell types (Stahl, *et al.* 1997; Tozeren, *et al.* 1995; van der, *et al.* 1997; Zhou, *et al.* 1998). Additionally, individual MDA-MB-231 cells are nearly twice the diameter of MCF-10A cells, resulting in a nearly 4-fold increase in catalytic surface area on a per cell basis. Since the 4-fold larger surface area of MDA-MB-231 cells appeared to be associated with only a ~2-fold increase in procoagulant potential over MCF-10A cells in the plasma recalcification assay, the underlying relationship between surface area and thrombogenicity remains to be characterized. Future studies that take advantage of circulating tumor cells isolated from patients over the course of varying disease states will overcome these discrepancies and provide more conclusive data linking coagulopathies and metastatic potential.

This study demonstrates that cultured breast-derived epithelial cell lines, MDA-MB-231 and MCF-10A, promote coagulation and the formation of occlusive thrombi under physiological levels of shear. While we show that the coagulation potential of these epithelial cell lines is dependent upon the extrinsic TF pathway, it remains to be determined if circulating tumor cells utilize these mechanisms to promote coagulation during transit within the vasculature and what the impact the procoagulant nature of circulating tumor cells has on metastasis.

Chapter 7: Conclusions and Future Directions

7.1 Evaluate the efficacy of WE treatment in a model of ischemic stroke

As shown in Chapter 3, our results demonstrated that the thrombin mutant WE acts as an antagonist to the platelet receptor GPIb, inhibiting platelet interactions with vWF under flow conditions. Moreover, WE has been shown to activate protein C, resulting in generation of the anticoagulant APC. In a baboon model of thrombosis, we showed that administration of WE was antithrombotic without causing bleeding side effects (Gruber, *et al.* 2007). Based on the observed dissociation of antithrombotic and antihemostatic effects of WE *in vivo*, we hypothesize that WE administration may provide a safe alternative to early treatment of stroke, as current approaches to treatment of ischemic stroke, such a tissue plasminogen activator (tPA) administration, are limited by bleeding side effects (Hacke, *et al.* 1995). Therefore, to extend the findings of platelet and anticoagulant activities of WE, future studies will determine the effect of WE administration in a murine middle cerebral artery occlusion (MCAO) model of acute ischemic stroke.

In future studies, designed to model ischemic stroke, cerebral ischemia will be induced in male mice by occlusion of the middle cerebral artery for 1 hour with a silicone-coated filament. Animals will be treated with saline, WE, or tPA during or after occlusion, then monitored for up to 1 week following MCAO with daily neurological assessments.

Our preliminary studies demonstrate that administration of WE during MCAO led to a significant improvement in neurological scores 24 hours post-MCAO as compared to vehicle or tPA treatment (Figure 7.1A). Analysis of infarcted brain tissue by 2,3,5-triphenyltetrazolium chloride (TTC) exclusion, indicated that the relative volume of TTC-defined infarct area of the affected hemisphere was significantly smaller in both WE- and tPA-treated than in vehicle-treated mice (Figure 7.1A,B).

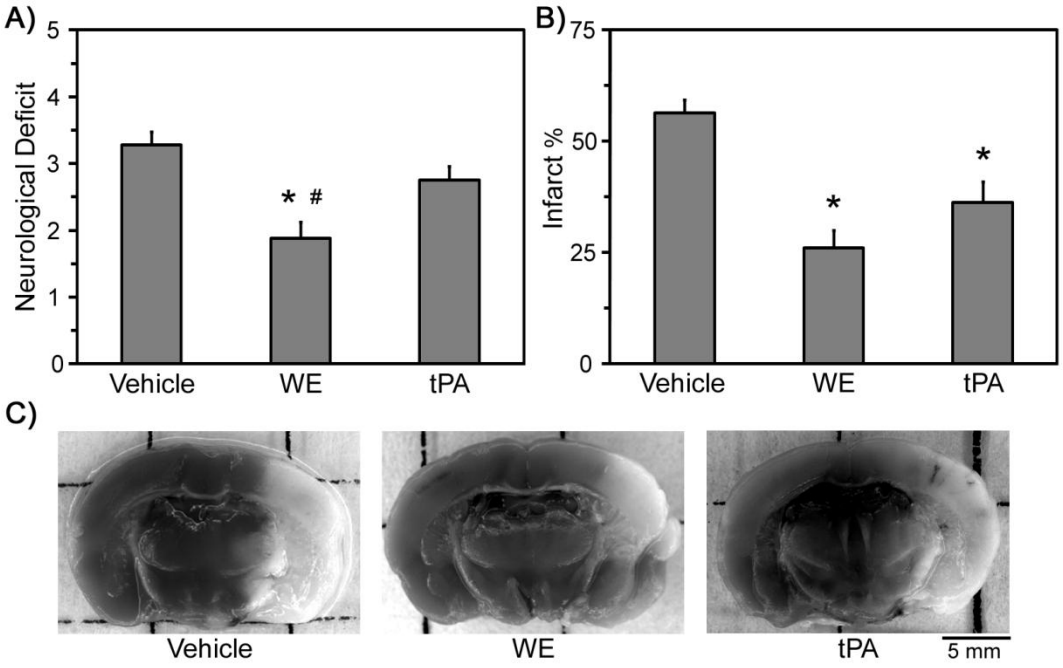

Figure 7.1. WE treatment during MCAO improves neurological performance scores and reduces infarct size. Mice were administered vehicle, WE (25 µg/kg), or tPA (2.5 mg/kg) during MCAO. A, Neurological deficits were scored 24 hours post-MCAO based on a 5 point scale, ranking neurological impairment from 0 for no neurological symptoms to 5 for a deceased animal (Tabrizi, *et al.* 1999). Following scoring, autopsy was performed and brain sections were stained with TTC. B, Images of the sections were analyzed by morphometric analysis to determine the percentage of TTC-defined infarcted tissue. C, Representative images of brain sections show the presence of TTC-defined infarct (lighter areas) and viable tissue (darker areas). Values are mean ± SEM, n=16-20. *P<0.05 versus vehicle treatment. #P<0.05 versus tPA. These experiments were performed by Sawan Hurst of the Gruber laboratory.

Our preliminary studies of animals monitored for 1 week after receiving saline, WE, or tPA treatment 2 hours post-MCAO demonstrate that both WE and tPA improved

neurological outcomes. On days 3 to 7 after MCAO, performance scores in WE- and tPA-treated mice were significantly better than in vehicle treated mice (Figure 7.2A). Both WE- and tPA-treated mice showed significant improvement in neurologic scores over the 7 days of observation, while neurological scores in vehicle-treated mice were unchanged (Figure 7.2A). Survival curves of WE-treated animals trended toward an increase in survival beyond vehicle-treated animals (Figure 7.2B), but require additional data to show significance.

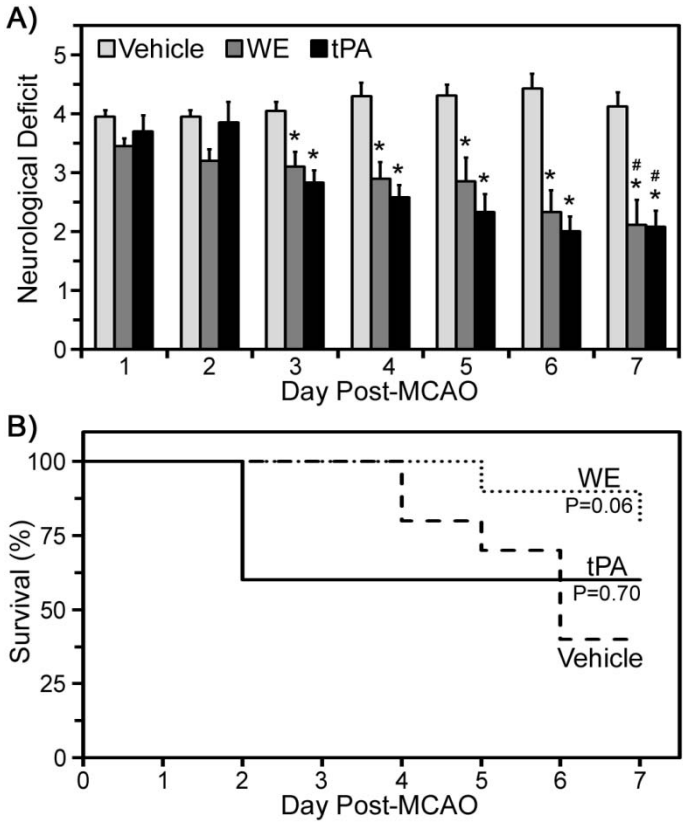

Figure 7.2. WE treatment post-MCAO improves 7-day neurological scores. Mice were infused with vehicle, WE (25 µg/kg/hr), or tPA (10 mg/kg/hr) 2 hours post-MCAO. A, Neurological deficits were scored daily for 1 week beginning at 24 hours post-MCAO (Day 1). Values are mean ± SEM, n=10. *P<0.05 versus vehicle. #P<0.05 versus corresponding treatment at Day 1. B, Animal survival was tracked for 1 week following MCAO and treatment. Data was generated by Sawan Hurst of the Gruber laboratory.

To evaluate the hemostatic effects of WE treatment, tail transection assays will be conducted for saline, WE, or tPA treated animals. Our preliminary studies show that tail bleeding times in WE-treated mice were comparable to vehicle-treated mice (Figure 7.3A). In contrast, tPA-treated mice had a significantly prolonged tail bleeding time in comparison to both vehicle and WE treatment. Blood volume lost from tPA-treated mice was more than three-fold greater than the blood loss from vehicle- or WE-treated mice (Figure 7.3B). These preliminary data provide the first evidence that administration of WE does not significantly interfere with the hemostasis of mice.

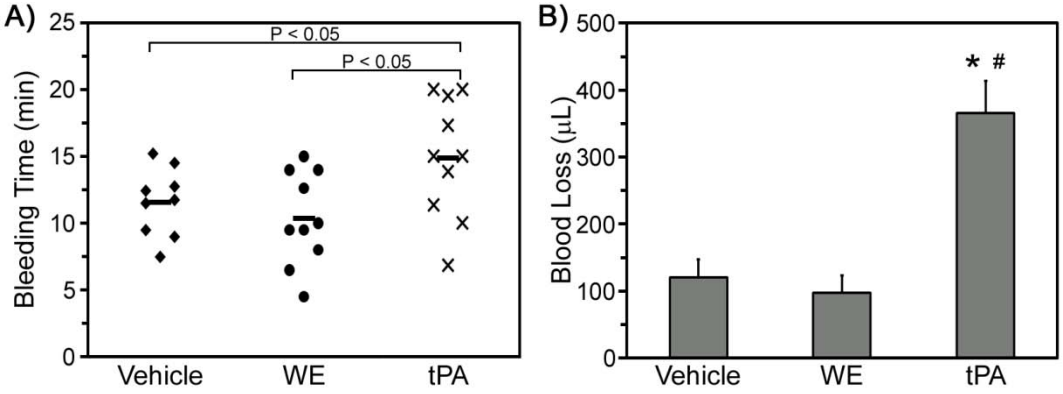

Figure 7.3. WE treatment does not increase bleeding time and blood loss. Anesthetized mice were administered a bolus of vehicle, WE (25 µg/kg), or tPA (2.5 mg/kg). Tails were transected where the diameter reached 1.5 mm and placed in a tube of water. The time until cessation of bleeding (A) and total volume of blood lost (B) were recorded. Mean bleeding times are indicated by the bold horizontal lines in A. Values are mean ± SEM. *P<0.05 versus vehicle. #P<0.05 versus WE. These experiments were conducted by Sawan Hurst and Erik Tucker of the Gruber laboratory.

Taken together, our preliminary data from MCAO studies suggest that WE has potential to improve neurological outcomes and reduce TTC-defined infarct size 24 hours after induction of ischemic stroke, with an efficacy comparable to tPA. Moreover, WE treatment 2 hours after MCAO may improve neurological performance over a period of 1

week. These studies show promise for WE treatment of ischemic stroke and prompt further investigations into the mechanisms of action of WE *in vivo*.

7.2 Characterize the fibrin(ogen) binding sites responsible for thrombin recruitment to thrombi under flow

In Chapter 4, studies were conducted to assess the localization of fibrin(ogen), FXa, prothrombin, and thrombin on thrombi formed under physiological shear flow. The results indicated that FXa and prothrombin associated with PS-exposing platelets, while thrombin was distributed over fibrin(ogen). The specificity and activity of thrombin is mediated by the occupancy of its 2 exosites (De Cristofaro, *et al.* 2003); therefore, thrombin-fibrin(ogen) interactions may have significant effects on the function of the enzyme. As thrombin is a critical mediator of thrombus formation, future studies will aim to determine the fibrin(ogen) binding sites required for thrombin-thrombi interactions. Thrombin binding sites on fibrin(ogen) are located on the Aα, Bβ, and γ chains, with a high affinity binding site on the alternatively spliced γ' chain (Meh, *et al.* 1996; Pospisil, *et al.* 2003). Clinical studies have indicated that elevated levels of γ' fibrinogen are associated with increased cardiovascular events, such as myocardial infarction (Lovely, *et al.* 2010; Mannila, *et al.* 2007). Importantly, when thrombin is bound to the γ' chain, it retains activity and is protected from inhibition by antithrombin (Weitz, *et al.* 1998). We hypothesize that the high affinity binding site on the γ' chain may play a critical role in supporting the binding of active thrombin to thrombi under physiologically relevant shear flow conditions. Future studies will use fibrinogen deficient plasmas reconstituted with specific fibrin(ogen) chains to test this hypothesis. Dissection of the molecular

mechanisms of thrombin binding to and retainment on thrombi will provide new insights into the role of thrombin in thrombus development and may provide an explanation for the increased cardiovascular events associated with high plasma γ' fibrinogen levels. These insights may reveal new drug targets for novel therapeutic agents designed to prevent the binding of active thrombin to thrombi for the prevention of thrombosis.

7.3 Extend the application of the *ex vivo* model of occlusive thrombus formation

Chapter 5 describes the development and characterization of an *ex vivo* model of occlusive thrombus formation on a collagen matrix. In accordance with animal models of occlusive thrombus formation, the time to occlusion was significantly increased by inhibitors of the platelet receptor $\alpha_{IIb}\beta_3$, inhibitors of thrombin or FXa, and by the anticoagulant APC. Therefore, this model provides an ideal platform for future studies to evaluate mechanisms of thrombus formation and to test the efficacy of antithrombotics.

To this accord, preliminary studies were conducted to determine the ability of immobilized laminin (a component of the ECM) or TF to support the development of occlusive thrombi under flow. In parallel to collagen (Figure 5.1), the results indicate that both laminin and TF support occlusive thrombus formation in a thrombin-dependent manner (Figure 7.4). Building upon these studies, future studies will be designed to determine the contribution of other ECM proteins, such as elastin and fibronectin, and platelet receptors, such as GPIb, to occlusive thrombus formation. Elucidation of cooperative roles of extracellular matrix proteins, platelet receptors, and coagulation

proteins in thrombus formation will provide a more complete picture of the molecular mechanisms of thrombus formation in the presence shear flow.

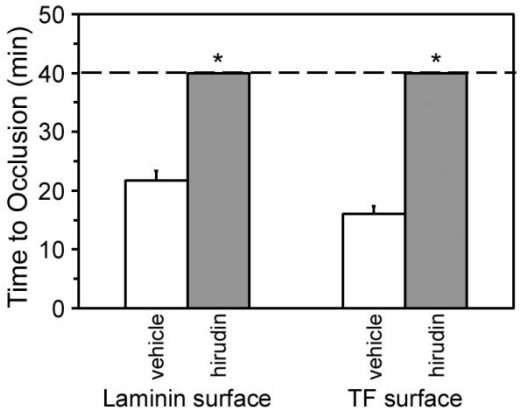

Figure 7.4. Immobilized laminin or tissue factor supports occlusive thrombus formation under a constant pressure gradient. Human whole blood in 0.38% sodium citrate was recalcified and perfused through a laminin- or tissue factor-coated glass capillary until occlusion. Blood flow was driven by a constant pressure difference. In selected experiments, blood was pretreated with vehicle or 20 μg/mL of the thrombin inhibitor, hirudin. Data are reported as mean ± SEM of at least three experiments. *P < 0.05 compared with occlusion time in the presence of vehicle on each respective surface. Figure adapted and reprinted with permission from John Wiley and Sons, Journal of Thrombosis and Haemostasis (White-Adams, *et al.* 2010).These experiments were performed by Ishan Patel and Patrick Simonson from the McCarty laboratory.

7.4 Characterization of the procoagulant activity of circulating tumor cells

Studies conducted in Chapter 6 utilized model cell lines to assess the procoagulant activity of breast tumor cells. The ability of breast tumor cells to promote clotting and support the formation of occlusive thrombi, support the hypothesis that the presence of procoagulant cancer cells in the vasculature (during metastasis) may contribute to cancer-associated thrombosis. In preliminary studies, circulating tumor cells were observed in peripheral blood samples from cancer patients (Figure 7.5). In contrast to leukocytes, which stain positive for CD45, a leukocyte-specific surface antigen (Kurtin, *et al.* 1985), circulating tumor cells stained positive for cytokeratin. As many malignancies are derived from epithelial tissue and these cytokeratin-positive cells are only observed in blood

samples from cancer patients, the cytokeratin positive cells are defined as circulating tumor cells (Chu, *et al.* 2000). To strengthen the link between the presence of circulating tumor cells and thrombosis, future studies will focus on characterizing the procoagulant activity of circulating tumor cells from cancer patient samples. In parallel to Chapter 6, determination of the ability of circulating tumor cells to support coagulation, the binding of coagulation factors, and the formation of occlusive thrombi will provide important new insights into the link between cancer and thrombosis.

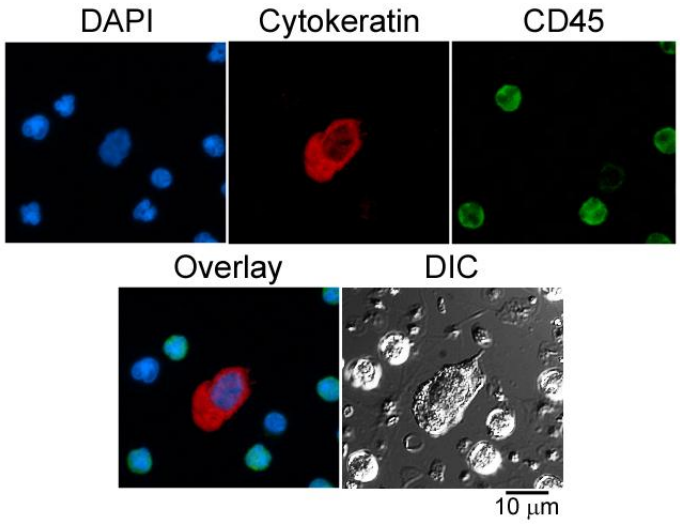

Figure 7.5. Single cell identification of a circulating tumor cell from a peripheral blood sample. Example of a pathologist-confirmed circulating tumor cell found in the peripheral blood of a prostate cancer patient. Top, fluorescent images of blood sample. The cell nuclei are stained *blue* with DAPI, the circulating tumor cell is stained with anti-cytokeratin AlexaFluor 555 (*red*), and leukocytes are stained with anti-CD45 (*green*). Bottom left, overlay image of DAPI, anti-cytokeratin, and anti-CD45 staining. Bottom right, differential interference contrast (DIC) image of the same field of view. These experiments and imaging were performed by Peter Kuhn's laboratory and Owen McCarty.

References

Aarts PA, van den Broek SA, Prins GW, Kuiken GD, Sixma JJ, Heethaar RM. Blood platelets are concentrated near the wall and red blood cells, in the center in flowing blood. *Arteriosclerosis*. 1988; 8:819-824.

Adams TE, Huntington JA. Thrombin-cofactor interactions: structural insights into regulatory mechanisms. *Arterioscler Thromb Vasc Biol*. 2006; 26:1738-1745.

Ahmad SS, London FS, Walsh PN. The assembly of the factor X-activating complex on activated human platelets. *J Thromb Haemost*. 2003; 1:48-59.

Ahmad SS, London FS, Walsh PN. Binding studies of the enzyme (factor IXa) with the cofactor (factor VIIIa) in the assembly of factor-X activating complex on the activated platelet surface. *J Thromb Haemost*. 2003; 1:2348-2355.

Ahn KC, Jun AJ, Pawar P, et al. Preferential binding of platelets to monocytes over neutrophils under flow. *Biochem Biophys Res Commun*. 2005; 329:345-355.

Anderson PJ, Nesset A, Bock PE. Effects of activation peptide bond cleavage and fragment 2 interactions on the pathway of exosite I expression during activation of human prethrombin 1 to thrombin. *J Biol Chem*. 2003; 278:44482-44488.

Andrews RK, Berndt MC. Platelet physiology and thrombosis. *Thromb Res*. 2004; 114:447-453.

Andrews RK, Lopez JA, Berndt MC. Molecular mechanisms of platelet adhesion and activation. *Int J Biochem Cell Biol*. 1997; 29:91-105.

Aslan JE, Thomas G. Death by committee: organellar trafficking and communication in apoptosis. *Traffic*. 2009; 10:1390-1404.

Auger JM, Kuijpers MJE, Senis YA, Watson SP, Heemskerk JWM. Adhesion of human and mouse platelets to collagen under shear: a unifying model. *FASEB J*. 2005; 19:825-827.

Awtry EH, Loscalzo J. Aspirin. *Circulation*. 2000; 101:1206-1218.

Ayala YM, Cantwell AM, Rose T, Bush LA, Arosio D, Di Cera E. Molecular mapping of thrombin-receptor interactions. *Proteins*. 2001; 45:107-116.

Baglia FA, Shrimpton CN, Emsley J, et al. Factor XI interacts with the leucine-rich repeats of glycoprotein Ib alpha on the activated platelet. *J Biol Chem*. 2004; 279:49323-49329.

Beguin S, Kumar R. Thrombin, fibrin and platelets, a resonance loop in which von Willebrand factor is a necessary link. *Thromb Haemost*. 1997; 78:590-594.

Bergmeier W, Stefanini L. Novel molecules in calcium signaling in platelets. *J Thromb Haemost*. 2009; 7 Suppl 1:187-190.

Bevers EM, Comfurius P, van Rijn JL, Hemker HC, Zwaal RF. Generation of prothrombin-converting activity and the exposure of phosphatidylserine at the outer surface of platelets. *Eur J Biochem*. 1982; 122:429-436.

Bevers EM, Comfurius P, Zwaal RF. Changes in membrane phospholipid distribution during platelet activation. *Biochim Biophys Acta*. 1983; 736:57-66.

Biondi-Zoccai GG, Abbate A, Liuzzo G, Biasucci LM. Atherothrombosis, inflammation, and diabetes. *J Am Coll Cardiol*. 2003; 41:1071-1077.

Blair P, Flaumenhaft R. Platelet alpha-granules: basic biology and clinical correlates. *Blood Rev*. 2009; 23:177-189.

Blom JW, Doggen CJ, Osanto S, Rosendaal FR. Malignancies, prothrombotic mutations, and the risk of venous thrombosis. *JAMA*. 2005; 293:715-722.

Blomback B, Hessel B, Hogg D, Therkildsen L. A two-step fibrinogen--fibrin transition in blood coagulation. *Nature*. 1978; 275:501-505.

Bock PE. Active-site-selective labeling of blood coagulation proteinases with fluorescence probes by the use of thioester peptide chloromethyl ketones. II. Properties of thrombin derivatives as reporters of prothrombin fragment 2 binding and specificity of the labeling approach for other proteinases. *J Biol Chem*. 1992; 267:14974-14981.

Bodary PF, Eitzman DT. Animal models of thrombosis. *Curr Opin Hematol*. 2009; 16:342-346.

Borsig L. The role of platelet activation in tumor metastasis. *Expert Rev Anticancer Ther*. 2008; 8:1247-1255.

Bouchard BA, Tracy PB. The participation of leukocytes in coagulant reactions. *J Thromb Haemost*. 2003; 1:464-469.

Bouillard JB, Bouillard S. De l'Obliteration des veines et de son influence sur la formation des hydropisies partielles: consideration sur la hydropisies passive et general. *Arch Gen Med*. 1823; 1:188-204.

Braun S, Pantel K, Muller P, et al. Cytokeratin-positive cells in the bone marrow and survival of patients with stage I, II, or III breast cancer. *N Engl J Med*. 2000; 342:525-533.

Butenas S, Branda RF, van't Veer C, Cawthern KM, Mann KG. Platelets and phospholipids in tissue factor-initiated thrombin generation. *Thromb Haemost*. 2001; 86:660-667.

Cailleau R, Mackay B, Young RK, Reeves WJ, Jr. Tissue culture studies on pleural effusions from breast carcinoma patients. *Cancer Res*. 1974; 34:801-809.

Calaminus SD, McCarty OJ, Auger JM, et al. A major role for Scar/WAVE-1 downstream of GPVI in platelets. *J Thromb Haemost*. 2007; 5:535-541.

Camerer E, Kolsto AB, Prydz H. Cell biology of tissue factor, the principal initiator of blood coagulation. *Thromb Res*. 1996; 81:1-41.

Camerer E, Qazi AA, Duong DN, Cornelissen I, Advincula R, Coughlin SR. Platelets, protease-activated receptors, and fibrinogen in hematogenous metastasis. *Blood*. 2004; 104:397-401.

Cantwell AM, Di Cera E. Rational design of a potent anticoagulant thrombin. *J Biol Chem*. 2000; 275:39827-39830.

Celi A, Merrill-Skoloff G, Gross P, et al. Thrombus formation: direct real-time observation and digital analysis of thrombus assembly in a living mouse by confocal and widefield intravital microscopy. *J Thromb Haemost*. 2003; 1:60-68.

Celikel R, McClintock RA, Roberts JR, et al. Modulation of alpha-thrombin function by distinct interactions with platelet glycoprotein Ib alpha. *Science*. 2003; 301:218-221.

Chiang AC, Massague J. Molecular basis of metastasis. *N Engl J Med*. 2008; 359:2814-2823.

Chu P, Wu E, Weiss LM. Cytokeratin 7 and cytokeratin 20 expression in epithelial neoplasms: a survey of 435 cases. *Mod Pathol*. 2000; 13:962-972.

Coller BS. Interaction of normal, thrombasthenic, and Bernard-Soulier platelets with immobilized fibrinogen: defective platelet-fibrinogen interaction in thrombasthenia. *Blood*. 1980; 55:169-178.

Coughlin SR. Protease-activated receptors in hemostasis, thrombosis and vascular biology. *J Thromb Haemost*. 2005; 3:1800-1814.

Crawley JT, Lane DA. The haemostatic role of tissue factor pathway inhibitor. *Arterioscler Thromb Vasc Biol*. 2008; 28:233-242.

Crawley JT, Zanardelli S, Chion CK, Lane DA. The central role of thrombin in hemostasis. *J Thromb Haemost*. 2007; 5 Suppl 1:95-101.

Dachary-Prigent J, Pasquet JM, Freyssinet JM, Nurden AT. Calcium involvement in aminophospholipid exposure and microparticle formation during platelet activation, a study using Ca^{2+}-ATPase inhibitors. *Biochemistry*. 1995; 34:11625-11634.

Dahl JP, Wang-Dunlop J, Gonzales C, Goad ME, Mark RJ, Kwak SP. Characterization of the WAVE1 knock-out mouse: implications for CNS development. *J Neurosci*. 2003; 23:3343-3352.

Dahlback B, Villoutreix BO. Regulation of blood coagulation by the protein C anticoagulant pathway: novel insights into structure-function relationships and molecular recognition. *Arterioscler Thromb Vasc Biol*. 2005; 25:1311-1320.

Davie EW, Kulman JD. An overview of the structure and function of thrombin. *Semin Thromb Hemost*. 2006; 32 Suppl 1:3-15.

De Candia E, Hall SW, Rutella S, Landolfi R, Andrews RK, De Cristofaro R. Binding of thrombin to glycoprotein Ib accelerates the hydrolysis of Par-1 on intact platelets. *J Biol Chem*. 2001; 276:4692-4698.

De Cristofaro R, De Candia E. Thrombin domains: structure, function and interaction with platelet receptors. *J Thromb Thrombolysis*. 2003; 15:151-163.

De Cristofaro R, De Candia E, Landolfi R, Rutella S, Hall SW. Structural and functional mapping of the thrombin domain involved in the binding to the platelet glycoprotein Ib. *Biochemistry*. 2001; 40:13268-13273.

Denis CV, Wagner DD. Platelet adhesion receptors and their ligands in mouse models of thrombosis. *Arterioscler Thromb Vasc Biol*. 2007; 27:728-739.

Di Cera E. Thrombin interactions. *Chest*. 2003; 124:11S-17S.

Di Cera E. Thrombin as procoagulant and anticoagulant. *J Thromb Haemost*. 2007; 5 Suppl 1:196-202.

Di Cera E, Cantwell AM. Determinants of thrombin specificity. *Ann N Y Acad Sci*. 2001; 936:133-146.

Di Cera E, Page MJ, Bah A, Bush-Pelc LA, Garvey LC. Thrombin allostery. *Phys Chem Chem Phys*. 2007; 9:1291-1306.

Doggett TA, Girdhar G, Lawshe A, et al. Selectin-like kinetics and biomechanics promote rapid platelet adhesion in flow: the GPIb(alpha)-vWF tether bond. *Biophys J*. 2002; 83:194-205.

Dong JF, Berndt MC, Schade A, McIntire LV, Andrews RK, Lopez JA. Ristocetin-dependent, but not botrocetin-dependent, binding of von Willebrand factor to the platelet glycoprotein Ib-IX-V complex correlates with shear-dependent interactions. *Blood*. 2001; 97:162-168.

Dong JF, Li CQ, Lopez JA. Tyrosine sulfation of the glycoprotein Ib-IX complex: identification of sulfated residues and effect on ligand binding. *Biochemistry*. 1994; 33:13946-13953.

Doroszewski J, Skierski J, Przadka L. Interaction of neoplastic cells with glass surface under flow conditions. *Exp Cell Res*. 1977; 104:335-343.

Dubois C, Panicot-Dubois L, Gainor JF, Furie BC, Furie B. Thrombin-initiated platelet activation in vivo is vWF independent during thrombus formation in a laser injury model. *J Clin Invest*. 2007; 117:953-960.

Dumas JJ, Kumar R, Seehra J, Somers WS, Mosyak L. Crystal structure of the GpIb alpha-thrombin complex essential for platelet aggregation. *Science*. 2003; 301:222-226.

Esmon CT, Owen WG. Identification of an endothelial cell cofactor for thrombin-catalyzed activation of protein C. *Proc Natl Acad Sci U S A*. 1981; 78:2249-2252.

Even-Ram S, Uziely B, Cohen P, et al. Thrombin receptor overexpression in malignant and physiological invasion processes. *Nat Med*. 1998; 4:909-914.

Falati S, Gross P, Merrill-Skoloff G, Furie BC, Furie B. Real-time in vivo imaging of platelets, tissue factor and fibrin during arterial thrombus formation in the mouse. *Nat Med*. 2002; 8:1175-1181.

Ferry JD. The mechanism of polymerization of fibrin. *Proc Natl Acad Sci U S A*. 1952; 38:566-569.

Forrester JV, Lackie JM. Adhesion of neutrophil leucocytes under conditions of flow. *J Cell Sci*. 1984; 70:93-110.

Fredenburgh JC, Stafford AR, Leslie BA, Weitz JI. Bivalent binding to gammaA/gamma'-fibrin engages both exosites of thrombin and protects it from inhibition by the antithrombin-heparin complex. *J Biol Chem*. 2008; 283:2470-2477.

Fulcher CA, Gardiner JE, Griffin JH, Zimmerman TS. Proteolytic inactivation of human factor VIII procoagulant protein by activated human protein C and its analogy with factor V. *Blood*. 1984; 63:486-489.

Furie B, Furie BC. Thrombus formation in vivo. *J Clin Invest*. 2005; 115:3355-3362.

Furie B, Furie BC. In vivo thrombus formation. *J Thromb Haemost*. 2007; 5 Suppl 1:12-17.

Furie B, Furie BC. Mechanisms of thrombus formation. *N Engl J Med*. 2008; 359:938-949.

Furie B, Furie BC, Flaumenhaft R. A journey with platelet P-selectin: the molecular basis of granule secretion, signalling and cell adhesion. *Thromb Haemost*. 2001; 86:214-221.

Garcia D, Crowther MA, Ageno W. Practical management of coagulopathy associated with warfarin. *BMJ*. 2010; 340:c1813.

George JN, Reimann TA, Moake JL, Morgan RK, Cimo PL, Sears DA. Bernard-Soulier disease: a study of four patients and their parents. *Br J Haematol*. 1981; 48:459-467.

Gorog P. A new, ideal technique to monitor thrombolytic therapy. *Angiology*. 1986; 37:99-105.

Gorog P, Ahmed A. Haemostatometer: a new in vitro technique for assessing haemostatic activity of blood. *Thromb Res*. 1984; 34:341-357.

Gray E, Mulloy B, Barrowcliffe TW. Heparin and low-molecular-weight heparin. *Thromb Haemost*. 2008; 99:807-818.

Gruber A, Cantwell AM, Di Cera E, Hanson SR. The thrombin mutant W215A/E217A shows safe and potent anticoagulant and antithrombotic effects in vivo. *J Biol Chem*. 2002; 277:27581-27584.

Gruber A, Marzec UM, Bush L, et al. Relative antithrombotic and antihemostatic effects of protein C activator versus low-molecular-weight heparin in primates. *Blood*. 2007; 109:3733-3740.

Gunay-Aygun M, Huizing M, Gahl WA. Molecular defects that affect platelet dense granules. *Semin Thromb Hemost*. 2004; 30:537-547.

Hacke W, Kaste M, Fieschi C, et al. Intravenous thrombolysis with recombinant tissue plasminogen activator for acute hemispheric stroke. The European Cooperative Acute Stroke Study (ECASS). *JAMA*. 1995; 274:1017-1025.

Hallam TJ, Rink TJ. Agonists stimulate divalent cation channels in the plasma membrane of human platelets. *FEBS Lett*. 1985; 186:175-179.

Harker LA, Kelly AB, Hanson SR. Experimental arterial thrombosis in nonhuman primates. *Circulation*. 1991; 83:IV41-55.

Heemskerk JW, Bevers EM, Lindhout T. Platelet activation and blood coagulation. *Thromb Haemost*. 2002; 88:186-193.

Heit JA, Mohr DN, Silverstein MD, Petterson TM, O'Fallon WM, Melton LJ, 3rd. Predictors of recurrence after deep vein thrombosis and pulmonary embolism: a population-based cohort study. *Arch Intern Med*. 2000; 160:761-768.

Hemker HC, Giesen PLA, Ramjee M, Wagenvoord R, Béguin S. The thrombogram: monitoring thrombin generation in platelet rich plasma. *Thromb Haemost*. 2000; 83:589-591.

Henrikson KP, Salazar SL, Fenton JW, 2nd, Pentecost BT. Role of thrombin receptor in breast cancer invasiveness. *Br J Cancer*. 1999; 79:401-406.

Hirata M, Hayashi Y, Ushikubi F, et al. Cloning and expression of cDNA for a human thromboxane A2 receptor. *Nature*. 1991; 349:617-620.

Huntington JA. Slow thrombin is zymogen-like. *J Thromb Haemost*. 2009; 7 Suppl 1:159-164.

Inauen W, Baumgartner HR, Bombeli T, Haeberli A, Straub PW. Dose- and shear rate-dependent effects of heparin on thrombogenesis induced by rabbit aorta subendothelium exposed to flowing human blood. *Arteriosclerosis*. 1990; 10:607-615.

Inoue O, Suzuki-Inoue K, McCarty OJT, et al. Laminin stimulates spreading of platelets through integrin {alpha}6beta1-dependent activation of GPVI. *Blood*. 2006; 107:1405-1412.

Italiano JE, Jr., Lecine P, Shivdasani RA, Hartwig JH. Blood platelets are assembled principally at the ends of proplatelet processes produced by differentiated megakaryocytes. *J Cell Biol*. 1999; 147:1299-1312.

Jackson SP. The growing complexity of platelet aggregation. *Blood*. 2007; 109:5087-5095.

Jackson SP, Schoenwaelder SM. Antiplatelet therapy: in search of the 'magic bullet'. *Nat Rev Drug Discov*. 2003; 2:775-789.

Jardin I, Ben Amor N, Bartegi A, Pariente JA, Salido GM, Rosado JA. Differential involvement of thrombin receptors in Ca2+ release from two different intracellular stores in human platelets. *Biochem J*. 2007; 401:167-174.

Jin J, Tomlinson W, Kirk IP, Kim YB, Humphries RG, Kunapuli SP. The C6-2B glioma cell P2Y(AC) receptor is pharmacologically and molecularly identical to the platelet P2Y(12) receptor. *Br J Pharmacol*. 2001; 133:521-528.

Kahn ML, Nakanishi-Matsui M, Shapiro MJ, Ishihara H, Coughlin SR. Protease-activated receptors 1 and 4 mediate activation of human platelets by thrombin. *J Clin Invest*. 1999; 103:879-887.

Kakkar AK, Lemoine NR, Scully MF, Tebbutt S, Williamson RC. Tissue factor expression correlates with histological grade in human pancreatic cancer. *Br J Surg*. 1995; 82:1101-1104.

Kalia N, Auger JM, Atkinson B, Watson SP. Critical role of FcR gamma-chain, LAT, PLCgamma2 and thrombin in arteriolar thrombus formation upon mild, laser-induced endothelial injury in vivo. *Microcirculation*. 2008; 15:325-335.

Kamath P, Krishnaswamy S. Fate of membrane-bound reactants and products during the activation of human prothrombin by prothrombinase. *J Biol Chem*. 2008; 283:30164-30173.

Kaneko N, Matsuda R, Hosoda S, Kajita T, Ohta Y. Measurement of plasma annexin V by ELISA in the early detection of acute myocardial infarction. *Clin Chim Acta*. 1996; 251:65-80.

Katritsis D, Kaiktsis L, Chaniotis A, Pantos J, Efstathopoulos EP, Marmarelis V. Wall shear stress: theoretical considerations and methods of measurement. *Prog Cardiovasc Dis*. 2007; 49:307-329.

Keuren JF, Wielders SJ, Ulrichts H, et al. Synergistic effect of thrombin on collagen-induced platelet procoagulant activity is mediated through protease-activated receptor-1. *Arterioscler Thromb Vasc Biol*. 2005; 25:1499-1505.

Kirchhofer D, Riederer MA, Baumgartner HR. Specific accumulation of circulating monocytes and polymorphonuclear leukocytes on platelet thrombi in a vascular injury model. *Blood*. 1997; 89:1270-1278.

Kisiel W, Canfield WM, Ericsson LH, Davie EW. Anticoagulant properties of bovine plasma protein C following activation by thrombin. *Biochemistry*. 1977; 16:5824-5831.

Kratzer MA, Born GV. Simulation of primary haemostasis in vitro. *Haemostasis*. 1985; 15:357-362.

Krem MM, Di Cera E. Dissecting substrate recognition by thrombin using the inactive mutant S195A. *Biophys Chem*. 2003; 100:315-323.

Krishnaswamy S, Church WR, Nesheim ME, Mann KG. Activation of human prothrombin by human prothrombinase. Influence of factor Va on the reaction mechanism. *J Biol Chem*. 1987; 262:3291-3299.

Kroll MH, Hellums JD, McIntire LV, Schafer AI, Moake JL. Platelets and shear stress. *Blood*. 1996; 88:1525-1541.

Kuijpers MJ, Munnix IC, Cosemans JM, et al. Key role of platelet procoagulant activity in tissue factor-and collagen-dependent thrombus formation in arterioles and venules in vivo differential sensitivity to thrombin inhibition. *Microcirculation*. 2008; 15:269-282.

Kulkarni S, Dopheide SM, Yap CL, et al. A revised model of platelet aggregation. *J Clin Invest*. 2000; 105:783-791.

Kurtin PJ, Pinkus GS. Leukocyte common antigen--a diagnostic discriminant between hematopoietic and nonhematopoietic neoplasms in paraffin sections using monoclonal antibodies: correlation with immunologic studies and ultrastructural localization. *Hum Pathol*. 1985; 16:353-365.

Lane DA, Philippou H, Huntington JA. Directing thrombin. *Blood*. 2005; 106:2605-2612.

Lawrence MB, McIntire LV, Eskin SG. Effect of flow on polymorphonuclear leukocyte/endothelial cell adhesion. *Blood*. 1987; 70:1284-1290.

Lawson JH, Mann KG. Cooperative activation of human factor IX by the human extrinsic pathway of blood coagulation. *J Biol Chem*. 1991; 266:11317-11327.

Leon C, Alex M, Klocke A, et al. Platelet ADP receptors contribute to the initiation of intravascular coagulation. *Blood*. 2004; 103:594-600.

Leon C, Hechler B, Vial C, Leray C, Cazenave JP, Gachet C. The P2Y1 receptor is an ADP receptor antagonized by ATP and expressed in platelets and megakaryoblastic cells. *FEBS Lett*. 1997; 403:26-30.

Liddington RC, Ginsberg MH. Integrin activation takes shape. *J Cell Biol*. 2002; 158:833-839.

Lipowsky HH, Kovalcheck S, Zweifach BW. The distribution of blood rheological parameters in the microvasculature of cat mesentery. *Circ Res*. 1978; 43:738-749.

Lipowsky HH, Usami S, Chien S. In vivo measurements of "apparent viscosity" and microvessel hematocrit in the mesentery of the cat. *Microvasc Res*. 1980; 19:297-319.

Lloyd-Jones D, Adams RJ, Brown TM, et al. Heart disease and stroke statistics--2010 update: a report from the American Heart Association. *Circulation*. 2010; 121:e46-e215.

Lord ST. Fibrinogen and fibrin: scaffold proteins in hemostasis. *Curr Opin Hematol*. 2007; 14:236-241.

Lovelock CE, Cordonnier C, Naka H, et al. Antithrombotic drug use, cerebral microbleeds, and intracerebral hemorrhage: a systematic review of published and unpublished studies. *Stroke*. 2010; 41:1222-1228.

Lovely RS, Falls LA, Al-Mondhiry HA, et al. Association of gammaA/gamma' fibrinogen levels and coronary artery disease. *Thromb Haemost*. 2002; 88:26-31.

Lovely RS, Kazmierczak SC, Massaro JM, D'Agostino RB, Sr., O'Donnell CJ, Farrell DH. Gamma' fibrinogen: evaluation of a new assay for study of associations with cardiovascular disease. *Clin Chem*. 2010; 56:781-788.

Lovely RS, Rein CM, White TC, et al. gammaA/gamma' fibrinogen inhibits thrombin-induced platelet aggregation. *Thromb Haemost*. 2008; 100:837-846.

Maas C, Meijers JCM, Marquart JA, et al. Activated factor V is a cofactor for the activation of factor XI by thrombin in plasma. *Proc Natl Acad Sci U S A*. 2010; 107:9083-9087.

Mackman N. The many faces of tissue factor. *J Thromb Haemost*. 2009; 7 Suppl 1:136-139.

Mann KG. Adding the vessel wall to Virchow's triad. *J Thromb and Haemost*. 2006; 4:58-59.

Mann KG, Butenas S, Brummel K. The dynamics of thrombin formation. *Arterioscler Thromb Vasc Biol*. 2003; 23:17-25.

Mannila MN, Lovely RS, Kazmierczak SC, et al. Elevated plasma fibrinogen gamma' concentration is associated with myocardial infarction: effects of variation in fibrinogen genes and environmental factors. *J Thromb Haemost*. 2007; 5:766-773.

Marguerie GA, Plow EF, Edgington TS. Human platelets possess an inducible and saturable receptor specific for fibrinogen. *J Biol Chem*. 1979; 254:5357-5363.

Masuda J, Takayama E, Satoh A, et al. Levels of annexin IV and V in the plasma of pregnant and postpartum women. *Thromb Haemost*. 2004; 91:1129-1136.

McCarty OJ, Abulencia JP, Mousa SA, Konstantopoulos K. Evaluation of platelet antagonists in in vitro flow models of thrombosis. *Methods Mol Med*. 2004; 93:21-34.

McCarty OJ, Larson MK, Auger JM, et al. Rac1 is essential for platelet lamellipodia formation and aggregate stability under flow. *J Biol Chem*. 2005; 280:39474-39484.

McCarty OJ, Mousa SA, Bray PF, Konstantopoulos K. Immobilized platelets support human colon carcinoma cell tethering, rolling, and firm adhesion under dynamic flow conditions. *Blood*. 2000; 96:1789-1797.

McCarty OJ, Zhao Y, Andrew N, et al. Evaluation of the role of platelet integrins in fibronectin-dependent spreading and adhesion. *J Thromb Haemost*. 2004; 2:1823-1833.

McNicol A, Israels SJ. Platelet dense granules: structure, function and implications for haemostasis. *Thromb Res*. 1999; 95:1-18.

Meh DA, Siebenlist KR, Mosesson MW. Identification and characterization of the thrombin binding sites on fibrin. *J Biol Chem*. 1996; 271:23121-23125.

Moroi M, Jung SM, Okuma M, Shinmyozu K. A patient with platelets deficient in glycoprotein VI that lack both collagen-induced aggregation and adhesion. *J Clin Invest*. 1989; 84:1440-1445.

Mosesson MW. Fibrinogen and fibrin structure and functions. *J Thromb Haemost*. 2005; 3:1894-1904.

Mosesson MW, Finlayson JS, Umfleet RA. Human fibrinogen heterogeneities. 3. Identification of chain variants. *J Biol Chem*. 1972; 247:5223-5227.

Muga KM, Melton LG, Gabriel DA. A flow dynamic technique used to assess global haemostasis. *Blood Coagul Fibrinolysis*. 1995; 6:73-78.

Munnix IC, Kuijpers MJ, Auger J, et al. Segregation of platelet aggregatory and procoagulant microdomains in thrombus formation: regulation by transient integrin activation. *Arterioscler Thromb Vasc Biol*. 2007; 27:2484-2490.

Nachman RL, Leung LL. Complex formation of platelet membrane glycoproteins IIb and IIIa with fibrinogen. *J Clin Invest*. 1982; 69:263-269.

Najean Y, Ardaillou N, Dresch C. Platelet lifespan. *Annu Rev Med*. 1969; 20:47-62.

Nesbitt WS, Kulkarni S, Giuliano S, et al. Distinct glycoprotein Ib/V/IX and integrin alpha IIb beta 3-dependent calcium signals cooperatively regulate platelet adhesion under flow. *J Biol Chem*. 2002; 277:2965-2972.

Nesbitt WS, Westein E, Tovar-Lopez FJ, et al. A shear gradient-dependent platelet aggregation mechanism drives thrombus formation. *Nat Med*. 2009; 15:665-673.

Ni H, Denis CV, Subbarao S, et al. Persistence of platelet thrombus formation in arterioles of mice lacking both von Willebrand factor and fibrinogen. *J Clin Invest*. 2000; 106:385-392.

Ni H, Papalia JM, Degen JL, Wagner DD. Control of thrombus embolization and fibronectin internalization by integrin alpha IIb beta 3 engagement of the fibrinogen gamma chain. *Blood*. 2003; 102:3609-3614.

Noble S, Pasi J. Epidemiology and pathophysiology of cancer-associated thrombosis. *Br J Cancer*. 2010; 102 Suppl 1:S2-9.

Offermanns S. Activation of platelet function through G protein-coupled receptors. *Circ Res*. 2006; 99:1293-1304.

Otten HM, Prins MH. Venous thromboembolism and occult malignancy. *Thromb Res*. 2001; 102:V187-194.

Panizzi P, Friedrich R, Fuentes-Prior P, et al. Novel fluorescent prothrombin analogs as probes of staphylocoagulase-prothrombin interactions. *J Biol Chem*. 2006; 281:1169-1178.

Papaioannou TG, Stefanadis C. Vascular wall shear stress: basic principles and methods. *Hellenic J Cardiol*. 2005; 46:9-15.

Paul BZ, Jin J, Kunapuli SP. Molecular mechanism of thromboxane A(2)-induced platelet aggregation. Essential role for p2t(ac) and alpha(2a) receptors. *J Biol Chem*. 1999; 274:29108-29114.

Phillips DR, Conley PB, Sinha U, Andre P. Therapeutic approaches in arterial thrombosis. *J Thromb Haemost*. 2005; 3:1577-1589.

Pieters J, Lindhout T, Hemker HC. In situ-generated thrombin is the only enzyme that effectively activates factor VIII and factor V in thromboplastin-activated plasma. *Blood*. 1989; 74:1021-1024.

Pineda AO, Chen ZW, Caccia S, et al. The anticoagulant thrombin mutant W215A/E217A has a collapsed primary specificity pocket. *J Biol Chem*. 2004; 279:39824-39828.

Pospisil CH, Stafford AR, Fredenburgh JC, Weitz JI. Evidence that both exosites on thrombin participate in its high affinity interaction with fibrin. *J Biol Chem*. 2003; 278:21584-21591.

Radomski MW, Palmer RM, Moncada S. The anti-aggregating properties of vascular endothelium: interactions between prostacyclin and nitric oxide. *Br J Pharmacol*. 1987; 92:639-646.

Ramakrishnan V, DeGuzman F, Bao M, Hall SW, Leung LL, Phillips DR. A thrombin receptor function for platelet glycoprotein Ib-IX unmasked by cleavage of glycoprotein V. *Proc Natl Acad Sci U S A*. 2001; 98:1823-1828.

Ratnoff OD, Bennett B. The genetics of hereditary disorders of blood coagulation. *Science*. 1973; 179:1291-1298.

Reed GL. Platelet secretory mechanisms. *Semin Thromb Hemost*. 2004; 30:441-450.

Renne T, Nieswandt B, Gailani D. The intrinsic pathway of coagulation is essential for thrombus stability in mice. *Blood Cells Mol Dis*. 2006; 36:148-151.

Renne T, Pozgajova M, Gruner S, et al. Defective thrombus formation in mice lacking coagulation factor XII. *J Exp Med*. 2005; 202:271-281.

Ribes JA, Ni F, Wagner DD, Francis CW. Mediation of fibrin-induced release of von Willebrand factor from cultured endothelial cells by the fibrin beta chain. *J Clin Invest*. 1989; 84:435-442.

Rick ME, Hoyer LW. Thrombin activation of factor VIII. II. A comparison of purified factor VIII and the low molecular weight factor VIII procoagulant. *Br J Haematol*. 1978; 38:107-119.

Ruggeri ZM, Bader R, de Marco L. Glanzmann thrombasthenia: deficient binding of von Willebrand factor to thrombin-stimulated platelets. *Proc Natl Acad Sci U S A*. 1982; 79:6038-6041.

Sadler JE. Structural biology. A menage a trois in two configurations. *Science*. 2003; 301:177-179.

Santoro SA, Rajpara SM, Staatz WD, Woods VL, Jr. Isolation and characterization of a platelet surface collagen binding complex related to VLA-2. *Biochem Biophys Res Commun*. 1988; 153:217-223.

Sebastiano C, Bromberg M, Breen K, Hurford MT. Glanzmann's thrombasthenia: report of a case and review of the literature. *Int J Clin Exp Pathol*. 2010; 3:443-447.

Segal JB, Brotman DJ, Necochea AJ, et al. Predictive value of factor V Leiden and prothrombin G20210A in adults with venous thromboembolism and in family members of those with a mutation: a systematic review. *JAMA*. 2009; 301:2472-2485.

Segers O, Castoldi E. Factor V Leiden and activated protein C resistance. *Adv Clin Chem*. 2009; 49:121-157.

Shearer MJ. Vitamin K and vitamin K-dependent proteins. *Br J Haematol*. 1990; 75:156-162.

Shen Y, Cranmer SL, Aprico A, et al. Leucine-rich repeats 2-4 (Leu60-Glu128) of platelet glycoprotein Ib alpha regulate shear-dependent cell adhesion to von Willebrand factor. *J Biol Chem*. 2006; 281:26419-26423.

Shen YM, Frenkel EP. Thrombosis and a hypercoagulable state in HIV-infected patients. *Clin Appl Thromb Hemost*. 2004; 10:277-280.

Siebenlist KR, Meh DA, Mosesson MW. Protransglutaminase (factor XIII) mediated crosslinking of fibrinogen and fibrin. *Thromb Haemost*. 2001; 86:1221-1228.

Siljander PR, Munnix IC, Smethurst PA, et al. Platelet receptor interplay regulates collagen-induced thrombus formation in flowing human blood. *Blood*. 2004; 103:1333-1341.

Sorensen HT, Mellemkjaer L, Olsen JH, Baron JA. Prognosis of cancers associated with venous thromboembolism. *N Engl J Med*. 2000; 343:1846-1850.

Soslau G, Class R, Morgan DA, et al. Unique pathway of thrombin-induced platelet aggregation mediated by glycoprotein Ib. *J Biol Chem*. 2001; 276:21173-21183.

Soule HD, Maloney TM, Wolman SR, et al. Isolation and characterization of a spontaneously immortalized human breast epithelial cell line, MCF-10. *Cancer Res*. 1990; 50:6075-6086.

Sporn LA, Marder VJ, Wagner DD. Inducible secretion of large, biologically potent von Willebrand factor multimers. *Cell*. 1986; 46:185-190.

Stahl S, Weitzman S, Jones JC. The role of laminin-5 and its receptors in mammary epithelial cell branching morphogenesis. *J Cell Sci*. 1997; 110 (Pt 1):55-63.

Sunnerhagen M, Forsen S, Hoffren AM, Drakenberg T, Teleman O, Stenflo J. Structure of the Ca(2+)-free Gla domain sheds light on membrane binding of blood coagulation proteins. *Nat Struct Biol*. 1995; 2:504-509.

Suzuki K, Dahlback B, Stenflo J. Thrombin-catalyzed activation of human coagulation factor V. *J Biol Chem*. 1982; 257:6556-6564.

Svensson J, Hamberg M, Samuelsson B. On the formation and effects of thromboxane A2 in human platelets. *Acta Physiol Scand*. 1976; 98:285-294.

Tabrizi P, Wang L, Seeds N, et al. Tissue plasminogen activator (tPA) deficiency exacerbates cerebrovascular fibrin deposition and brain injury in a murine stroke model:

studies in tPA-deficient mice and wild-type mice on a matched genetic background. *Arterioscler Thromb Vasc Biol*. 1999; 19:2801-2806.

Tesselaar ME, Romijn FP, Van Der Linden IK, Prins FA, Bertina RM, Osanto S. Microparticle-associated tissue factor activity: a link between cancer and thrombosis? *J Thromb Haemost*. 2007; 5:520-527.

Thornber K, McCarty OJ, Watson SP, Pears CJ. Distinct but critical roles for integrin alphaIIbbeta3 in platelet lamellipodia formation on fibrinogen, collagen-related peptide and thrombin. *FEBS J*. 2006; 273:5032-5043.

Tozeren A, Kleinman HK, Grant DS, Morales D, Mercurio AM, Byers SW. E-selectin-mediated dynamic interactions of breast- and colon-cancer cells with endothelial-cell monolayers. *Int J Cancer*. 1995; 60:426-431.

Tracy PB, Eide LL, Mann KG. Human prothrombinase complex assembly and function on isolated peripheral blood cell populations. *J Biol Chem*. 1985; 260:2119-2124.

Trousseau A. Phlegmasia alba dolens. Clinique Medicale de l'Hotel-Dieu de Paris. Paris, France: The Syndenham Society; 1865:654-712.

Tucker EI, Marzec UM, White TC, et al. Prevention of vascular graft occlusion and thrombus-associated thrombin generation by inhibition of factor XI. *Blood*. 2009; 113:936-944.

Utsugi T, Schroit AJ, Connor J, Bucana CD, Fidler IJ. Elevated expression of phosphatidylserine in the outer membrane leaflet of human tumor cells and recognition by activated human blood monocytes. *Cancer Res*. 1991; 51:3062-3066.

van der P, Vloedgraven H, Papapoulos S, et al. Attachment characteristics and involvement of integrins in adhesion of breast cancer cell lines to extracellular bone matrix components. *Lab Invest*. 1997; 77:665-675.

Vanschoonbeek K, Feijge MAH, van Kampen RJW, et al. Initiating and potentiating roles of platelets in tissue factor-induced thrombin generation in the presence of plasma: subject-dependent variation in thrombogram characteristics. *J Thromb Haemost*. 2004; 2:476-484.

Vicente V, Houghten RA, Ruggeri ZM. Identification of a site in the alpha chain of platelet glycoprotein Ib that participates in von Willebrand factor binding. *J Biol Chem*. 1990; 265:274-280.

Wagner CL, Mascelli MA, Neblock DS, Weisman HF, Coller BS, Jordan RE. Analysis of GPIIb/IIIa receptor number by quantification of 7E3 binding to human platelets. *Blood*. 1996; 88:907-914.

Walker FJ, Sexton PW, Esmon CT. The inhibition of blood coagulation by activated Protein C through the selective inactivation of activated Factor V. *Biochim Biophys Acta*. 1979; 571:333-342.

Walmsley MJ, Ooi SK, Reynolds LF, et al. Critical roles for Rac1 and Rac2 GTPases in B cell development and signaling. *Science*. 2003; 302:459-462.

Ward CM, Andrews RK, Smith AI, Berndt MC. Mocarhagin, a novel cobra venom metalloproteinase, cleaves the platelet von Willebrand factor receptor glycoprotein Ib alpha. Identification of the sulfated tyrosine/anionic sequence Tyr-276-Glu-282 of glycoprotein Ib alpha as a binding site for von Willebrand factor and alpha-thrombin. *Biochemistry*. 1996; 35:4929-4938.

Weeterings C, Adelmeijer J, Myles T, de Groot PG, Lisman T. Glycoprotein Ib alpha-mediated platelet adhesion and aggregation to immobilized thrombin under conditions of flow. *Arterioscler Thromb Vasc Biol*. 2006; 26:670-675.

Wegener KL, Campbell ID. Transmembrane and cytoplasmic domains in integrin activation and protein-protein interactions (review). *Mol Membr Biol*. 2008; 25:376-387.

Weisel JW. Fibrinogen and fibrin. *Adv Protein Chem*. 2005; 70:247-299.

Weiss HJ, Turitto VT, Baumgartner HR. Role of shear rate and platelets in promoting fibrin formation on rabbit subendothelium. Studies utilizing patients with quantitative and qualitative platelet defects. *J Clin Invest*. 1986; 78:1072-1082.

Weitz JI, Leslie B, Hudoba M. Thrombin binds to soluble fibrin degradation products where it is protected from inhibition by heparin-antithrombin but susceptible to inactivation by antithrombin-independent inhibitors. *Circulation*. 1998; 97:544-552.

White-Adams TC, Berny MA, Patel IA, et al. Laminin promotes coagulation and thrombus formation in a factor XII-dependent manner. *J Thromb Haemost*. 2010; 8:1295-1301.

White TC, Berny MA, Tucker EI, et al. Protein C supports platelet binding and activation under flow: role of glycoprotein Ib and apolipoprotein E receptor 2. *J Thromb Haemost*. 2008; 6:995-1002.

Woldhuis B, Tangelder GJ, Slaaf DW, Reneman RS. Concentration profile of blood platelets differs in arterioles and venules. *Am J Physiol*. 1992; 262:H1217-1223.

Woulfe D, Yang J, Brass L. ADP and platelets: the end of the beginning. *J Clin Invest*. 2001; 107:1503-1505.

Wu KK, Thiagarajan P. Role of endothelium in thrombosis and hemostasis. *Annu Rev Med*. 1996; 47:315-331.

Xu H, Bush LA, Pineda AO, Caccia S, Di Cera E. Thrombomodulin changes the molecular surface of interaction and the rate of complex formation between thrombin and protein C. *J Biol Chem*. 2005; 280:7956-7961.

Xu J, Kochanek KD, Murphy SL, Tejada-Vera B. Deaths: final data for 2007. *Natl Vital Stat Rep*. 2010; 58:1-135.

Yamamoto K, Yamamoto N, Kitagawa H, Tanoue K, Kosaki G, Yamazaki H. Localization of a thrombin-binding site on human platelet membrane glycoprotein Ib determined by a monoclonal antibody. *Thromb Haemost*. 1986; 55:162-167.

Yuan Y, Kulkarni S, Ulsemer P, et al. The von Willebrand factor-glycoprotein Ib/V/IX interaction induces actin polymerization and cytoskeletal reorganization in rolling platelets and glycoprotein Ib/V/IX-transfected cells. *J Biol Chem*. 1999; 274:36241-36251.

Yun TH, Baglia FA, Myles T, et al. Thrombin activation of factor XI on activated platelets requires the interaction of factor XI and platelet glycoprotein Ib alpha with thrombin anion-binding exosites I and II, respectively. *J Biol Chem*. 2003; 278:48112-48119.

Zambrowicz BP, Friedrich GA, Buxton EC, Lilleberg SL, Person C, Sands AT. Disruption and sequence identification of 2,000 genes in mouse embryonic stem cells. *Nature*. 1998; 392:608-611.

Zhou JN, Ljungdahl S, Shoshan MC, Swedenborg J, Linder S. Activation of tissue-factor gene expression in breast carcinoma cells by stimulation of the RAF-ERK signaling pathway. *Mol Carcinog*. 1998; 21:234-243.

Zucker MB, Nachmias VT. Platelet activation. *Arteriosclerosis*. 1985; 5:2-18.

Zwaal RF, Comfurius P, Bevers EM. Surface exposure of phosphatidylserine in pathological cells. *Cell Mol Life Sci*. 2005; 62:971-988.

Zwaal RF, Schroit AJ. Pathophysiologic implications of membrane phospholipid asymmetry in blood cells. *Blood*. 1997; 89:1121-1132.

Biographical Sketch

Michelle Anne Berny was born on June 26, 1984 in Astoria, Oregon to Michael and Dana Berny. On September 4, 2010, she was married to Christopher Lang.

Michelle attended Astoria High School and, upon graduation, enrolled at Oregon State University (OSU). During her undergraduate studies, she became involved in a variety of research areas through internships at the OSU Seafood Research Center, the City of Eugene Wastewater Department, and the laboratory of Dr. Joseph McGuire at OSU. In June of 2006, she earned her Bachelor of Science degree in Biological Engineering.

Michelle continued her education at Oregon Health & Science University (OHSU), joining the laboratory of Dr. Owen McCarty in the Department of Biomedical Engineering in July 2006. After her first year of graduate school, she received a Whitaker fellowship to conduct her second year of graduate research in the laboratory of Dr. Johan Heemskerk at the University of Maastricht in the Netherlands. Michelle returned from Europe to finish her graduate research centered on the role of the coagulation enzyme thrombin in blood clot formation.

During her graduate studies at OHSU, she was awarded an Achievement Rewards for College Scientists scholarship, a NIH fellowship in Molecular Hematology, a Young Investigator Award from the International Society on Thrombosis and Haemostasis, an OHSU Educational Achievement award, and awards for research presentations. Michelle has received research funding through an American Heart Association predoctoral fellowship and the Pacific Division Alan E. Leviton Student Research Award from the AAAS. Michelle has presented her research in peer-reviewed journals and at conferences throughout the U.S. and Europe. Current publications and presentations are listed below:

Publications

1. White TC, **Berny MA**, Robinson DK, Yin H, DeGrado WF, Hanson SR, McCarty OJT, "The leech product saratin is a potent inhibitor of platelet integrin α2β1 and VWF binding to collagen" *FEBS Journal*; 2007 Mar; 274(6):1481-91.

2. Gruber A, Marzec U, Bush L, Fernández JA, **Berny MA**, Tucker EI, McCarty OJT, Di Cera E, Griffin JH, Hanson SR, "Relative antithrombotic and antihemostatic effects of protein C activator versus low molecular weight heparin in primates" *Blood*; 2007 May 1; 109(9):3733-40.

3. **Berny MA**, White TC, Tucker EI, Bush-Pelc LA, Di Cera E, Gruber A, McCarty OJT, "Thrombin Mutant W215A/E217A Acts as a Platelet GPIb Antagonist" *Arterioscler Thromb Vasc Biol*; 2008 Feb. 1; 28(2):329-334. (With Editorial; Awarded 2009 Karl Link New Investigator Award in Thrombosis)

4. White TC, **Berny MA**, Tucker EI, Urbanus RT, de Groot PG, Fernández JA, Griffin JH, Gruber A, McCarty OJT, "Protein C supports platelet binding and activation under flow: role of glycoprotein Ib and apolipoprotein E receptor 2" *J Thromb Haemost*; 2008 Jun; 6(6):995-1002. (Cover Figure)

5. White-Adams TC, **Berny MA**, Tucker EI, Gertz JM, Gailani D, Urbanus RT, de Groot PG, Gruber A, McCarty OJT, "Identification of Coagulation Factor XI as a Ligand for Platelet Apolipoprotein E Receptor 2 (ApoER2)" *Arterioscler Thromb Vasc Biol*; 2009 Oct; 29:1602-1607. (With Editorial)

6. Eshel-Green T, **Berny MA**, Conley RB, McCarty OJT, "Effect of sex difference on platelet adhesion, spreading and aggregate formation" *Thrombosis and Haemostasis*; 2009 Oct; 102:958-965.

7. Vartanian KB, **Berny MA**, McCarty OJT, Hanson SR, Hinds MT, "Cytoskeletal structure regulates endothelial cell immunogenicity independent of fluid shear stress" *Am J Physiol Cell Physiol*; 2010 Feb; 298(2):C333-41.

8. **Berny MA**, Munnix ICA, Auger JM, Schols SEM, Cosemans JMEM, Panizzi P, Bock PE, Watson SP, McCarty OJT, Heemskerk JWM, "Spatial distribution of factor Xa, thrombin, and fibrin(ogen) on thrombi at venous shear" *PLoS-ONE*; 2010 Apr; 5(4):e10415.

9. **Berny MA**, Patel IA, Simonson P, White-Adams TC, Gruber A, Rugonyi S, McCarty OJT, "Rational design of an ex vivo model of thrombosis" *Cell Mol Bioengineering*; 2010 Jun; 3(2):187-189.

10. White-Adams TC, Tucker EI, **Berny MA**, Gailani D, Gruber A, McCarty OJT, "Laminin supports the initiation of coagulation and thrombus formation in the presence of flow" *J Thromb Haemost*; 2010 Jun; 8(6): 1295-301.

11. Tucker EI, Marzec UM, **Berny MA**, Hurst S, Bunting S, McCarty OJT, Gruber A, Hanson SR, "Safety and antithrombotic efficacy of moderate platelet count reduction by thrombopoietin inhibition in primates" *Sci Transl Med*; 2010 Jun; 2(37): 37ra44.

12. **Berny MA**, Aslan JE, Tormoen GW, Patel IA, Bock PE, Gruber A, McCarty OJT, "Promotion of experimental thrombus formation by the procoagulant activity of breast cancer cells" (in press: *Phys Biol*)

Presentations

1. **Berny MA**, White TC, Tucker EI, Di Cera E, Gruber A, McCarty OJT, "The thrombin mutant W215A/E217A acts as a platelet antagonist through inhibition of thrombin activation and GPIb binding to VWF" XXIst Congress of the International Society on Thrombosis and Haemostasis, Geneva, Switzerland (Jul. 2007).

2. **Berny MA**, White TC, Melinte IA, Tucker EI, Swanson CE, Robinson DK, Mousa SA, Gruber A, McCarty OJT, "Factor XI mediates platelet lamellipodia formation and tethering and rolling under shear conditions" XXIst Congress of the International Society on Thrombosis and Haemostasis, Geneva, Switzerland (Jul. 2007).

3. **Berny MA**, White TC, Tucker EI, Swanson CE, Robinson DK, Gertz J, Gruber A, McCarty OJT, "Factor XI mediates platelet lamellipodia formation and tethering and rolling under shear conditions" 9th United Kingdom - 1st Netherlands Platelet Meeting, London, UK (Sep. 2007).

4. **Berny MA**, "Whitaker International Fellowship 2007-2008" Whitaker Alumni Symposium, St. Louis, MO (Oct. 2008)

5. **Berny MA**, Munnix ICA, Feijge MA, Bock PE, McCarty OJT, Heemskerk JWM, "Heterogeneous localization of coagulation factors in flow-dependent thrombus formation" Annual Meeting of the Biomedical Engineering Society, St. Louis, MO (Oct. 2008).

6. Fuchs BK, **Berny MA**, White TC, Conley TB, Eshel T, McCarty OJT, "Characterization of the procoagulant activity of platelets on laminin under shear flow" Annual Meeting of the Biomedical Engineering Society, St. Louis, MO (Oct. 2008).

7. **Berny MA**, Munnix ICA, Schols SEM, Bock PE, McCarty OJT, Heemskerk JWM, "Heterogeneous localization of coagulation factors in an ex vivo model of thrombus formation" XXIInd Congress of the International Society on Thrombosis and Haemostasis, Boston, MA (July. 2009). (Presented in Abstract Symposia for highly rated abstracts)

8. **Berny MA**, "Whitaker Fellowship 2007-2008" Annual Meeting of the Biomedical Engineering Society – Whitaker Session, Pittsburgh, PA (Oct. 2009).

9. **Berny MA**, "Characterization of the procoagulant activity of circulating tumor cells" Gordon Research Conference on Hemostasis, Waterville Valley, NH (Jul. 2010).